JOHANNES GUTENBERG UNIVERSITÄT MAINZ

Formulation and Characterization of Colloidal Formulations Loaded with Free Amino Acids for Dermal Delivery

DISSERTATION

zur Erlangung des akademischen Grades

"Doktor der Naturwissenschaften"

im Promotionfach Pharmazie

am Fachbereich Chemie, Pharmazie, Geographie, und Geowissenschaften

der Johannes-Gutenberg-Universität, Mainz

vorgelegt von

Birhanu Nigusse Kahsay

Geboren in Ayba/Alaje, Tigray, Äthiopia

Mai 2023

Dekanin	Prof. Dr. Eva Rentschler
1. Berichterstatter	Prof. Dr. Peter Langguth
2. Berichterstatter	Prof. Dr. Dr. Reinhard Neubert
Tag der mündlichen Prüfung	_____

DEDICATED TO MY LATE MOTHER

TABLE OF CONTENTS

LIST OF FIGURES

LIST OF TABLES

ACRONYMS AND ABBREVIATIONS

- AA: Amino acid
- AD: Atopic dermatitis
- ADAM: Adamantane HCl
- CE: Cornified envelope
- CORs: Corneocytes
- CPEs: Chemical permeation enhancers
- DAD: Diod array detector
- DER: Dermis
- DMSO: Dimethyl sulfoxide
- EDTA: Ethylenediaminetetraacetic acid
- EP: Epidermis
- FAAs: Free amino acids
- FMOC-Cl: 9-fuorenylmethoxycarbonyl chloride
- G'': Loss modulus
- G': Storage modulus
- GABA: γ-aminobutyric acid
- HET-CAM: Hen's egg test chorioallantoic membrane
- ICCVAM: Inter-agency coordinating committee on the validation of alternative methods
- $K_{COR/W}$: COR-water partition coefficient
- $K_{O/W}$: Octanol–water partition coefficient
- K_P: Skin permeation coefficients
- $K_{SC/V}$: SC-vehicle partition coefficient
- L-Ala: L-Alanine
- L-Arg: L-Arginine
- L-Asn: L-Asparagine
- L-Asp: L-Aspartate
- L-Cit: L-Citrulline
- L-Cys: L-Cysteine
- L-Gln: L-Glutamine
- L-Glu: L-Glutamate
- L-Gly: L-Glycine
- L-His: L-Histidine
- L-Ile: L-Isoleucine

- L-Leu: L-Leucine
- L-Lys: L-Lysine
- L-Met: L-Methionine
- LOD: Limit of detection
- LOQ: Limit of quantification
- L-Orn: L-Ornithine
- L-Phe: L-Phenylalanine
- L-Pro: L-Proline
- L-Ser: L-Serine
- L-Thr: L-Threonine
- L-Trp: L-Tryptophan
- L-Tyr: L-Tyrosine
- L-Val: L-Valine
- MEBHGs: Microemulsion based hydrogels
- MEs: Microemulsions
- MW: Molecular weight
- NMFs: Natural moisturizing factors
- O/W: Oil-in-water
- OECD: Organization for Economic Co-operation and Development
- PBS: Phosphate-buffered saline
- PHSC: Powdered human stratum corneum
- PS: Psoriasis
- RP-HPLC: Reversed phase high performance liquid chromatography
- SC: Stratum corneum
- SST: System suitability test
- Tau: Taurine
- TEWL: Trans-epidermal water loss
- VEP: Viable epidermis
- W/O: Water-in-oil
- WHO: World Health Organization

ABSTRACT

Free amino acids (FAAs) constitute the largest component (~40%) of the natural moisturizing factors (NMF). They play a critical role in skin barrier function and skin hydration. They are also responsible for maintaining the acidic pH of the skin. However, their content can decrease because of environmental and pathological conditions such as dry skin associated with atopic dermatitis (AD) and psoriasis (PS). The depleted skin FAAs can potentially be substituted by topical delivery of these compounds through appropriate formulation design. The present work, therefore, aimed at preparation and characterization of colloidal formulations loaded with plant-based and synthetic FAAs for topical application.

The FAA contents of 59 different plant species and mushroom were investigated to identify potential natural sources for these compounds. The samples were collected, dried, extracted and the concentration of 27 FAAs was analyzed using LC-ESI–MS/MS. Among the tested samples, the natural resource with the highest amount of those FAAs was selected. 18 FAAs that are also the major components of the NMF (namely L-Ala, L-Arg, L-Asn, L-Asp, L-Gln, L-Glu, L-Gly, L-His, L-Ile, L-Lue, L-Lys, L-Met, L-Orn, L-Phe, L-Pro, L-Ser, L-Thr, and L-Val) were extracted and purified from the selected source. A selective and accurate HPLC/DAD method was then developed and validated for simultaneous analysis of the 18 FAAs in the formulations during assay, partitioning and permeation studies. Then the skin partitioning behavior of the selected FAAs was studied using different skin models. The corneocyte -water partition coefficient ($K_{COR/W}$), skin permeation coefficients (K_P) and associated factors were studied as per standard protocols. The experimental K_P values were compared with those results obtained using four selected mathematical models. Finally, different colloidal formulations (microemulsions (MEs) and microemulsion based hydrogels (MEBHGs) loaded with the plant/mushroom-based FAAs and synthetic FAAs were prepared and characterized. The skin permeation of these colloidal formulations was compared with each other and with marketed hydrophilic cream (H-Cream) loaded with the same FAAs.

The results indicate that all 27 FAAs were detected at different concentrations in most of the investigated plant and mushroom sources. Among the tested samples, oyster mushroom contained high concentration of the dominant FAAs in the NMF. The validated RP-HPLC/DAD method for the simultaneous analysis of 18 FAAs was linear over the concentration range of 5-80 µM with a R^2 > 0.995. It was also sensitive, precise, accurate, and robust. The corneocyte-water partitioning studies suggest that FAAs are suitable candidates for the corneocytary pathway. The $K_{COR/W}$ values of the human corneocyte (COR) and that of pig ear skin were better correlated compared to that of human COR and keratin. The initial concentrations of the FAAs, presence of lipid in the stratum corneum (SC) and permeation enhancers affect the $K_{COR/W}$ values. The FAAs have very low K_P values indicating the

need for skin permeation enhancers during formulation design. Even though new mathematical models that consider the corneocytary pathway could better predict the skin permeation of FAAs, the tested models are able to reasonably predict the skin permeation of FAAs (from aqueous vehicle). The prepared colloidal formulations (MEs and MEBHGs) had the desired physico-chemical and particle properties and were non-irritant. The FAAs permeated into the deeper layers of the SC from the MEs and MEBHGs better than from H-cream. The MEs prepared from the mushroom extracts and those prepared using synthetic sources have similar physico-chemical characteristics. In summary, it can be concluded that FAAs that originate from nature or through chemical synthetic routes can be appropriately delivered into and through the skin's SC using colloidal carrier systems.

ZUSAMMENFASSUNG

Freie Aminosäuren (FAAs) stellen den größten Bestandteil (~40%) der natürlichen Feuchthaltefaktoren (NMF) dar. Sie spielen eine entscheidende Rolle bei der Funktion der Hautbarriere und der Hautfeuchtigkeit. FAAs sind auch dafür verantwortlich, den sauren pH-Wert der Haut aufrechtzuerhalten. Ihr Gehalt kann jedoch aufgrund von Umweltbedingungen und pathologischen Prozessen wie z.B. trockener Haut in Verbindung mit atopischer Dermatitis (AD) und Psoriasis (PS) abnehmen und, möglicherweise, durch eine topische Applikation dieser Verbindungen ersetzt werden. Die vorliegende Arbeit hatte daher zum Ziel, geeignete Formulierungen, die mit pflanzlichen und synthetischen FAAs für die topische Anwendung beladen sind, herzustellen und zu charakterisieren.

Der FAA-Gehalt von 59 verschiedenen Pflanzenarten und Pilzen wurde untersucht, um potenzielle natürliche Quellen für diese Verbindungen zu identifizieren. Die Proben wurden gesammelt, getrocknet, extrahiert und die Konzentration von 27 FAAs wurde mittels LC-ESI–MS/MS analysiert. Unter den getesteten Proben wurde die natürliche Ressource mit der höchsten Menge dieser FAAs ausgewählt. 18 FAAs, die auch die Hauptbestandteile des NMF sind (nämlich L-Ala, L-Arg, L-Asn, L-Asp, L-Gln, L-Glu, L-Gly, L-His, L-Ile, L-Lue, L-Lys, L-Met, L-Orn, L-Phe, L-Pro, L-Ser, L-Thr, and L-Val) wurden aus der ausgewählten Quelle extrahiert und gereinigt. Anschließend wurde eine selektive und genaue HPLC/DAD-Methode entwickelt und für die gleichzeitige Analyse der 18 FAAs in den Formulierungen während Assay-, Verteilungs- und Permeationsstudien validiert. Anschließend wurde das Hautverteilungsverhalten der ausgewählten FAAs unter Verwendung verschiedener Hautmodelle untersucht. Der Korneozyten-Wasser-Verteilungskoeffizient ($K_{COR/W}$), Hautpermeationskoeffizienten (K_P) und zugehörige Faktoren wurden gemäß Standardprotokollen untersucht. Die experimentellen K_P Werte wurden mit den Ergebnissen verglichen, die unter Verwendung von vier ausgewählten mathematischen Modellen erhalten wurden. Schließlich wurden verschiedene kolloidale Formulierungen (Mikroemulsionen (MEs) und Hydrogele auf Mikroemulsionsbasis (MEBHGs), die mit FAAs auf Pflanzen-/Pilzbasis und synthetischen FAAs beladen waren, hergestellt und charakterisiert. Die Hautpermeation dieser kolloidalen Formulierungen wurde miteinander und mit vermarkteten hydrophilen Mitteln verglichen Creme (H-Cream), die mit den gleichen FAAs beladen ist.

Die Ergebnisse zeigen, dass alle 27 FAAs in den meisten untersuchten Pflanzen- und Pilzquellen in unterschiedlichen Konzentrationen nachgewiesen wurden. Von den untersuchten Proben enthielt der Austernpilz eine hohe Konzentration der wichtigsten FAAs im NMF. Die validierte RP-HPLC/DAD-Methode zur simultanen Analyse von 18 FAAs war über den Konzentrationsbereich von 5-80 µM mit einem $R^2 > 0,995$ linear. Die Methode war empfindlich, präzise, genau und robust. Die Korneozyten-Wasser-Verteilungsstudien legen nahe, dass FAAs geeignete Kandidaten für den Korneozyten-Weg

sind. Die $K_{COR/W}$-Werte der menschlichen Korneozyten (COR) und der Schweineohrhaut korrelierten besser im Vergleich zu denen von menschlichem COR und Keratin. Die Anfangskonzentrationen der FAAs, das Vorhandensein von Lipid im Stratum corneum (SC) und die Permeationsverstärker beeinflussen die $K_{COR/W}$-Werte. Die FAAs haben sehr niedrige K_P-Werte, was auf die Notwendigkeit von Hautpermeationsverstärkern bei der Formulierungsentwicklung hinweist. Obwohl neue mathematische Modelle, die den korneozytären Weg berücksichtigen, die Hautpermeation von FAAs besser vorhersagen könnten, sind die getesteten Modelle in der Lage, die Hautpermeation von FAAs (aus wässrigem Träger) angemessen vorherzusagen. Die hergestellten kolloidalen Formulierungen (MEs und MEBHGs) hatten die gewünschten physikalisch-chemischen und Partikeleigenschaften und waren nicht reizend. Die FAAs drang aus den MEs und MEBHGs besser in die tieferen Schichten des SC ein als aus der H-Creme. Die aus den Pilzextrakten hergestellten MEs und die unter Verwendung synthetischer Quellen hergestellten haben ähnliche physikalisch-chemische Eigenschaften. Zusammenfassend kann geschlussfolgert werden, dass FAAs, die aus der Natur oder auf chemischen Synthesewegen stammen, mit kolloidalen Trägersystemen angemessen in und durch das SC der Haut transportiert werden können.

ACKNOWLEDGMENTS

I would like to express my deepest gratitude and appreciation to my supervisor, Prof. Dr. Peter Langguth for allowing me to finalize my PhD project at Johannes Gutenberg University (JGU), Mainz and for his guidance and constructive feedback on my PhD project. I am very thankful for the golden opportunity he gave to me.

I am deeply grateful to my supervisor, Prof. Dr. Dr. h.c. Reinhard Neubert, for his unreserved support and scientific guidance throughout the PhD Project and for his personal advice, encouragement and positive influence on my life.

I thank Prof. Dr. Peter Imming for allowing me to perform the PhD research work in his laboratory and for arranging the financial and material resources during my stay at Martin Luther University Halle-Wittenberg.

I also thank Prof. Dr. Tsige Gebre-Mariam, Prof. Dr. Johannes Wohlrab, and Dr. Lucie Moeller for advising me on key scientific aspects of my work (especially during the initial phase of the project).

I acknowledge JGU staff who helped me a lot. Special thanks to Dr. Nicole Merbitz for her unreserved support during the application and registration process at JGU-Mainz. I also thank Luise Meiser for her assistance in the rheology measurement of the formulations.

I am thankful to Mr. Jörg Ziegler, Leibniz Institute of Plant Biochemistry, for allowing me to use the LC-MS/MS instrument and for his support in arranging the necessary materials during the analysis.

I would like to offer my special thanks to Dr. Adrian Richter, Dr. Andreas Beuchel, Markus Lang, Paul Palme, Lea Mann, and Christoph Hage for their excellent assistance during my stay at Martin Luther University Halle-Wittenberg.

The Ethiopian Biodiversity Institute is acknowledged for supplying the plant materials. Special thanks to Yared Tareke who helped me during collection of the plant and fungus species.

I greatly acknowledge the financial support provided by the German Academic Exchange Service (DAAD) under the Tri-Sustain Project during the beginning of the PhD research work.

I would like to express my deepest gratitude to my son Elnathan Birhanu and my sister Sindu Nigusse for their love and support; this endeavor would not have been possible without them.

I am also very grateful to friends, colleagues, and other people who have been on my side during this project. Special thanks to Mrs. Bianka Huber and Pia Gaffron.

CHAPTER 1: INTRODUCTION

1.1 The human skin

The human skin is a complex organ and covers the whole-body surface. It makes up the largest organ of the human body, with a surface area of approximately 1.5-2.0 m^2, and accounts for about 16 % of total body weight. Its most important function is to form an effective barrier between the 'outside' and the 'inside' of the organism [Proksch et al., 2008]. It provides a barrier to water loss and also protects against diverse forms of chemical (irritants, allergens), physical (mechanical injury, UV-irradiation), and microbial (bacteria, fungus, virus) assailants. It has a dominant role in regulating body temperature, enhancing metabolic functions, and synthesizing vitamin D [Yannas, 2001].

The human skin is composed of three layers (Fig. 1), that are: the epidermis, the dermis, and subcutaneous tissue. The subcutaneous tissue (hypodermis) is the deepest layer of the skin. This tissue is filled with fat cells, fibroblasts, and macrophages [Narasimha and Shivakumar, 2010]. The middle layer of the skin, the dermis, is rich in blood vessels, lymphatic vessels, and nerve endings. In addition to the hair follicles, sebaceous glands, and sweat glands, the dermis is filled with scattered fibroblasts, macrophages, leukocytes, and mast cells. One square centimeter of skin contains about 10 hair follicles, 15 sebaceous glands, 12 nerves, 100 sweat glands, 360 cm of nerves, and three blood vessels on average [Barry, 1983].

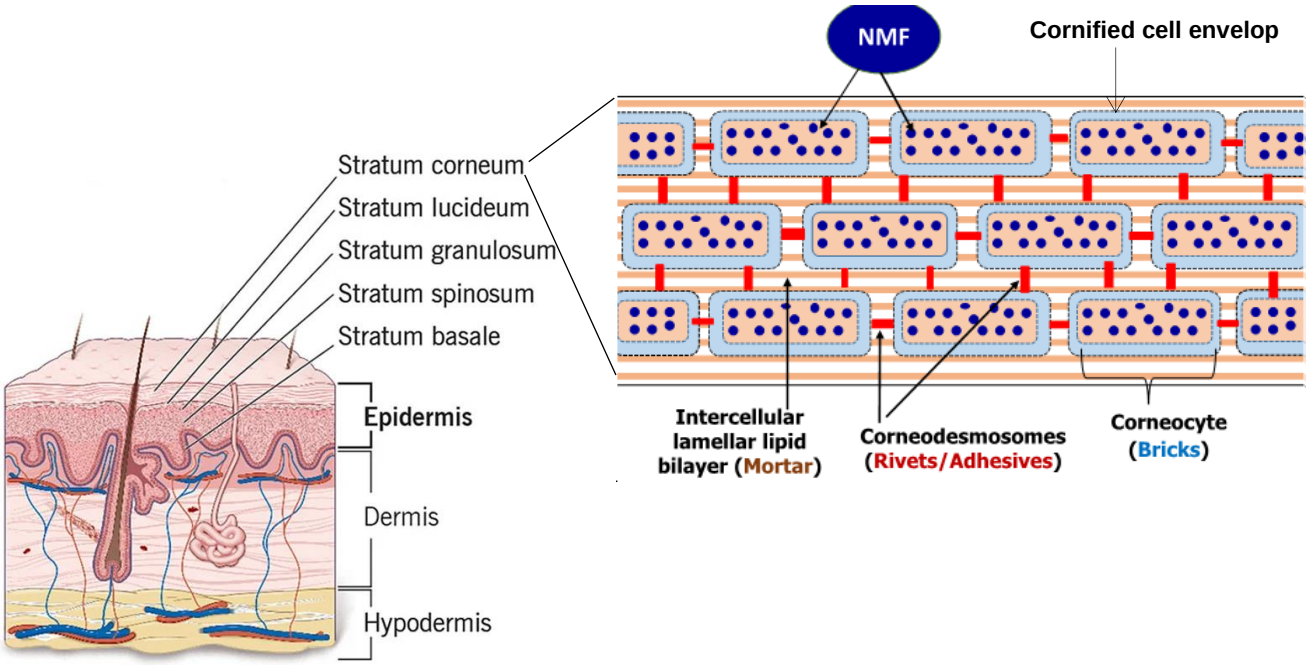

Fig. 1: The layers of the human skin [Harding, 2004].

The epidermis is the outermost layer of the skin that protects the body from the external environment. Stratified epidermis is about 100–150 μm thick. It forms an effective barrier against obnoxious stimuli from outside and simultaneously functions as a semipermeable membrane, helping to maintain proper moisture within the body. Keratinocytes, which make up about 90% of the cells, are the most common cells of the epidermis. In addition to keratinocytes, the normal epidermis contains Langerhans cells, Melanocytes, and Merkel cells.

The epidermis consists of five sub-layers. From outside to inside these layers are stratum corneum (SC) (horny cell layer), stratum lucidum (clear layer), stratum granulosum (granular cell layer), stratum spinosum (prickle cell layer), and stratum basale (basal cell layer). Stratum basale, the deepest sub-layer of the epidermis where keratinocytes are produced, is composed of a single layer of basal cells; and forms the boundary to the dermis. It holds approximately 8% of the water in the epidermis. However, with aging, this layer becomes thinner and loses the ability to retain water. Stratum spinosum, with a thickness of 50 to 150 μm [Anderson and Parrish, 1982], refers to the 10 to 20 cell layers that lie on top of the basal cell layer. Spinosum cells, also called prickle cells, have little spines on the outside of their membrane. Stratum granulosum is composed of 2 to 4 granular cell layers and has a typical thickness of about 3 μm [Anderson and Parrish, 1982]. Cornification called keratinization of keratinocytes begins in this sublayer. Stratum lucidum, also called the clear layer, can only be found in soles and palms and is a highly refractive sub-layer. Its cells become more densely packed and flatter during turn-over. The SC, which is the outermost layer of the epidermis, is a flat dead tissue packed with keratin fibers (corneocytes).

1.2 The stratum corneum (SC)

The SC, approximately 10–20 μm thick [Walters and Roberts, 2019], is the exterior sub-layer of the epidermis which forms the main barrier for diffusion of the permeants through the skin [Wertz and Downing, 1989]. This barrier property may be related in part to its low hydration of 15–20% compared to the usual 70% for the total body mass. The water content of the skin is remarkably high in viable epidermis (70% water) and drops to 15–30% water at the junction between the stratum granulosum and SC [Verdier-Sévrain and Bonté, 2007]. This difference in water content separates the SC from the body, helping to conserve water and other important solutes within the viable epidermis. The steep water gradient (at the lower part of the SC) initiates important keratinocyte functions such as the proteolysis of filaggrin. This intern facilitates the production of components of the natural moisturizing factors (NMF) in the deeper part of the SC. This significant difference in the water content also parallels the increase in SC lipids secretion. Both processes are essential for skin barrier function and SC hydration. It is estimated that water loss due to ‘insensible perspiration’ is restricted to 0.5 μl/cm^2 /hr, or 250 ml of water per day for a normal adult [Walters and Roberts, 2019]. The SC also has very high

density (1.4 g/cm^3 in the dry state) and low surface area for solute transport. Hence, in addition to its low hydration, these properties contribute to its barrier function [Walters and Roberts, 2019].

The SC is composed of cells called corneocytes (COR) which are inter-dispersed within the lipid matrix to assume a ‘‘bricks (CORs) and mortar (lipids)’’ arrangement [Fig 1]. The proper function of these two components of the SC assures skin integrity and hydration [Verdier-Sévrain and Bonté, 2007]. The extracellular lipid and intra-cellular keratin contribute 10 % and 90% of the dry weight of the SC respectively [Narasimha and Shivakumar, 2010]. Lipids in the SC exist principally in the form of triglycerides, fatty acids, cholesterol, and phospholipids.

1.3 Corneocytes (CORs) and their role in skin barrier function

The SC is composed of 15-25 layers of hexagonal-shaped flat, hard, keratin-rich dead cells named horny cells or CORs [Walters and Roberts, 2019]. Each cell has diameter and thickness of approximately 40 µm and 0.5 µm respectively. CORs are the physical barrier of the SC as the level of hydration of the SC is one of the key elements for the skin barrier function [Bouwstra, et al., 2003]. When hydrated, CORs contribute to skin aspect and sensorial surface properties.

COR are surrounded by a cornified envelope (CE) [Kalinin et al., 2002]. CE is a highly cross-linked protein shell. Together with keratin filaments the CE is useful for both the flexibility and mechanical resilience of the SC [Verdier-Sévrain and Bonté, 2007]. The impermeable CE provides structural support to the cell and resists invasion by microorganisms and deleterious environmental agents; however, it does not appear to have a significant role in regulating permeability. The CE is composed of different structural proteins such as involucrin, loricrin, small proline-rich protein, filaggrin and cystatin S, cross-linked by transglutaminase enzymes [Gittler et al., 2013].

CORs originate in the deepest layer of the epidermis, the stratum spinosum, as cells called keratinocytes [Yang et al., 2017]. As suggested by their name, keratin is the primary constituent of keratocytes. As these cells move up through the layers of the epidermis to the SC, they lose their nucleus and flatten out. It is at this point that they're considered CORs. Hence, CORs are filled with keratin filaments in addition to amino acids and other small molecules (collectively referred to as natural moisturizing factors (NMFs)) [Verdier-Sévrain and Bonté, 2007]. Keratin and NMFs provide the major water holding capacity of the SC thus regulating skin flexibility, firmness, and smoothness. Hence, water present in healthy skin *in vivo*, i.e., about 15–30% per weight of dry SC [Caspers et al., 2000] is tightly bound [Walkley, 1972; Hansen and Yellin, 1972].

1.4 Natural moisturizing factors (NMFs) and their role

The NMF is a mixture of hygroscopic molecules that keeps the SC hydrated by maintaining hydration in the COR. Much of the NMF is represented by FAAs and their derivatives (Pyrrolidone carboxylic acid (PCA) and urocanic acid), derived from the proteolysis of epidermal filaggrin. Other components found within but also external to the CORs include lactates, urea, sugars, and electrolytes (Table 1) [Rawlings and Harding, 2004]. The NMF compounds are present in high concentrations within COR (making up approximately about 10% of COR mass), and they represent 20% to 30% of the dry weight of the SC [Strianse, 1974; Fowler, 2012].

The principal role of the NMF is to maintain adequate hydration of the SC of skin. By doing so it serves three major functions: (1) it contributes to optimum SC barrier function; (2) it allows hydrolytic enzymes to function in the process of desquamation; and (3) it maintains plasticity of the skin, protecting it from damage [Rawlings et al, 1994; Fowler, 2012]. Hygroscopic components of the NMF are reported as very efficient humectant [Rawlings et al., 1994]. They attract and bind water from the atmosphere, drawing it into the CORs.

Table 1: Chemical composition of NMF [Rawlings and Harding, 2004]

Chemical	Composition (%)
Free amino acids (FAAs)	40
Pyrrolidone carboxylic acid (PCA)	12
Lactate	12
Sugars	8.5
Urea	7
Chloride	6
Sodium	5
Potassium	4
Ammonia, uric acid, glucosamine, creatine	1.5
Calcium	1.5
Magnesium	1.5
Phosphate	0.5
Citrate and formiate	0.5

NMFs are very important to maintain tissue flexibility [Williams and Barry, 2004]. Approximately two-third of water contained within the SC is free water, with the remainder being bound [Fowler, 2012]. Moreover, the elasticity of the SC is not affected by increasing the level of free water [Jokura et al., 1995]. This means only the NMF-bound water is responsible for providing the skin with its elastic qualities. Therefore, replenishing or replacing the supply of the NMF in the skin through the external application of topical formulations that contain the major components of NMF (such as FAAs) can be considered as a successful treatment approach for xerotic skin.

1.5 Free amino acids (FAAs) and their benefit for the skin

Amino acids (AAs), often called “the building blocks of life”, are primary metabolites which play a vital role in nutrition and health maintenance [Leuchtenberger et al., 2005; Mueller and Huebner 2003]. They are very safe for humans [Hitoshi et al., 2012]. They can be used as ingredients in cosmetic and pharmaceutical products and as special nutrients in the medical field (Ikeda 2003; Park and Lee, 2008). AA are commonly exploited in transfusions [Naylor et al., 1989; Louard et al., 1990; Stoimenova et al., 2013]. They are also used as intermediate precursors to produce antibiotics and in the manufacture of artificial sweeteners such as aspartame [Newsholme et al., 1985; Tang et al., 1994; Demain, 2000; Garg et al., 2008]. AAs, administered individually or in combination, are also very important for the treatment of many disease conditions. They are used in treatment of brain metabolism and neurotransmission imbalances [Meletis and Barker, 2005], treatment and/or prevention of cardiovascular disease, obesity, diabetes, metabolic syndrome, and infection [Wu, 2009], liver disease [Lee and Kim, 2019], and improving and/or maintaining physical conditions [Takaoka et al., 2019].

There are 20 standard AAs, and structurally each AA consists of one basic primary amino (-NH_2) group (except proline (L-Pro)) and one acidic carboxylic (-COOH) group with a side chain `R´, specific to the AA (Fig. 2; Fig S1). L-Pro is classified as an imino acid. Its α-amine is a secondary amine with its nitrogen having two covalent bonds to carbon (to the α-carbon and side chain carbon), rather than primary amine.

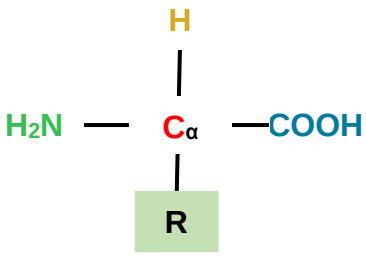

Fig. 2: Structure of alpha amino acids

Based on their nutritional requirements, the standard AAs can be classified into two groups [Wu et al., 2013]: essential and non-essential AAs. Essential AAs are those that are not synthesized by the body and must be supplied as supplement. L-Histidine (L-His), L-isoleucine (L-Ile), L-leucine (L-Leu), L-lysine (L-Lys), L-methionine (L-Met), L-phenylalanine (L-Phe), L-threonine (L-Thr), L-tyrosine (L-Try), and L-valine (L-Val) are classified in this group. Non-essential AAs are synthesized in the body and there is no diet dependency for them. L-Alanine (L-Ala), L-arginine (L-Arg), L-asparagine (L-Asn), L-aspartic acid (L-Asp), L-cysteine (L-Cys), L-glutamic acid (L-Glu), L-glutamine (L-Gln), L-glycine (L-Gly), L-Pro, serine (L-Ser), and L-Tyr are included as non-essential AAs. Some AAs (L-Arg, L-Cys, L-Gly, L-Gln, L-Pro, and L-Tyr) are considered as semi-essential as their synthesis can be limited under special

pathophysiological conditions. The standard AAs can also be classified into aliphatic (L-Gly, L-Ala, L-Val, L-Leu, and L-Ile), aromatic (L-Phe, L-Tyr, L-Trp), acidic (L-Asp, L-Glu), basic (L-Lys, L-Arg, L-His), imino acid (L-Pro), sulfur (L-Cys, L-Met), and hydroxyl (L-Ser, L-Thr, L-Tyr) AAs based on the type of the functional group (R group). They can also be grouped into polar and non-polar AAs based on the characteristics of the functional group. The polar AAs can be further classified into neutral (L-Tyr, L-Ser, L-Thr, L-Cys, L-Gln, and L-Asn), acidic (L-Glu, L-Asp), and basic (L-Lys, L-His and L-Arg). The non-polar AAs can further be classified into aromatic (L-Phe and L-Trp) and alkyl (L-Gly, L-Ala, L-Val, L-Leu, L-Ile, L-Met, L-Pro). AA can also be categorized into alpha, beta, gamma, and delta AAs based on the site of attachment of the functional groups.

In addition to the standard AAs, there are other classes of AAs, namely non-protein AAs, non-alpha AAs, and modified protein AAs. Non-protein AAs are not naturally encoded by genetic code but found in free state as intermediates of metabolic pathway for standard AAs. L-Ornithine (L-Orn) and L-citrulline (L-Cit) are intermediates in urea biosynthesis. In the non α-AA group, the -NH_2 group is not attached to the α-C atom but some other carbon atom (e.g., γ-aminobutyric acid (GABA)). On the other hand, modified protein AAs are those that are modified after they are incorporated into protein. For example, L-Pro and L-Lys undergo hydroxylation to become hydroxyproline and hydroxylysine and they are essential for formation of mature collagen. Each of the AAs can be found bound (to peptides and proteins) or in free form. The 20 standard AAs plus L-Cit and L-Orn (Table S1) can be found in free form and are important for our skin.

Free amino acids (FAAs) are indispensable for healthy skin. They are active compounds used in therapeutic and cosmetic treatments for several skin diseases and/or just for hydrated and young skin maintenance. The SC maintains its hydration level at ~15% by retention of FAAs that act as emollients [Jacobson et al., 1990; Seguchi et al., 1996; Kim et al., 2012]. They constitute the largest component (~40%) of the so-called NMF (Table 1) [Jokura et al., 1995] and are very important in maintaining the moisture balance of skin. Filaggrin, one of the most important skin proteins specifically located in granular keratinocytes and lower CORs of the SC [Hsu et al., 2011], is the source of FAAs. The composition of FAAs in skin and the composition of filaggrin show a high degree of similarity [Solano, 2020]. Moreover, a decrease in the amount of FAAs contributes to the pathogenesis of xerotic skin conditions [Horii et al., 1989], and this is correlated with low filaggrin content in the epidermis. These indicate that selective proteolysis of filaggrin is the source of FAAs and during terminal differentiation filaggrin may act as a NMF.

There are some reports on the most dominant FAAs of the NMF. As reported by Caspers et al., L-Ser (~ 36%), L-Gly (~ 22%) and L-Ala (~13%) are the most dominant ones [Caspers et al., 2001]. Citrulline (Cit), ornithine (Orn), L-His and L-Arg all account for 6–8%. In another study by Burke et al., [1966], L-

Ser, L-Gly, Cit, L-Ala, L-His, and L-Thr, in that order, are the dominant FAAs in the SC of human skin and account for as much as 80%. L-Met, L-Cys, and L-Trp are present in smallest concentrations; and L-Pro is obscured because of the large amount of Cit masking its presence. Twenty-three (23) FAAs were detected in human CORs in a study by Hussain et al., (2019) at different concentrations.

When topically applied, FAAs help to improve all skin types and are suitable for all ages. Supplementation of FAAs (alone or in combination) has been proven to be beneficial to the beauty and health of human skin. Among others, the three neutral ones (L-Gly, L-Pro and L-Leu) and three cationic ones (L-His, L-Lys and L-Arg) are the most common FAAs in skincare products [Solano, 2020]. L-Gly and L-Pro are by far the two most abundant AAs in collagen, and they play an important role in its production [Albaugh et al., 2017]. They are not only abundant constituents of collagen but also regulators of the synthesis of this protein [Wu et al., 2011]. L-Pro and L-Leu can attenuate wrinkles when paired together [Solano, 2020]. L-Pro, and its precursors L-Glu and pyrroline-5-carboxylate, increases collagen synthesis in human fibroblast cells [Karna et al., 2001].

A study by Murakami et al conducted on hairless mice showed that mixtures consisting of branched-chain AAs (L-Leu, L-Ile and L-Val) plus L-Arg, L-Gln or L-Pro significantly increased the synthesis of dermal collagen [Murakami et al., 2012]. L-Leu in combination with L-Gly and L-Pro, has been used for attenuation of skin wrinkles [Kawashima et al., 2013].

L-His, which is the key building block of the skin protein filaggrin [Koyama et al., 1984], has antioxidant and soothing properties for skin. It can improve the severity of atopic dermatitis (AD) by significantly increasing both filaggrin formation and skin barrier function [Irvine et al., 2011; Tan et al., 2017]. It helps in boosting the production of collagen and elastin in the lower layers of the skin. L-His also plays an important role in preserving the moisture of SC. L-Arg and L-His residues in filaggrin undergoes deimination, so that urocanic acid (UCA) and citrulline residues appear. UCA has photoprotective on the skin [Barresi et al., 2010]. It has also a buffering effect to maintain the relatively acidic pH of the SC (around 5.5) and this contributes to the inhibition of pathogenic fungal and bacterial growth. In cosmetics, L-Cit is mainly used as a skin conditioning agent with potential antioxidant benefits.

Many AAs are very important in wound healing. Among others, L-Arg [Shi et al., 2003; Stechmiller et al., 2005], combination of L-Lys and L-Arg [Solano, 2020], L-Orn [Shi et al., 2002], and AA mixtures (L-Ala, L-Asp, L-Glu, L-Gly, L-Ile, L-Ser, L-Leu, L-Lys, L-Met, L-Thr, L-Phe, L-Pro, L-Trp, L-Tyr, and L-Val) [Badiu et al., 2010; Corsetti et al., 2010] are reported for their benefit in wound healing. The supplementation of L-Leu has an anabolic effect on protein metabolism in skin wounds [Zhang et al., 2004]. L-Lys is one of the essential AAs that have been extensively studied for skin care products as it is very important for proper elastin and collagen functions. Supplementations that contain this compound have also been proposed for prevention of acne and cold sore [Solano, 2020]. It is also

very useful to strengthen the skin surface. L-Glu increases pro-collagen mRNA levels and collagen content [Bellon et al., 1987, Bellon et al., 1995]. A study by Ishikawa et al. indicates that a combination of FAAs such as L-Ala, L-Gly, L-Ile, and L-Leu reduces pigmentation in B16F0 melanoma cells [Ishikawa et al.,2007].

Ala and Ser are moisturizing agents added to some skincare products. As for FAAs, L-Ser and L-Ala play a general role in water retention in the SC. L-Ser is one of the most abundant AAs in filaggrin, the main skin protein that helps to maintain pH and hydration at the SC. L-Ser rich products have been proposed for improving skin hydration in atopic dermatitis [Kim et al., 2012]. L-Thr plays a necessary role in the formation of collagen and elastin [Jiravanichanun et al., 2006] which both help with healthy skin and wound healing. This AA is precursor for L-Gly, the main AA in collagen. L-Thr and L-Ser are among the most important AA for keeping the SC in a hydrated state [Solano, 2020]. Asp and Glu are excitatory neurotransmitters, and excessive use of these AAs may contribute to nociception and inflammatory pain in peripheral tissues including the skin [Omote et al., 1998]. L-Gln has been proposed as a stimulator of collagen biosynthesis [Karna et al., 2001]. It is frequently proposed for improving wound healing because it inhibits protein breakdown [Williams et al., 2002; Xi et al., 2012]. High levels of L-Gln are needed for regulation of the acid-base balance. L-Asn is needed for cell growth. Deprivation of L-Asn with the bacterial enzyme asparaginase is used to inhibit cell proliferation [Durden, 2016] and such approach has been used for malignant cells. This could also be applied to the treatment of cell hyperproliferation of keratinocytes, as occurring in psoriasis.

L-Met and L-Cys are another group of AAs. These (sulfur-containing) AAs are the sources of sulfur for several functions. L-Cys found in keratin can be sourced from L-Met and it plays an important role in the formation of the disulfide bridges present in the integumentary skin structures [Miniaci et al., 2016]. These AAs are very useful for the formation of skin structural glycosaminoglycanes and polysaccharides [Danzberger et al., 2018]. L-Met can also be used as a vehicle for zinc for the treatment of acne and inflammatory cutaneous lesions as antioxidant complexes [Solano, 2020]. L-Phe and L-Tyr are not very abundant in collagen, elastin, or keratins. However, these aromatic AAs are important as precursors of melanin, which absorbs the harmful sunlight UV and thus is the main cutaneous photoprotective pigment for avoiding DNA damage and skin cancer types [Brenner and Hearing, 2008; Fajuyigbe et al., 2018]. L-Trp is another aromatic AA that is not abundant in skin proteins. Hence, there are only very few studies on its role in skin health. However, this AA is the precursor of melatonin, a hormone involved in skin protection against oxidative stress. L-Orn is a non-protein AA that can improve skin condition subjectively and objectively when applied to the skin [Kirisako et al., 2012].

In general, none of the FAAs can be considered as the most important one, as they are complementary to each other. They are very important though when it comes to maintaining healthy skin. When added to skincare products, they improve hydration while making the skin more resilient to harmful environmental stressors. They also have anti-aging benefits by boosting the natural production of elastin and collagen. They can work together with other beneficial ingredients such as glycerides, ceramides, hyaluronic acid and peptides. They work especially well in combination with peptides and can be included in many peptide boosters. They are versatile ingredients that are a nice addition to other active skin care ingredients such as antioxidants, plant extracts and omega fatty acids.

1.6 Nature based sources of FAAs

FAAs for cosmeceutical, pharmaceutical, and food applications can be sourced in four different ways, namely through chemical synthesis, extraction (from natural resources), fermentation, and enzymatic synthesis [Leuchtenberger et al., 2005; Ikeda, 2003]. Even though there are a great advancements in biotechnology and chemical synthesis, the demand for herbal medicines by customers is still high. Recent report by the world health organization (WHO) indicated that about 80% of world population utilizes herbal medicines as first-line primary healthcare [Nagalingam, 2017; Srivastava et al., 2018; Sharma et al., 2019]. This revival of public interest in herbal medicine has been attributed to several reasons including: (a) herbal medicines are a mixture of bioactive molecules that may act synergistically [Sandberg and Corrigan, 2001; Segneanu et al., 2017]; (b) they could be more effective compared to their synthetic counterparts [Thornfeldt, 2005]; (c) they have a lot of economic advantages and may be used by people at all economic stages; (d) they have less and/or no side effects, interactions, and contraindications [Segneanu et al., 2017]; and (e) they have complex (structural diversity) and may have multiple stereo centers [Phillipson, 2001]. There is also a general trust that herbal medicines are superior as compared to chemically manufactured products. Herbal medicines are the modern trend in the field of health, beauty, and fashion when it comes to the cosmetic industry and there is a greater demand for herbal materials. Herbal remedial approaches are also believed to lead people towards self-medication [Bandaranayake, 2006]. Finally, in the cosmeceutical sector, use of a single natural source for a mixture of bioactive molecules such as FAAs has considerable economic advantage over using FAAs produced individually through any of the other production techniques.

Understanding the above-mentioned benefits, the WHO has been working toward increasing the use of herbal medicines [WHO, 2013] and currently about 25% of new drugs approved by the European Medical Agency (EMA) and Food and Drug Administration (FDA) and/or are directly or indirectly herbal based [Newman and Cragg, 2012; Calixto, 2019]. Hence, research on plant-based bioactive molecules is among the top research topics in the consmecutical and/or pharmaceutical sector

[Segneanu et al., 2017; Azmir et al., 2013; Chikezie et al., 2015]. In line with this, some countries have been broadly using their natural resources (plants) for cosmeceutical and/or pharmaceutical applications [Ji et al., 2017; Ruhsam and Hollingsworth, 2018]. Ethiopia is one of the countries endowed with a diversity of biological resources. It is one of the six regions which are rich in the biodiversity of plant and is land of about 6500–7000 species of higher plants of which 12% are endemic [Berhan and Egziabher, 2009]. Use of such sustainable and natural ingredients for cosmeceutical applications has several benefits to the population in fostering sustainability and natural remedial approaches. Moreover, most of the FAAs can be sourced from a single plant and this has a lot of benefits than the use of individual FAAs obtained through different options.

1.7 Dermatological disorders associated with SC barrier dysfunction

The hygroscopic properties of the SC are maintained by the presence of NMF. However, both extrinsic and intrinsic factors can affect the production of NMF and its components (including FAAs). If water content of the SC falls below a critical level, enzymatic function required for normal desquamation is impaired, leading to COR adhesion and accumulation on the cutaneous surface [Verdier-Sévrain and Bonté, 2007]. These abnormal changes result in the visible appearance of roughness, dryness, scaling, and flaking [Watkinson et al., 2001]. Many factors such as low humidity, surfactant, sun, and wind can lower the water content of the SC, causing improper desquamation and the appearance of dry, flaky skin. For example, the function of hydrolytic enzymes responsible for the proteolysis of filaggrin and the generation of FAAs is impaired at low humidity (< 10% relative humidity) and, consequently, induces skin surface dryness [Katagiri et al., 2003]. The SC can also be damaged when the skin's natural moisturizing process is disrupted by ultraviolet (UV) radiation. There is an age-related decline in NMF. For instance, in senile xerosis, a common dry skin condition in elderly people, there is a reduced synthesis of pro-filaggrin and decreased FAA amount [Horii et al., 1989]. A reduced level in NMF is one of the reasons why in dry skin the hydration level is lower than in normal skin [Rawlings et al, 1993]. In skin, which is exposed to the daily cleansing agents, much of the soluble NMF is washed out of the superficial SC [Caspers et al., 2001]. Disease conditions such as atopic dermatitis (AD), ichthyosis vulgaris, psoriasis (PS), and age can also be the causes for the lower level of the FAAs in the skin [Verdier-Sévrain and Bonté, 2007; Takada et al., 2012]. Hence, the barrier function of the SC should be monitored continuously.

The SC barrier dysfunction can be investigated (by investigating its components) using any of the available bioengineering techniques. Among these, measurement of Transepidemal water loss (TEWL) is a marker for skin barrier function, since it depends on skin hydration, skin blood flow and skin temperature. Increased TEWL is associated with increased skin permeability and absorption of chemicals [Rubio et al., 2011]. The removal of consecutive SC layers by means of tape stripping is a minimally invasive and widely used technique [Lademann et al., 2009; Zhai et al., 2013]. The method

has been applied for experimentally induced impairment of barrier function [Jungersted et al., 2010], for penetration studies [Jakasa et al., 2007], to evaluate the composition of the skin (lipids and other components [Jungersted et al., 2013]), and for assessment of epidermal biomarkers in skin diseases [Koppes et al., 2016; Clausen et al., 2018]. A consistent method has been developed, using a specialized tape (D-squame tape), and standardized pressure [Koppes et al., 2016; Breternitz et al., 2007]. Despite the efforts to standardize the method, the number of strips taken varies between studies. The human skin is described as shinny and red after the removal of 30–40 strips, and it is generally agreed that the SC has been removed [de Jongh et al., 2007; Peppelman et al., 2015]. Other measurements of skin barrier function include SC hydration [Gruber et al., 2011; Williams et al., 2010], SC cohesion, surface pH and paracellular permeability of the water-soluble tracer lanthanum [Gruber et al., 2011].

After the SC dysfunction is investigated, the best way to overcome such disease condition seems to be the delivery of the major components of the SC (such as components of the NMF) to the human skin. The delivery of the required amount of the drug to the target site within the skin requires detailed knowledge of the compounds of interest, choosing the appropriate drug delivery pathway, understanding the critical factors affecting the delivery, and then designing of appropriate formulation.

1.8 Hydrophilic drug delivery into and through the SC

Dermal delivery of a drug is a complex process involving several steps: (i) the release of drug from the formulation; (ii) drug partitioning into the SC; (iii) drug diffusion across the SC; (iv) drug partitioning from the SC into viable epidermis layers; and v) diffusion across the viable epidermis layers into the dermis [Kalia and Guy, 2001]. Ideal physico-chemical properties of drug candidates for (trans)dermal delivery include: (a) adequate solubility in oil and water such that the membrane concentration gradient would be high, (b) low molecular weight (< 500 Daltons), (c) high potency of the actives (dose < 50 mg/day or ideally, < 10 mg/day), (d) high lipophilicity (logP in the range of 1–3), (e) two or less hydrogen-bonding groups, and (f) a low melting point (< 200 ^{0}C) [Pathan and Setty, 2009].

The delivery of hydrophilic molecules such as FAAs into and through the SC is highly challenging. It requires detailed understanding of the diffusion/permeation pathway and critical factors that can affect the whole process. The pathways for epidermal permeation of active molecules are through the intercellular lipid matrix, intracellular permeation through the CORs, and appendageal penetration [Kim et al., 2020]. The appendages comprise only a fractional area for permeation and their contribution to epidermal permeation is usually small [Kim et al., 2020]. Due to this it is well documented that drug interaction with the SC is possible with (1) CORs (keratin, NMFs and proteins of CE); (2) intercellular lipids [Hansen et al., 2009]. As there is a common consensus that transport occurs mainly via the

intercellular lipids [Walters and Roberts, 2019], interactions of small hydrophilic molecules with CORs is neglected.

It is well documented that occlusion effectively enhances skin permeation of hydrophilic compounds by increasing the partitioning of the compounds into the SC [Williams and Barry, 2004]. CORs may also offer a permeation pathway across the SC for hydrophilic molecules through the controversially discussed continuous desmosome-COR route [Peck et al., 1994; Sznitowska et al., 1998; Barry, 2002; Jain et al., 2002; Panchagnula et al., 2004; Lademann et al., 2007; Otberg et al., 2008]. There is also significant evidence that the CORs are accessible for at least a few – permeants. Water can also enter the CORs very effectively [Kasting and Barai, 2003; Bouwstra et al., 2003]. Moreover, several larger hydrophilic and even lipophilic molecules (usually dyes) were visualized inside the COR [Yu et al., 2003; Jacobi et al., 2006]. Disintegrating desmosomes could serve as an entrance through the cornified envelop (CE) into the CORs in the apical SC [Boddé et al., 1991]. These evidence suggest that the preferred delivery path for small hydrophilic molecules such as FAAs could be the corneocytary pathway. Hence, studying the partitioning behavior of these compounds to the COR is very important to prove this.

Many factors can affect the permeation of drugs through the CORs. As outlined in Eq 1, drug permeation rate through the SC can be represented by the steady-state flux equation:

$$J_{SS} = \frac{KD\Delta C_V}{h} \qquad \text{(Eq. 1)}$$

Where J_{ss} is drug flux, K is partition coefficient of the solute between the membrane and the vehicle ($K= C_S/C_V$), D is diffusion coefficient in the skin membrane, C_S and C_V are solute concentrations in the skin membrane and vehicle respectively, and h is path length. Thus, effective penetration enhancers can increase the drug delivery by increasing the diffusion coefficient of the drug in the SC, increasing the drug concentration in the vehicle, and improving the partitioning between the drug formulation and the SC.

Even though the common factors could be those mentioned above, other related aspects can affect the delivery system. In 1983 a 10-factor guide (for percutaneous absorption) was suggested by [Wester and Maibach, 1983]. This was later expanded to 15 in 2012 [Ngo and Maibach, 2012], and modified in 2013 [Hui et al., 2013(a); Hui et al., 2013(b)]. Clinical relevance and complexities were added to it in 2017 [Li et al., 2017]. Recently, 20 clinically relevant factors that can affect the percutaneous absorption of drugs and chemicals were identified by [Law et al., 2019]. Example of the factors that can affect dermal delivery include (1) relevant physico-chemical properties ((particle size/molecular weight, lipophilicity, pH, pKa, partition coefficient), (2) vehicle/formulation, (3) drug

exposure conditions (dose, duration, surface area, exposure frequency), (4) skin appendages (hair follicles, glands) as sub-anatomical pathways, (5) skin application sites (regional variation in penetration), (6) population variability (premature, infants, and aged), (7) skin surface conditions (hydration, temperature, pH), and (8) skin health and integrity (trauma, skin diseases). Even though all the stated factors can affect percutaneous absorption, it is wise to further identify the most critical parameters. Among others, detailed knowledge of the rate-limiting barrier and the key physico-chemical determinants that control molecular flux through the skin are the most important ones [Surber, 1990]. The primary barrier lies within the SC [Rougier et al., 1990]. Thus, it is to be expected that the overall kinetic process will depend mainly on the pharmacokinetic parameters governing the permeation of compounds through this membrane. On the other hand, the partition coefficient (K) of a drug can be taken as a critical physico-chemical indicator that controls the drug flux through the skin membrane (for example the SC). Thus, for a given thickness of SC and a specific anatomical site, the penetration flux value of a substance depends mainly on its SC-vehicle partition coefficient ($K_{SC/V}$) [Rougier et al., 1987, Rougier et al., 1990; Vecchia and Bunge, 2002; Hansen et al., 2011]. Hence, determination of the $K_{SC/V}$ value of drug substances is very critical to understand the permeation properties of drugs into or through the SC.

Considering the detailed anatomical heterogeneity of the SC, previous models assume that interactions with the CORs are regulated by a partition coefficient [Raykar et al., 1988; Nitsche et al., 2006] at drug concentrations far away from saturation. However, non-linear concentration influences indicating saturable processes are being repeatedly reported in literature. These include binding studies using isolated keratin protein [Banning and Heard, 2002; Heard et al., 2003] and SC-donor partition coefficients ($K_{SC/don}$) of several drugs [Kubota et al., 1993; Surber et al., 1990; Banning and Heard, 2002; Heard et al., 2003]. Lately, experimental methods were established to quantify the tendency of compounds to interact with the CORs in terms of a COR-intercellular lipids partition coefficient ($K_{cor/lip}$) [Hansen et al., 2008]. This method provides a general idea of the overall extent of COR uptake. However, it does not allow insight into the mechanism of interaction. Some datasets of experimentally measured partition coefficients into extracted SC lipids are reported for some compounds [Raykar et al., 1988; Hansen et al., 2008]. A correlation between the octanol–water partition coefficient ($K_{O/W}$) and the lipid-donor partition coefficient ($K_{lip/don}$) according to a power law (linear free energy relationship) has been employed [Mitragotri, 2002; Yu et al., 2003; Nitsche et al., 2006]. Similar correlations have also been proposed to exist between the COR–water partition coefficient ($K_{cor/w}$) and $K_{O/W}$ [Anderson and Cassidy, 1973; Anderson et al., 1988; Raykar et al., 1988; Hansen et al., 2008]. Furthermore, partition coefficients into callus shavings and delipidized SC have been proposed as a model to investigate compound binding to COR proteins [Raykar et al., 1988; Surber et al., 1990; Abdulmajed et al., 2004].

1.9 Hydrophilic drug permeation enhancers

To facilitate the permeation of molecules through the SC, chemical permeation enhancers (CPEs) have been extensively studied. To date, more than 350 CPEs have been demonstrated to enhance skin permeability [Karande et al., 2005], including sulfoxides, terpenes, pyrrolidones, laurocapram, fatty alcohols, fatty acids, alcohols such as glycol, urea, and surfactants [Chen et al., 2014]. The different CPEs are very different with respect to their physico-chemical properties and therefore are expected to influence the molecular properties of the SC in various ways [Williams and Barry, 2012].

To be considered as a candidate for a CPE, a chemical compound should meet the following desirable criteria [Williams and Barry, 2012]: (1) it should be nontoxic (should not cause allergic and/or irritation effects) (2) it should work unidirectional, i.e. enhance drug penetration into the skin whilst preventing the loss of endogenous material from the body; (3) it should be cosmetically appliable with a proper skin feel; (4) it should have a rapid but reproducible and predictable effect; (5) upon the withdrawal of CPE from skin, its barrier properties should restore quickly and utterly; (6) it should be compatible with drugs and other excipients in the formulation; (7) it should be colourless and odourless; and (8) it should not have any pharmacological activity. No CPE has yet been developed which possesses all the above-mentioned ideal properties. Despite showing some limitations, a consistent group of chemical compounds has been used over the years safely and effectively in dermal and transdermal drug delivery systems.

The mechanisms of action of CPEs are different based on the nature of the compound. There are four main types of CPEs that can interact with the SC [Williams and Barry, 2012]: (a) CPEs that cause swelling and increase the hydration of SC by denaturing or modifying the conformation of SC keratin; (b) CPEs that affect desmosomes, specialized protein complexes responsible for cohesion between corneocytes; (c) CPEs that lower the barrier resistance of lipid bilayers by affecting lipid domains; (d) CPEs that alter the solvent nature of the SC by affecting the partitioning of active compounds into the tissue. For hydrophilic drug substances, that need to be delivered through the corneocytary pathway, appropriate CPEs should be selected based on the targeted delivery.

CPEs for hydrophilic molecules such as FAAs work by increasing the partitioning property of the drug to the skin or by their interaction with the CORs or keratin. As seen from Eq. 1, partition coefficient (K), diffusion coefficient (D) and drug concentration in the vehicle (C_V) are the parameters that change the rate of drug penetration. Hydrophlic CPEs can penetrate the SC and change its chemical and solvent properties. This allows for the increase of the K value of the drug, co-enhancer and co-solvent into the SC and their increased solubility within the SC [Barry, 2001]. Examples of hydrophilic CPEs include water, N-methyl-2-pyrrolidone, 2-pyrrolidone, dimethylsulfoxide (DMSO), propylene glycol, and transcutol® P.

Water increases the flux of both hydrophilic and lipophilic drugs and hence is one of the very effective natural penetration enhancers. Drug penetration can be increased by a factor of 2-3 when the skin is hydrated [Scheuplein and Blank, 1971; Blank et al, 1984]. The two pyrrolidones, N-methyl-2-pyrrolidone and 2-pyrrolidone, have been investigated for their permeation effect for many years. Both are dissolved in water in all proportions and can enhance the permeation of both hydrophilic and lipophilic compounds [Williams and Barry, 2004]. Propylene glycol is another well-established CPE that has been used as a co-solvent in topical and transdermal products. It mainly increases drug permeation by improving the partition properties of drugs into the SC. It reduces drug-tissue binding by solvating the α-keratin [Barry, 1987].

DMSO is an aprotic solvent that interacts with keratin (like pyrrolidones) when applied in low concentration (20%) [Haque and Talukder, 2018]. Many studies indicate that it is used as a CPE for both hydrophilic and lipophilic compounds. It can improve the drug penetration via a number of mechanisms [Williams and Barry 2004; Lane, 2013]: (a) interactions with keratin, such as changing the intercellular keratin conformation, from α helical to a β sheet, as well as displacement of bound water from keratin; (b) extraction of skin lipids; and (c) interactions with the lipid alkyl chains in the SC. DMSO has small molecular size and it can easily penetrate the region of protein sub-unit [Haque and Talukder, 2018]. It then displaces the protein-water and hampers the native configuration of the protein (by interfering with hydrogen bonding and hydrophobic interactions). This causes the drug/compounds to be become loose or flexible areas to penetrate through the SC. However, skin's impermeable characteristics return to normal immediately after removing DMSO [Barry, 1987]. It passes through the skin very quickly. There is also a gradual removal of protein-DMSO by competitive bonding with cellular water [Barry, 1987]. DMSO can also interact with the polar head groups of lipids, thus destabilizing the regular lipid structure, making it more fluid and less resistant to drug diffusion [Williams and Barry, 2004]. This CPE may also change the solubility properties of SC for the permeant, by affecting the aqueous domain in the lipid bilayers, and hence facilitate drug partitioning from the vehicle into the SC [Williams and Barry, 2004; Lane et al., 2012].

Transcutol® P represents a non-toxic, potent, biodegradable hydrophilic CPE that can significantly enhance skin penetration of different drugs [Nina et al., 2015]. The main mechanism of this CPE to enhance permeation is to increase the partition parameter of the drug into the skin [Haque and Talukder, 2018]. This may be because of the close solubility parameter of transcutol® P with skin (10.62 $(cal/cm^3)^{1/2}$) [Liron and Cohen, 1984]. It has been used in several dermal and transdermal commercial products [Lane, 2013]. Isopropyl myristate is the most common ester investigated as a CPE which has been used in commercial products [Lane, 2013]. It can integrate itself within the lipid bilayers and causes a more fluid structure, facilitating the drug flux [Leopold and Lippold, 1995]. Moreover, a study

by Santos et al. indicates that Isopropyl myristate can increase drug solubility in the SC [Santos et al., 2012].

1.10 Colloidal carrier systems for dermal delivery of peptides

Dermal and transdermal delivery of therapeutic peptides is very difficult mainly because of their physicochemical properties (polarity, size) and several techniques and vehicles have been investigated to improve their percutaneous transit [Goebel and Neubert, 2008]. These include iontophoresis, electroporation, sonophoresis, microneedle system, thermal poration, powder jects, and colloidal systems (such as microemulsions (MEs)).

Many studies demonstrate that carrier systems in the nano-size range such as MEs are able to improve the dermal and transdermal delivery of different pharmaceutical and cosmeceutical actives due to their exceptional skin penetration enhancing capacity [Getie et al., 2005; Goebel and Neubert, 2008; Goebel et al., 2011; Goebel et al., 2012; Heuschkel et al., 2008; Heuschkel et al., 2009; Sahle et al., 2013; Sahle et al., 2014; Sommer et al., 2018]. MEs are thermodynamically stable, optically isotopic, transparent systems of oil, water, and surfactant/co-surfactants mix [De Gennes and Taupin, 1982; Langevin, 1992; Sommer et al., 2018]. They are transparent to slightly opalescent systems with low viscosity (dynamic viscosity < 300 mPa•s), low interfacial tension (close to zero), Newtonian fluid behavior, and can be formed spontaneously without any energy input. They have high solubilization capacity. The essential conditions for the formation of a ME system are the creation of a very low interfacial tension between the oil and the aqueous phase, as well as the existence of a highly fluid interfacial surfactant film which is associated with the oil phase [Schulman et al., 1959; Kreilgaard, 2002]. A single surfactant is not able to create this very low interfacial tension and short chain cosurfactants are added, which can penetrate the amphiphilic interfacial layer and increase its curvature and fluidity [De Gennes and Taupin, 1982; Attwood, 1994].

According to the major components, MEs appear in different microstructures. They are categorized as water-in-oil (w/o) or oil-in-water (o/w) MEs. MEs with droplet size of less than 150 nm can be formed with such systems [Sommer et al., 2018]. This results in the term “ME” generating some confusion as to the characteristics of these systems. If the system contains similar amounts of water and oil, a bicontinuous structure can be observed with continuous domains separated by surfactant-rich interfaces. The most frequent emulsions applied in pharmaceutics are o/w [Lopes, 2014]. Additionally, o/w emulsions are the most appropriate for topical application, as they allow the penetration of hydrophilic substances through the SC of the skin.

MEs are suitable carrier systems for the dermal delivery of peptides. This could be due to their high solubilization capacity for both lipophilic and hydrophilic drugs in addition to thermodynamic stability and ease of preparation [Goebel and Neubert, 2008; Sommer et al., 2018]. Some studies indicate

that MEs have been used as carrier systems for biologically active peptides [Getie et al., 2005; Goebel and Neubert, 2008; Neubert et al., 2018]. Hence these carrier systems can also be used for the delivery of FAAs into and through the SC.

As stated in section 1.6, the level of NMFs including FAAs can decline in dry skin conditions due to many disease conditions such as atopic dermatitis, ichthyosis vulgaris, psoriasis, environmental conditions, and age [Verdier-Sévrain and Bonté, 2007; Kwan et al., 2012; Takada et al., 2012]. The treatment option for such a condition involves the delivery of the major components of the NMF (FAAs) into the human skin [Arezki et al., 2017]. Hence, designing these compounds in the form of MEs and MEBHGs can be considered as one way to overcome such health problems.

1.11 Analytical methods for the analysis of FAAs

The quality, safety, and efficacy of products loaded with FAAs should be ensured after formulating the colloidal preparations. In line with this, a rapid, selective, and accurate method for the simultaneous analysis of the different FAAs in different formulations is of broad interest in the cosmeceutical and/or pharmaceutical sector. Several methods have been described for the determination of FAAs, including capillary electrophoresis, cation-exchange chromatography, gas chromatography (GC), high-performance liquid chromatography (HPLC), and liquid chromatography-mass spectrometry (LC-MS/MS) [Bidlingmeyer et al., 1984; Hsieh and Chen, 2007; Mustafa et al., 2007; Zhao et al., 2012; Hussain et al., 2019]. Among the available methods, the combination of pre-column derivatization followed by chromatographic separation by HPLC is the most convenient approach [González-Castro et al., 1997; Kriukova et al., 2018]. The determination of the concentration of compounds by this technique requires derivatization into derivative molecules that fluoresce or absorb in the ultraviolet-visible (UV-Vis) wavelength range. Several reagents including but not limited to phenylisothiocyanate (PITC) [Shi et al., 2013], o-phthaldialdehyde (OPA) [Dai et al., 2014], 9-fluorenylmethyl chloroformate (Fmoc-Cl) [Shangguan et al., 2001; López-Cervantes et al., 2006], naphthalene dicarboxaldehyde (NDA) [Manica et al., 2003], 5-dimethylamino-1-naphthalenesulfonyl chloride (dansyl-Cl) and 4-dimethylaminoazobenzene-4-sulfonyl chloride (dabsyl chloride) [Kang et al., 2006], 2,4-dinitrofluorobenzene (DNFB) [Zhang et al., 2012], and 6-aminoquinolyl-N-hydroxysuccinimidylcarbamate (AQC) [Palace et al., 1999] have been used for this purpose.

Each of the above-mentioned derivatizing reagents has its drawbacks. PITC derivatization causes in hydrolysis and there is by-products that interfere with the analyte of interest [González-Castro et al., 1997]. This derivatization technique has poor sensitivity. Moreover, the derivatization process itself and removal of excess solvent are time-consuming. There is high solvent consumption, and the analysis time is time is long when the AQC is used for derivatization [Mayer and Fiechter, 2013]. OPA

and NDA are not able to derivatize secondary amino acids such as Pro and hydroxyproline; and the resulting AA derivatives are unstable, especially with OPA [Dai et al., 2014, Zhang and Sun, 2004]. Dansyl chloride reacts with both OH and NH_2 groups and it lacks selectivity [Kang et al., 2006]. In addition to this, the derivatization with this reagent is slow and the resulting derivatives have poor stability.

On the other hand, use of Fmoc-Cl as derivatizing agent has been commonly used due to its unique benefits. The derivatization is done at room temperature, requires very short time, and the resultant derivatives are very stable [Haynes et al., 1991]. This reagent rapidly reacts quantitatively with both primary and secondary amino compounds in mild alkaline buffers [Bank et al., 1996]. Moreover, the resulting derivatives have high sensitivity in the UV region [Catrinck et al., 2014]. Hence, such derivatization techniques can be used for the determination of the content of FAAs during assay and skin permeation studies in cosmeceutical and/or pharmaceutical preparations.

Despite Fmoc-Cl based techniques are frequently reported, the available methods have several drawbacks with respect to fulfilling method requirements and their applicability in sectors such as cosmeceutical and/or pharmaceutical industries where there is a strict regulatory requirement. The available methods are mainly applicable to determine the concentration of FAAs in biological matrixes (e.g., plant extracts). The reported methods are time-consuming and require excessive material/resources. Moreover, the common limitation of the reversed-phase -HPLC (RP-HPLC) method for the analysis of FAAs, namely difficulty of separation/resolution from the solvent peak and among the analyte peaks, and poor retention of polar amino acids on the RP columns is still the major problem and needs further investigation. Hence, there is an ongoing demand for a rapid, selective, and accurate analytical method for the simultaneous analysis of FAAs in pharmaceutical and/or cosmeceutical industries.

1.12 Aim of the study

FAAs, the major constituents of the NMFs, are very important for healthy skin. The reduction and/or lack these and other NMF components causes various SC abnormalities that manifest clinically as areas of dry skin with flaking, scaling, or even cracking [Marstein et al., 1973; Horii et al., 1989; Denda et al., 1992; Harding et al., 2000; Watkinson et al., 2001]. The NMF components including FAAs is essentially absent in skin conditions such as psoriasis and ichthyosis [Harding et al., 2000; Sybert et al., 1985]. It reduces significantly in other diseases such as AD [Palmer and Irvine, 2006; Kezic et al., 2011] and xerosis [Jacobson et al., 1990]. The content of FAAs can also be decreased substantially due to bathing and exposure to UV light [Rawlings and Harding, 2004]. Moreover, the FAA content of the SC can be dramatically reduced due to aging [Jacobson et al., 1990]. Studies also show that there is a significant correlation between the hydration of the skin and its FAA content [Horii et al., 1989]. All

these reports indicate that the skin can be susceptible to different disease conditions if the concentration of the FAAs in the SC is absent or reduced significantly. The formulation strategy to overcome such disease condition is to deliver these compounds into the appropriate site(s) within the skin. As the majority of the above skin diseases are due to abnormal desquamation, the dermal administration of the FAAs can be considered as treatment strategy for such conditions, and to the best of our knowledge, no studies have been done on this area.

Even though FAAs can be sourced from synthetic, enzymatic, or biotech-based sources, they can also be obtained from natural products. This has significant economic and therapeutic advantage especially in resource constraint countries like Ethiopia. To date, however, little effort has been made to investigate the FAAs content of Ethiopian plants and fungi so as to deliver them into the SC. Thus, the FAA content of selected natural products should be investigated to know if the required FAA mixture could be obtained from a single source. After appropriate natural sources are identified, the FAAs separation and purification method should also be optimized.

The delivery of the FAAs into and through the SC is very challenging due to the hydrophilic nature of the molecules and structural complexity of SC. To our knowledge, there are no reports on the skin partitioning and permeation characteristics of the FAAs. Furthermore, much work is not yet conducted whether the mathematical models could predict the permeation properties of FAAs or not. Hence, the $K_{COR/W}$ should be investigated in selected skin types. The effect of different factors including CPEs on the $K_{COR/W}$ should also be investigated. In addition to this, the permeation properties of the FAAs (K_P values) should be studied. The applicability of the most common mathematical models for the prediction of the skin permeation of FAAs should also be investigated.

Finally, the transport of FAAs across the various skin layers after topical application of FAA-based formulations hasn't yet been investigated. Besides, to the best of our knowledge, to date, there is no study suggesting the best formulation strategy for the delivery of FAAs into and across the SC of the skin. Therefore, further studies are needed to provide supporting evidence for the skin health benefits of topically delivered FAAs. In line with this, there is no reported HPLC method for the simultaneous analysis of the FAAs in topical formulations, Therefore, a simple, selective, and accurate HPLC method should be developed and validated for the assay and *ex vivo* permeation studies.

In general, this PhD research will attempt to address the following four research questions that have emanated from the aforementioned research gaps.

1. Which Ethiopian plants and fungi are endowed with considerable amount of FAAs?
2. How can FAAs be quantified in topical formulations during permeation and assay studies?
3. Which permeation pathway is suitable for the topical application of FAAs?

4. What is the best formulation strategy to deliver FAA into and through the SC of the skin?

This study, therefore, aims at preparing and characterizing colloidal formulations loaded with plant based and chemical synthetic FAAs for dermal delivery. To address the four main research questions specified above, the following specific objectives were set:

1. Analysis of FAA content of selected Ethiopian plants and fungi using LC-ESI-MS/MS method.
2. Development and validation of RP-HPLC/DAD method for simultaneous analysis of 18 FAAs in topical formulations.
3. Study the $K_{COR/W}$ and K_P of the FAAs using appropriate skin models.
4. Prepare and characterize different colloidal preparations (MEs, MEBHGs).

CHAPTER 2: OVERALL PUBLICATION SUMMARY

The dissertation was prepared based on the data obtained from four manuscripts (two published and two submitted for publication). Each manuscript/publication is directly related to the PhD research focus/topic (as described in section 1.12).

The first publication involved on the investigation of the FAA contents of selected Ethiopian plant and fungus species. A total of 59 different plant species and mushroom were included in the study and the concentrations of 27 FAAs were analyzed using a sensitive LC-ESI–MS/MS method. All the 27 FAAs were detected at different concentrations in most of the investigated samples indicating that the desired FAAs can be extracted from a single natural resource.

The second publication was on the validation of a rapid, reliable, and appropriate RP-HPLC/DAD method for the simultaneous determination of 18 FAAs. The samples were derivatized with Fmoc-Cl and chromatographic separation was performed on InfinityLab Poroshell 120 E.C 18 (3 x 50) mm, 2.7 µm column at 25 ^{0}C. Mobile phase consisting of water and acetonitrile adjusted to appropriate pH was pumped in gradient mode at a flow rate of 0.7 mL/min. The analytical method was linear over the concentration range of 5-80 µM with a $R^2 > 0.995$. The HPLC/DAD method was sensitive, precise, accurate, and robust.

The third submitted manuscript deals with permeation characteristics of FAAs through the corneocytary pathway. Appropriate skin model systems and critical parameters were selected and investigated. The COR-water uptake coefficients ($K_{COR/W}$) and corneocyte permeation coefficient ($K_{P(COR)}$)) of the selected FAAs were studied. The effect of different factors including hydrophilic CPEs was assessed. The results indicated that FAAs are suitable candidates for the corneocytary pathway. The $K_{COR/W}$ values of the human COR and that of pig ear skin were better correlated. The permeation studies indicated that the available mathematical models under-predicted the skin diffusion/permeation of the FAAs suggesting the need for new mathematical models.

The fourth submitted manuscript was on the preparation and characterization of different colloidal and standard preparations loaded with FAAs. MEs, MEBGs, and H-Cream were prepared and characterized (for physico-chemical, particle, *ex vivo* permeation, and toxicity). The results indicated that FAAs could not permeate into deeper layers of the SC from a conventional hydrophilic cream. They permeated into the deeper layers of the SC from the MEs and MEHGs indicating that colloidal carrier systems are convenient for the delivery of FAAs.

The author list and the title of the 2 published and 2 unpublished manuscripts is as list below.

1) Birhanu Nigusse Kahsay, Jörg Ziegler, Peter Imming, Tsige Gebre-Mariam, Reinhard H. H. Neubert. Lucie Moeller* (2021). Free amino acid contents of selected Ethiopian plant and fungi species: a search for alternative natural free amino acid sources for cosmeceutical applications. Amino Acids (2021) 53:1105–1122. https://doi.org/10.1007/s00726-021-03008-5
2) Birhanu Nigusse Kahsay, Lucie Moeller, Peter Imming, Reinhard H. H. Neubert* & Tsige Gebre-Mariam* (2022). Development and Validation of a Simple, Selective, and Accurate Reversed-Phase Liquid Chromatographic Method with Diode Array Detection (RP-HPLC/DAD) for the Simultaneous Analysis of 18 Free Amino Acids in Topical Formulations. Chromatographia volume 85, pages 665–676. https://doi.org/10.1007/s10337-022-04160-0
3) Birhanu Nigusse Kahsay, Lucie Moeller, Johannes Wohlrab, Reinhard H.H. Neubert, Tsige Gebre-Mariam (2022). Corneocytary pathway across the stratum corneum. Part III: Identification of model systems and parameters to study dermal delivery of free amino acids (manuscript submitted to "Skin Pharmacology and Physiology").
4) Birhanu Nigusse Kahsay,Sophie Luise Meiser, Johannes Wohlrab, Reinhard H.H. Neubert, Peter Langguth (2023). Delivery of free amino acids into and through the stratum corneum of the skin using microemulsions and microemulsion-based hydrogels: Formulation, characterization, and ex-vivo permeation studies (manuscript submitted to journal of "die Pharmazie").

The introduction part for each manuscript was emanated from chapter one of this dissertation. The materials section (3.1) was combined for all the four manuscripts to avoid repetitions. The methodology, results, discussion, and conclusion parts are as shown in the following sections (chapter 3-5). Figures, Tables, and chapters of the publications are re-numbered. The results and discussion section which were merged together in the published manuscripts are now separated into the corresponding sections (chapter 4 and 5). The abstract and conclusion parts are merged for all the research topics to make an overall abstract (as shown at the beginning of this dissertation) and conclusion (chapter 6) respectively. The author's contribution for each manuscript is mentioned in the first parts of the results section of each research topic (chapter 4).

CHAPTER 3: MATERIALS AND METHODS

3.1. Materials

The plants and fungi species were collected from Gullele Botanical Garden and local supermarkets found in Addis Ababa, Ethiopia. All the L-amino acid standards (L-Ala, L-Cys, L-Ser, L-Pro, L-His, L-Cit, L-Gly, L-Orn, L-Thr, L-Trp, L-Arg, L-Met, L-Asp, L-Glu, L-Asn, L-Gln, γ-aminobutyric acid (GABA), L-Leu, L-Ile, L-Val, L-Phe, L-Lys, O-acetylserine, oxyproline, methionine oxide, taurine (Tau), and L-Tyr) were purchased from Sigma-Aldrich (St. Louis, USA). Norvaline, n-pentane, sodium borate, boric acid, 9-fuorenylmethoxycarbonyl chloride (Fmoc-Cl), sodium hydroxide, Brij O10, 2-phenoxyethanol, triethanolamine, Transcutol® P, and AmberLite™ XAD™16N Polymeric Adsorbent were also commercial products from Sigma-Aldrich Chemie GmbH (Steinheim, Germany). Chromabond® Multi 96 filter plates and Chromabond® Sorbent HR-X were from Macherey–Nagel (Düren, Germany). Chloroform and 1-Adamantanamine (ADAM) were sourced from Thermo Fischer Scientific (Heysham, United Kingdom). Carbopol® 934 was obtained from SERVA Electrophoresis GmbH (Heidelberg, Germany). Ultrapure water (resistivity 18.2 MΩ) purified by TKA X-CAD ultrapure water purification system (Thermo Fisher Scientifc, Waltham, MA, USA) was used at all steps where water was required except for the HPLC analysis. HPLC grade water, acetonitrile, and methanol were commercial products of Fischer Chemical (Loughborough, UK). Analytical grade glacial acetic acids, triethylamine, dimethyl sulphoxide (DMSO), N-methylpyrollidone (NMP), and phosphate-buffered saline (PBS) originated from Carl Roth GmbH + Co. KG (Karlsruhe, Germany). Propylene glycol (PG) was sourced from Caesar and Loretz GmbH (Hilden, Germany). 2-Pyrrolidone (Soluphor® P) was purchased from BASF (Ludwigshafen, Germany). The enzymes dispase II and trypsin were purchased from Sigma-Aldrich Chemie GmbH (Steinheim, Germany). The pig ear skin samples were obtained from a local pig slaughterhouse and the PHSC was sourced from a local cosmetic foot salon. Keratin particles were obtained from Skinomics GmbH. Isopropyl myristate and Poloxamer P407 were sourced from Caesar and Loretz GmbH (Hilden, Germany). D-Squame stripping discs were purchased from CuDerm (Dallas, TX, USA). Pig ear was obtained from local pig slaughterhouse in Halle/Saale, Germany.

3.2. Free amino acid contents of selected Ethiopian plant and fungi species: a search for alternative natural free amino acid sources for cosmeceutical applications

The analysis of FAAs was conducted as per the method reported elsewhere [Ziegler et al. 2019]. The procedure is briefly described in the following sections.

3.2.1. Sample extraction

Each sample was collected in triplicate and the collected samples were freeze dried (Alpha 2–4-LSC, Martin Christ Gefriertrocknungsanlagen GmbH, Germany). Five milligrams (5 mg) of each of the

lyophilized samples was weighed using dual range analytical balance (Model XA105, Mettler Toledo, USA) and transferred to a 2 mL Eppendorf tube. A steal bead of 5 mm in diameter was inserted to each Eppendorf tube and the samples were pulverized in a mixer mill (Model MM 301, Retsch GmbH, Germany) at 25 s^{-1} for 50 s. Two hundred microliters (200 µL) of extraction solvent [a mixture of water and 10 mM norvaline (1 mL: 5 µL)] was added to each sample and the samples were mixed thoroughly for 20 min on a vortex (JK Janke and Kunkel IKA, model IKA VIBRAX-VXR). The samples were then centrifuged (Model 5415C, Eppendorf®, Germany) at 10,000×*g* for 5 min and the supernatant was transferred to a 1.5 mL Eppendorf tube. This solution was again centrifuged (Model 5415C, Eppendorf®, Germany) at 10,000×*g* for 5 min and the supernatant was transferred to a new 1.5 mL Eppendorf tube. This solution was stored in deep freezer at − 80 °C until the next process.

3.2.2. Standard preparation

Twenty millimolar (20 mM) stock solution of each amino acid standard was prepared in ultra-pure water. Five microliters (5 µL) of each of the resulting solutions was transferred to a 2 mL Eppendorf tube and the resulting mixture was diluted to 500 µL with the same solvent. Finally, serial standard solutions were prepared for each amino acids and the internal standard to get a final concentration of 0, 2, 4, 8, 16, 64 and 128 pmol/µL after derivatization. These standard solutions were stored in deep freezer until the next step.

3.2.3. Sample derivatization and processing

After thawing at room temperature, 25 µL of the standard and sample solutions were transferred to 1.5 mL Eppendorf tubes. Fifty microliters (50 µL) of 0.5 M sodium borate buffer pH 7.9 and 100 µL 6 mM Fmoc-Cl solution (in acetone) were added to each solution and the resulting mixture was incubated for at least 5 min after mixing. Five hundred microliters (500 µL) of *n*-pentane was added to each solution, mixed thoroughly, centrifuged (Model 5415C, Eppendorf®, Germany) at 10,000×*g* for 1 min and the upper (organic phase) was discarded. This step was repeated two more times. After the last extraction step and removal of the organic phase, the tubes were opened and allowed to stand in a fume hood for evaporation of any residual organic solvent.

3.2.4. Solid-phase extraction

Solid-phase extraction (SPE) was conducted using Chromabond Multi 96-well plate (Macherey–Nagel, Düren, Germany) containing 50 mg/well HR-X-resin (Macherey–Nagel, Düren, Germany). First, the SPE plate was conditioned by 1 mL of methanol followed by 1 mL of water. In this and all subsequent steps, the liquid was passed through the resin by centrifugation at 500×*g* for 5 min using JS5.3 swingout rotor in an Avanti J-26XP centrifuge (Beckman Coulter, Fullerton, CA, USA). 500 µL of 5% (v/v) acetonitrile was added to the sample and standard solutions mentioned in “Sample derivatization and processing”. Then, the resulting solutions were quantitatively loaded onto the SPE plate, washed with 1 mL of water and the flow through was discarded after centrifugation. In the next step, 1 mL of

methanol was added into the 96-deep well plate and eluted to a new block by centrifugation. Finally, the eluates were transferred from the 96-deep well block to 2 mL Eppendorf tubes, and allowed to evaporate under vacuum in an Eppendorf Concentrator (Model 5301, Eppendorf, Hamburg, Germany) at 45 °C for 45 min. Finally, the samples were centrifuged (Model 5415C, Eppendorf®, Germany) at 10,000×*g* for 10 min and the supernatant was transferred to the 96-well plate and the plate was placed in LC–MS/MS auto-sampler.

3.2.5. LC-ESI–MS/MS analysis

Chromatographic separation was achieved using Agilent 1290 liquid chromatography system equipped with Zorbax Eclipse Plus C18 Rapid Resolution HD column (2.1 × 50 mm, 1.8 µm, Agilent). The column temperature was maintained at 30 °C. Gradient elution with solvent A (0.2% v/v acetic acid in water) and solvent B (0.2% v/v acetic acid in acetonitrile) was used as mobile phase at a flow rate of 700 µL/min. Solvent A was held constant at 75% for 0.3 min and decreased to 50% over the next 6.7 min. Then, it was held at 2% over the next 0.7 min and increased to 75% for the next 0.4 min. Ten microliters (10 µL) and 4 µL were injected into the auto-sampler for the sample and standard solutions, respectively.

Detection was done using API 3200 Triple Quadrupole LC–MS/MS system equipped with an ESI Turbo Ion Spray interface, operated in the negative ion mode (AB Sciex). The ion source parameters were set as follows: curtain gas was used at a pressure of 30 psi. The ion spray voltage was − 4500 V and the ion source temperature was set at 350 °C. Both the nebulizing and drying gas pressure were set at 50 psi. Triple quadrupole scans were acquired in the multiple reaction monitoring (MRM) mode with Q1 and Q3 set at “unit” resolution. Scheduled MRM was performed with a window of 90 s and a target scan time of 0.5 s. The mass spectrum (MS) parameters describing the MRMs for each FMOC-Cl derivatized amino acid were as reported by Ziegler et al. [2019].

3.2.6. Data analysis

The data analysis was done by automatic integration using Analyst software. A calibration curve was constructed using the standard solutions and from the graph the slope of the regression line was determined. The concentration (conc.) of each FAA was calculated in nmol/mg from the calibration curve.

3.3. Development and validation of a simple, selective, and accurate reversed-phase liquid chromatographic method with diode array detection (RP-HPLC/DAD) for the simultaneous analysis of 18 free amino acids in topical formulations

3.3.1. Preparation of microemulsion

In this study, Brij O10, Transcutol® P, and isopropyl myristate were used as a surfactant, co-surfactant, and oil phases respectively; and a water solution containing a mixture of the eighteen FAAs was used as the aqueous phase. An appropriate amount of Brij O10, Transcutol® P, and isopropyl myristate were weighed using an analytical balance (Type 870-13, KERN & SOHN GmbH, Germany), transferred to a glass vial, and mixed thoroughly using a magnetic stirrer (Model MR 3001, Heidolph Instruments GmbH & Co. KG Schwalbach, Germany). An aqueous solution containing a mixture of the 18 FAAs was prepared separately and this was slowly added to the surfactant/co-surfactant/oil mixture at room temperature with gentle stirring. The final mixture (that contains the selected FAAs) was gently shaken for complete mixing and stored in glass vials until analysis.

3.3.2. Preparation of standard solutions

Twenty millimolar (20 mM) stock solutions of each of the selected FAAs were prepared in 2-mL Eppendorf tubes using water as solvent. Then, 50 µL of each stock solution was transferred to a 1.5-mL Eppendorf tube and diluted to 1,000 µL with the same solvent to obtain a stock solution of 1 mM. A series of six standard solutions having a concentration of 50, 100, 200, 400, 600, and 800 µM were then prepared by transferring the appropriate volume of the stock solution and diluting with water in separate 1.5 µL Eppendorf tubes. One hundred microliters (100 µL) of each of the standard solutions were transferred to 1.5 mL Eppendorf tubes. Two hundred microliters (200 µL) of 0.5 M sodium borate buffer pH 8.6 and 400 µL 6 mM Fmoc-Cl solution (in acetonitrile) were added to each solution. The resulting solutions were mixed very well and incubated for 10 min for complete derivatization. Three hundred microliters (300 µL) of 12.5 mM Adamantine HCl (ADAM) (in water: acetonitrile, 1:3 v/v) were added to each solution to terminate the reaction. The solutions were mixed again and incubated for another 2 min; centrifuged (Model Mega Star 3.0R, VWR International, LLC, Darmstadt, Germany) at 10,000 x g for 5 min, and the supernatant was transferred to an HPLC autosampler vial. The concentrations of the final standard solutions were in the range of 5-80 µM.

3.3.3. Preparation of sample and placebo solutions

A stock solution of microemulsions containing about 2.5 mg/mL of the respective FAA was extracted using methanol as solvent. The resulting solutions were then filtered through Whatman filter paper No. 42, and 40 µL of the filtrate was further diluted to 200 µL with bi-distilled water. The placebo solutions (formulations without FAAs) were prepared in the same manner. Then, 100 µL of each solution was derivatized as per the procedure mentioned in the standard preparation (starting from the addition of 200 µL of 0.5 M sodium borate buffer pH 8.6).

3.3.4. HPLC chromatographic conditions

The chromatographic apparatus consists of Shimadzu HPLC system (Shimadzu Corporation, Tokyo, Japan) with Solvent Delivery Module LC-40D, Auto-sampler Module SIL-40C, Diode Array Detector Module SPD-40M, Column Oven Module CTO-40C, and System Controller Module CBM-40. Chromatographic separations were carried out on InfinityLab Poroshell 120 E.C 18 (3 x 50) mm, with a particle size of 2.7 µm (Agilent Technologies Germany GmbH & Co. KG, Waldbronn, Germany). Solvent A and solvent B consisted of water and acetonitrile, respectively, and each contained 0.2% glacial acetic acid and 0.1% trimethylamine as pH adjusters. The gradient system was adjusted as follows (time (min), %B): 0/15, 4/15, 7/23, 16/23, 18/38, 21/38, 27/60, 28/15, and 29/15. The auto-sampler temperature was maintained at 4 °C; 10 µL of each sample was injected. The column temperature was maintained at 25 °C and the detection of the derivatized samples was performed using a DAD. The total run time was set at 29 min.

3.3.5. Validation parameters

Before performing the validation activities, method development was conducted to optimize the sample pretreatment, derivatization process, and chromatographic conditions. Robustness of the final experimental setup was also investigated using the "one-factor-a-time" method ("one-variable-at-a-time procedure") [Dejaegher and Heyden, 2007]. Analysis parameters such as pH, composition and flow rate of mobile phase, column temperature, column age, and solution stability were included in the robustness study. The effect of all these deliberate changes on the retention time, tailing factor, theoretical plate numbers (N), repeatability of peak areas, and resolution were studied. After method development, the RP-HPLC/DAD method was validated in accordance with International Conference on Harmonization (ICH) guidelines on validation of analytical procedures [ICH, 2005]. Validation parameters including limit of detection (LOD), limit of quantification (LOQ), specificity/selectivity, linearity, range, accuracy, precision, and robustness were investigated. A system suitability test (SST) was also carried out throughout the validation work.

System suitability test (SST) was conducted using standard solutions at the assay concentration of 20 µM after derivatization. The test was carried out by injecting standard solutions of all FAAs, each at a concentration of 20 µM, in six replicates. Chromatographic parameters such as retention time, peak area, tailing factor, number of theoretical plates (efficiency), height equivalent to the theoretical plate (HETP), tailing factor, and resolution were evaluated to assess the suitability of the HPLC system. The acceptance criteria for %RSD of retention time and peak area in replicate injections was less than 2 and that of tailing factor was less than 2. The limit for efficiency was not less than 2000 and that of HETP was not more than 2. A resolution value of 1.5 or greater between two peaks was taken aa s threshold value to ensure whether the sample components are well (baseline) separated to a degree at which the area or height of each peak may be accurately measured.

The specificity/selectivity of the analytical method was evaluated by analyzing the standard solution, FAA-loaded formulations, and the placebo samples (formulation without the FAAs) at the working concentration of 20 µM. The acceptance criterion for this test was % interference of less than 5 at the retention time of the respective analytes.

The linearity and range were evaluated using standard solutions of the FAAs at concentrations ranging from 5-80 µM. The concentration of each FAA was plotted against its corresponding peak area and linear regression equations were calculated. R^2 values of greater than 0.995 was taken as acceptance criteria for the linearity. The LOD and LOQ parameters were calculated by multiplying the S/Slope ratio by 3 and 10, respectively (where S is standard deviation of the Y-intercepts of the five calibration curves and slope is the mean slope of the five calibration curves), according to the ICH guidelines [ICH, 2005]. This estimate was further confirmed by the independent analysis of real samples prepared at the detection and quantification limits.

The accuracy/recovery of the method was determined by preparing three sample solutions at 50%, 100%, and 150% of the target concentration (20 µM) and calculating the recovery of each analyte as percentage recovery. The overall recovery of 90-110 % was taken as a threshold value for this test.

The precision of the method was determined by measuring the repeatability (intra-day) and intermediate precision (inter-day) of the retention times and peak areas measured for each FAA. The intra-day variability was measured by the same analyst over one day, while inter-day precision tests were carried out by the same analyst at different days using different batches of reagents. The precision was determined by measuring the repeatability of the retention time and peak areas on replicate injections (n = 6) at the sample solutions at the assay concentration (20 µM) and reported as percentage of relative standard deviation (%RSD). The threshold value for precision was % RSD of less than 2 % for both the retention time and peak area.

3.3.6. Application of the method in a routine test

After performing the validation work, the applicability of the method was tested on final topical preparations. In addition to the microemulsion stated in the above section, micro emulsion-based hydrogels were prepared to check its applicability. The microemulsion-based topical hydrogels were prepared using Carbopol® 934 and Poloxamer P_{407} as polymers. A 2 % Carbopol® 934 dispersion was prepared in bi-distilled water, and this was mixed with the already prepared microemulsion (1:1 w/w). Then a few drops of triethanolamine were added to neutralize the resulting solution and form the hydrogel. The Poloxamer P_{407} based hydrogel was prepared using the cold method. The prepared microemulsion was cooled to 4 ^{0}C. Then Poloxamer P_{407} (prepared in water and stored at 4 ^{0}C) was added under continuous mixing while maintaining the temperature at 4 ^{0}C. The final concentration of Poloxamer P_{407} in the hydrogel was 16 % w/w. A few drops of 2-phenoxyethanol were added as a

stabilizer in both preparations. The content of FAAs in the formulations was determined following the final experimental conditions of this method. Each experiment was done in triplicate.

3.4. Corneocytary pathway across the stratum corneum: Identification of model systems and parameters to study dermal delivery of free amino acids.

The experiment was done following standard protocols [Raykar et al., 1988; Surber et al., 1990]. Three skin models, namely, PHSC isolated from adult foot calluses, SC isolated from pig ear skin, and keratin particles isolated from chicken feathers were used. The effect of different variables on the $K_{COR/W}$ was examined. Previously validated HPLC method [Kahsay et al., 2022] was used to determine the concentration of FAAs in the skin partitioning and permeation studies. The detailed procedure is mentioned in the following sections.

3.4.1. Preparation of powdered human stratum corneum

Adult foot calluses were carefully collected from a local beauty salon. The collected skin samples were grounded to powder. To remove the lipid content of the SC, preweighed SC samples were placed in a glass beaker containing 100 mL 2:1 chloroform: methanol and were gently agitated for 24 hr at 25 ^{0}C. The delipidated SC samples were then removed, rinsed twice with fresh chloroform/methanol, and dried. Lipid content was determined by the change in weight of the SC after solvent extraction. The delipidated SC samples (isolated corneocytes) were then used for the partitioning experiment.

3.4.2. Preparation of stratum corneum from pig ear

The epidermis of the pig ear was separated from the dermis following previously reported methods [Kitano and Okada, 1983; Ellison et al., 2020]. Briefly, after removing the subcutaneous tissue with a scalpel, the skin samples were cut into pieces (~1 mm) and each skin sample was stored for up to a maximum of 3 days in phosphate-buffered saline at 4 ^{0}C prior to the experiment. Four techniques were used to loosen the dermal-epidermal junction [Jian et al., 2019 (a-c)]. The first method was heat treatment in water. In this method, the skin sample was submerged in water at 60 ^{0}C for 50 sec. Then the epidermis was gently peeled off from the dermis using forceps. The second technique was heat treatment on the metal where the tissue was sandwiched in aluminum foil and pressed on a slide warmer at 50 ^{0}C for 45 sec. The third method involved the use of Ethylenediaminetetraacetic acid (EDTA) (20 mM Na_2EDTA prepared in 15 mM sodium phosphate buffer in normal saline and adjusted to pH 7.2). The skin sample was then immersed in this solution at 37 °C for 5 hr. The fourth technique involved enzymatic treatment (treatment with dispase II). Dispase powder was reconstituted in Ca^{2+}/Mg^{2+}-free PBS at a final concentration of 10 mg/ml (or about 6–10 µg/ml) This was then diluted to a final concentration of 2 µg/ml with Ca^{2+}/Mg^{2+}-free PBS to provide a dispase digestion solution. The skin sample was then immersed in the diluted dispase II solution at 4 ^{0}C for 24 hr. Finally, the

SC/epidermis layer was gently peeled from the dermis with dissection forceps. The separated sheets were washed with Ca^{2+}/Mg^{2+}-free PBS twice. The thin sheets of SC/epidermis were then placed (dermal side down) on a filter paper soaked with 0.1% trypsin for 24 hr at 4 ^{0}C. After digestion of the epidermal layer, the SC was gently rinsed and then dried at 37 ^{0}C in an incubator. To remove the lipid content of the SC, pre-weighed SC samples were then placed in a glass beaker containing 100 mL 2:1 chloroform: methanol and gently agitated for 24 hr at 25 ^{0}C. The delipidated SC samples (isolated corneocytes) were then removed, rinsed twice with fresh chloroform/methanol, and dried. Lipid content was determined by the change in weight of the SC after solvent extraction.

3.4.3. Preparation of keratin particles from chicken feather

The keratin particles used for the uptake experiment were extracted from poultry feathers as per the method reported elsewhere [Shavandi et al., 2017]. Briefly, raw feathers were thoroughly washed with detergent and rinsed with water and ethanol. They were dried in an oven at 60 °C and cut into small filaments. Then, about 3 g of clean feathers were chemically treated in a Soxhlet device with petroleum ether for 12 hrs to remove the fatty matters, followed by washing with distilled water and drying at room temperature. The pretreated feathers were immersed in 150 mL of a solution containing urea (0.33 mol/L), L-cysteine (100 mmol/L), and Tris (25 mmol/L) at pH 8. The mixture was stirred at 70 °C for 2 h under an N_2 atmosphere. After being filtered, a keratin solution was obtained. The solution was acidified, and the keratin was precipitated with ethanol. Subsequently, the keratin sedimentation was washed five times with distilled water and lyophilized. The extracted keratin particles were used without any modification. The experiments were conducted in triplicate.

3.4.4. Partitioning of FAAs into isolated powdered human stratum corneum

The SC-vehicle partition coefficient ($K_{SC/V}$) of the FAAs (the ratio of the compound concentration in the tissue (per gram of dried tissue weight) and in the vehicle at equilibrium was determined as per previously reported methods with slight modification [Raykar et al., 1988; Surber et al., 1990]. In a typical experiment, 500 µL of the vehicle solution (1 mM) and an accurately weighed, dry skin sample (3—8 mg) were placed in a screwcap borosilicate glass vial, which was capped with a Teflon septum. The vial contents were equilibrated (24 hr), with gentle occasional agitation, for various time intervals at 25 ^{0}C. The experiments were conducted in quintuplicate. At the end of the experiment, the decrease in drug concentration in the vehicle is assumed to be exactly equal to the uptake of the drug by the SC [Raykar et al., 1988; Surber et al., 1990].

The w/w concentration of FAAs in the COR and adjacent solution were determined at equilibrium by calculating the mass of FAAs absorbed in the hydrated COR per 1000mg of dry COR and and mass of FAAs per 1000mg of water respectively. Finally, the $K_{COR/W}$ was calculated from the ratio of the two

w/w concentrations as per Eq. 2 [Nitsche et al., 2006]. The experiments were conducted six times and average results were reported.

$$K_{COR/W} = \frac{\text{Mass of FAAs absorbed in the hydrated COR per unit mass of dry COR}}{\text{Mass of FAAs per unit mass of water in the adjucent solution}} \quad \text{(Eq. 2)}$$

3.4.5. Effects of different factors on $K_{COR/W}$

The effect of factors such as equilibration time, skin model, initial concentration of FAAs, separation technique, delipidation of SC, and penetration enhancer on $K_{SC/V}$ were investigated. Except for the effect of penetration enhancers, the variables were checked using water as a vehicle and the SC-water partition coefficients ($K_{SC/W}$) were determined. To investigate the effect of penetration enhancers on the $K_{COR/W}$ of FAAs, 1mM of the respective FAAs were prepared in water. Then 500 µL of the vehicle solution and an accurately weighed, dry skin sample (3—8 mg) were placed in screwcap borosilicate glass vials, which were capped with a Teflon septum. About 150 µL of the selected chemical penetration enhancer was added. The vial contents were equilibrated, with gentle occasional agitation, for predetermined time intervals at 25 ^{0}C. An aliquot of the vehicle (100 µL) was removed from the vial. Concentrations of the FAAs in the vehicle were then determined and, from this, the concentration in the skin was calculated by subtracting the concentration obtained in the vehicle from the concentration of the standard solution. The concentrations were determined by an RP-HPLC/DAD method and the experiments were conducted in quintuplicate.

3.4.6. RP-HPLC/DAD analysis of FAAs

The concentrations (C_i and C_v) were determined as per a validated RP-HPLC/DAD method [Kahsay et al., 2022]. Briefly, at the end of each experiment, the solutions were centrifuged (Model Mega Star 3.0R, VWR International, LLC, Darmstadt, Germany) at 10,000 x g for 10 min. An aliquot of the vehicle (50 µL) was transferred into a 1.5 ml Eppendorf tube and diluted to 100 µL with water. Two hundred microliters (200 µL) of 0.5 M sodium borate buffer pH 8.6 and 400 µL 6 mM Fmoc-Cl solution (in acetonitrile) were added to each solution. The resulting solutions were mixed and incubated for 10 min for complete derivatization. Three hundred microliters (300 µL) of 12.5 mM ADAM (in water: acetonitrile, 1:3 v/v) were added to each solution to terminate the reaction. The solutions were mixed again and incubated for another 2 min; centrifuged (Model Mega Star 3.0R, VWR International, LLC, Darmstadt, Germany) at 10,000 x g for 5 min, and the supernatants were transferred to an HPLC autosampler vials. The chromatographic apparatus consisted of the Shimadzu HPLC system (Shimadzu Corporation, Tokyo, Japan) with Solvent Delivery Module LC-40D, Auto-sampler Module SIL-40C, Diode Array Detector Module SPD-40M, Column Oven Module CTO-40C, and System Controller Module CBM-40. Chromatographic separations were carried out on InfinityLab Poroshell 120 E.C 18 (3 x 50) mm, with a particle size of 2.7 µm (Agilent Technologies Germany GmbH & Co.

KG, Waldbronn, Germany). Solvent A and solvent B consisted of water and acetonitrile, respectively, and each contained 0.2% glacial acetic acid and 0.1% trimethylamine as pH adjusters. The gradient system was programmed as follows (time (min), %B): 0/15, 4/15, 7/23, 16/23, 18/38, 21/38, 27/60, 28/15, and 29/15. The auto-sampler temperature was maintained at 4 ^{0}C; 10 µL of each sample was injected. The column temperature was maintained at 25 ^{0}C and the derivatized samples was detected with a diode array detector. The total run time was set at 29 min. Calibration curve solutions in the range of 5-80 µM were prepared, derivatized in the same manner, and the concentration of each of the FAAs in the vehicles were calculated from the slope and regression line of the respective calibration curves.

3.4.7. *In vitro* skin permeation of FAAs

Following the separation of the epidermis and dermis parts of the pig ear skin in dispase II solution, the dermis was discarded, and the epidermal membrane floated onto the surface of water and taken up onto a Whatman No.1 filter paper (Whatman International). The resultant epidermal sheets were blotted dry with tissue paper, stored flat, and wrapped in aluminum foil at 4–8 ^{0}C until use. The prepared epidermal sheets were cut into circular discs (1 cm ^{2}). The skin was visually assessed and those samples with the desired integrity were used for the test. The skin samples were then sandwiched between the donor (3 mL) and acceptor (having a volume of 5 mL and an orifice diameter was 9 mm) compartments of Franz cell (SES GmbH Analytical Systems Bechenheim, Germany). Prior to the experiment, the acceptor compartment was filled with water and maintained at 37 ^{0}C and stirred at 600 rpm throughout the experiment. After equilibrating for 30 min, an infinite dose (400 mL) of saturated solutions of the FAAs was introduced to the donor compartment. At appropriate time intervals, 100 µL of the acceptor was withdrawn and immediately replaced by an equal volume of fresh receptor solution at the same temperature (32 ^{0}C) as the receptor chamber. The experiments were conducted under unoccluded conditions for a duration of 24 hr. Acceptor samples were appropriately diluted and analyzed by HPLC as described below. Three replicates from each skin donor were employed in the study for each permeation experiment. Sink conditions (where the concentration of the penetrant in the acceptor does not exceed 20 % of the saturated solubility of penetrant in the vehicle [Akomeah et al., 2004]) were maintained throughout the experiment, to ensure adequate driving force for diffusion is maintained.

The cumulative amount of solute permeating per unit skin surface area was plotted against time and steady-state fluxes (J_{SS}, rates of solute transfer) were derived from the linear portion of the concentration-time profiles in accordance with Fick's law. The experimental permeability coefficient (K_P) which relates the flux to the concentration gradient across the membrane was calculated by normalizing J_{SS} with the saturated solubility of permeant in the donor fluid (C_V). The experiment was conducted in triplicate and the average results were used for the comparison. The K_P values from

mathematical models were calculated using the most commonly used models namely, empirical and mechanistic models. Accordingly, Potts & Guy [1992], Cleek and Bunge [1995], and modified Robinson [Wilschut et al., 1995] models were selected from the empirical models and Mitragotri [2003] model was selected from the mechanistic models. The calculations for the predictive KP values according to these models were done as per the calculations shown in Table 2 (Eq. 3 to 6).

Table 2: Mathematical models for calculating skin permeation coefficient (Kp).

S/N	Model	Calculation of K_P or Log K_P	Eqaution
1	Potts & Guy	$\log K_p(cm/s) = -6.3 + 0.71 \log K_{OW} - 0.006MW$	(Eq. 3)
2	Bunge and Cleek	$\mathrm{Log\ K_p\ (cm/s)} = -6.36 - 0.006\mathrm{MW} + 0.74 \log \mathrm{K_{OW}}$	(Eq. 4)
3	Modified Robinson	$K_p\ (cm/s) = \dfrac{1}{\dfrac{1}{K_{lip} + K_{pol}} + \dfrac{1}{K_{aq}}}$	(Eq. 5)
		Where, $\log K_{lip} = -1.286 + 0.620 \log K_{OW} - 0.159\sqrt{MW}$	
		$K_{pol} = \dfrac{0.0001519}{\sqrt{MW}}$	
		$K_{aq} = \dfrac{2.5}{\sqrt{MW}}$	
4	Mitragotri	$K_P\ (cm/s) = K_P^{fv} + K_P^{lateral} + K_P^{pore} + K_P^{shunt}$	(Eq. 6)
		Where. $\mathrm{Log\ K_P^{fv}\ (cm/s)} = 5.6 + 10^{-6}\ \mathrm{K_{OW}^{0.7}}\ exp(-0.46r^2)$	
		$K_P^{lateral} = 8\ x\ 10^{-10}\ K_{OW}^{0.7}$	
		$K_P^{pore} = 1.2\ x\ 10^{-2}\ exp\ (-1.5r)$	
		$K_P^{shunt} = 2\ x\ 10^{-9}$	

Where, K_P: Permeation coefficient, K_{ow}: Octanol-water partition coefficient, MW: Molecular weight, and r= radius in Å

The octanol-water partition coefficient (log K_{OW}) reported by Waterbeemd et al. [1994] was used in calculating the predicted values. For comparison, the linear correlation coefficient R^2 and the mean absolute errors (MAEs) between the predicted skin permeability and measured data have been computed. MAE between predicted permeability and experimental data was calculated by Eq. 7 [Lian et al., 2008]:

$$\mathrm{MAE} = / \frac{(log\ K_p^{obs} - logK_p^{pre})}{logK_p^{obs}} / \qquad \text{(Eq. 7)}$$

Where $log\ K_p^{obs}$ is the experimental value and $logK_p^{pre}$ is the predicted value.

3.5. Delivery of free amino acids into and through the stratum corneum of the skin using microemulsions and microemulsion-based hydrogels: Formulation, characterization, and ex-vivo permeation studies

3.5.1. Preparation and purification of FAA enriched crude extract:

The extraction and purification process of FAAs from oyster mushroom was standardized and validated. Briefly, samples were collected from local supermarkets in Addis Ababa. Any dirt on the surface of the samples was manually removed and the samples were gently dried in a drying oven at 40 ^{0}C until constant weight. The dried samples were powdered using a mortar and pestle and stored in tightly packed vials until further use. 200 g of the dried samples was mixed with 500 mL of 80% methanol in water and extracted using a magnetic stirring bar at 500 RPM for 6 hours. The samples were then sonicated for another 1 hour and filtered through whatman filter number 1. The residue from the filtration was further extracted with 400 mL of 80% methanol using sonication (1h). The filtered extracts from the two extractions were pooled and the methanol was evaporated under reduced pressure at 40°C. The concentrated mushroom extracts were separated and purified using the pre-treated AmberLite™ XAD™16N resin. The operating conditions were conducted within the recommended operating conditions from the resin manufacturer at room temperature. After conditioning the resin with methanol followed by water (at a rate of 2 bed volume per hour (2 BV/h), 1 BV = 1 m^3 solution per m^3 resin), the crude extract was loaded to the separation and purification column containing the pre-treated AmberLite™ XAD™16N resin (at sample loading rate of 2 BV/h). Then the FAAs were eluted using 80% methanol at an elution rate of 2 BV/h. The fractions which gave positive response to the ninhydrin test were pooled. The methanol was evaporated under reduced pressure at 40°C. Finally, the water extract was freeze dried (Alpha 2–4-LSC, Martin Christ Gefriertrocknungsanlagen GmbH, Germany), transferred to a glass vial and stored at -4 ^{0}C until further study. The yield was 13.40 ± 0.91 w/w on dried basis.

3.5.2. Selection of formulation ingredients

Surfactant: Among others, Brij® O10, a Polyoxyethylene (10) oleyl ether, was selected as surfactant. It has a single polar long POE chain linked to the oleyl group through polyhydric sorbitan and this can promote the permeation of the FAAs to the desired site. Increasing water content in Brij® O10-based MEs increased the ME existence area. Brij® O10 hydrophilic chains are strongly hydrated and connected with hydrogen bonds, allowing the interaction with more water droplets [Podlogar et al., 2004]. These properties make this surfactant to be used in aqueous emulsions to assist in the (trans)dermal delivery of drugs.

Co-surfactant: Transcutol® P is non-irritant, an effective solubilizer and skin penetration enhancer. It has been used for decades in dermal applications without adverse effects being reported [Osborne, 2011]. In our study on the effect of different permeation enhancers on the corneocyte-water partitioning properties of the FAAs, it was found that Transcutol® P has the highest positive effect among the tested corneocyte diffusion enhancers. Hence, due to its unique properties, it was selected as co-surfactant in preparing the MEs.

Permeation enhancer: To deliver the required quantity of FAAs, DMSO was used as additional permeation enhancer. It is one of the first and intensively studied hydrophilic penetration enhancers. It does not disrupt the lipid layer of the SC if used in pharmaceutically and cosmetically relevant concentrations (less than 30%). Hence, the permeation enhancing effect of DMSO for the topical application of hydrophilic drugs appears to be realized via the corneocytes [Mueller et al., 2019].

Oil phase: Isopropyl myristate (IPM) was selected as an oil phase as its usage in the (trans)dermal system has add-on benefit being biocompatible permeation enhancer [Kantaria et al., 2003; Zidan et al., 2017; Furuishi et al., 2019]. Taking into account the above-mentioned specifics, we conjectured that the encapsulation of FAAs in Brij® O10 /Transcutol/ IPM/ water/ DMSO in the form of MEs may result in enhanced permeation of FAAs across the epidermal barrier and can achieve greater dermal bioavailability. It is well documented that O/W MEs have improved permeation as compared to bicontinuous MEs and W/O MEs [Araujo et al., 2010; Cichewicz et al., 2013]. Hence, the MEs were prepared in an O/W ME type.

Gelling agents: The low viscosity of MEs is often considered a limitation for application to the skin. To overcome this problem, their viscosity has been increased with the addition of polymers Carbopol® 934 and Poloxamer® 407.

Active ingredient: The MEs and MEBHGs were prepared using both the standard FAAs containing these FAAs and the FAA enriched extracts. Among the several plants investigated earlier, oyster mushroom was found to be a good alternative source of most of the FAAs [Kahsay et al., 2021]. Hence, FAAs enriched extract was prepared from this fungus (section 2.5.1). The extract contains 18 FAAs (L-Ala, L-Arg, L-Asn, L-Asp, L-Gln, L-Glu, L-Gly, L-His, L-Ile, L-Leu, L-Lys, L-Met, L-Orn, L-Phe, L-Pro, L-Ser, L-Thr, and L-Val). Similar FAAs were incorporated in the standard formulation.

3.5.3. Preparation of MEs and MEBHGs

Oil-in-water MEs loaded with FAAs were prepared by mixing all the components of the ME (Table 3). The oil, surfactant/co-surfactant mixture and hydrophilic phase containing the FAAs were mixed in a glass vial until a clear and homophasic ME is formed. The MEs which contain 18 FAAs were prepared using both the standard FAAs (ME1-ME3) and the FAA enriched crude extracts obtained from oyster

mushroom (ME4). The prepared MEs were stored in glass vials at room temperature. MEBHGs were prepared using two different gelling agents (Carbopol® 934 and Poloxamer 407). Carbopol® 934 based hydrogels were prepared by incorporating Carbopol® 934 to ME1. Then few drops of triethanolamine was added to increase the viscosity. Poloxamer® 407 gels were prepared by the cold method applied to ME1 and ME4. In that process, MEs were first cooled to 4 ^{0}C and then the required amount of Poloxamer® 407 was added slowly with continuous mixing to the ME while the temperature was kept at 4 °C. The final hydrogel was mixed and stored at 4 ^{0}C until a clear hydrogel was formed. A few drops of 2-phenoxyethanol were added to both gels as stabilizer (1% of the total ME gel). The MEBHGs were stored in glass vials protected from light.

Table 3: Composition of different MEs and MEBHGs loaded with FAAs

S/N	Ingredients	Formulation composition (% W/W)						
		ME1	ME2	ME3	ME4	MEBHG1	MEBHG2	MEBHG3
1	Free amino acid standard mixture*	0.5	0.5	0.5	-	0.5	0.5	-
2	Free amino acid mushroom extract**	-	-	-	0.5	-	-	0:5
3	Brij® O10: Transcutol® P (1:1)	26	32	38	26	26	26	26
4	Isopropyl myristate	4	8	12	4	4	4	4
5	Water: DMSO (9:1)	70	60	50	70	70	70	70
6	Carbopol® 934	-	-	-	-	1	-	-
7	Poloxamer 407	-	-	-	-	-	16	16
8	2-phenoxyethanol	-	-	-	-	1	1	1

*The FAA standard mixture contains 18 FAAs (L-Ala, L-Arg, L-Asn, L-Asp, L-Gln, L-Glu, L-Gly, L-His, L-Ile, L-Leu, L-Lys, L-Met, L-Orn, L-Phe, L-Pro, L-Ser, L-Thr, and L-Val). **The mushroom extract contains all the stated FAAs.

3.5.4. Preparation of FAA loaded non-ionic hydrophilic cream

FAA mixture (5 mg) was incorporated into 1 g of non-ionic hydrophilic cream (DAC). The cream is composed of non-ionic emulsifying alcohol (21%), 2-ethylhexyl laureate (10%), glycerol (85%) (4.5%), potassium sorbate (0.14%), anhydrous citric acid (0.07%), and double distilled water (63.79%).

3.5.5. Characterization of MEs and MEBHGs

The physical stability of the MEs was routinely evaluated at ambient conditions by visual inspection of the samples over a period of time (12 months). Any physical change, such as phase separation, turbidity, flocculation of the droplets and/or precipitation of dispersed lipids, was taken as indicators of instability. The isotropicity of the formulation was verified using a cross-polarised light microscope (Zeiss Axiolab Pol, Carl Zeiss MicroImaging GmbH, Jena, Germany) where a clear system that appears as dark background was categorized as ME.

The refractive index of stable MEs was obtained using an Abbe refractometer (Carl-Zeiss, Jena, Germany) at 25 ± 2 ^{0}C. The viscosity of the MEs was measured at 25 ± 0.2 ^{0}C using a rotational viscometer (Anton Paar GmbH, Graz, Austria). The pH values of the samples were evaluated using a digital pH meter (S20-K, Mettler Toledo, Switzerland). Readings were made in triplicate and the average, and the RSD was calculated.

The particle sizes and zeta potentials were determined with the Malvern Instruments Zetasizer Nano ZS by Malvern Panalytical GmbH (Kassel, Germany). For particle size measurements, samples were diluted at 1:10 in water and measured in triplicate with 15 runs each at 25 °C in back scattering mode. The average results and the polydispersibility index (PDI) were calculated. The zeta potential was determined in triplicate by diluting each sample 1:1 in 0.1 x PBS at pH 7.4 (25 °C) with 50 runs per measurement.

Rheological measurements of the gel formulations were carried out at 32 ^{0}C by a rotational viscometer equipped with a cone-and-plate geometry of 25 mm diameter (the cone angle was 1°) (HAAKE RheoStress 1, Thermo Fisher Scientific). All the formulations were subjected to frequency sweep measurements at a fixed deformation amplitude in the LVR (below the critical strain level) by varying the angular frequency (100 to 0.1 rad/s). The storage modulus (G') represents the elastic portion of the viscoelastic behavior, which quasi describes the solid-state behavior of the hydrogel and the loss modulus (G'') characterizes the viscous portion of the viscoelastic behavior, which can be seen as the liquid-state behavior of the sample were evaluated and compared. Steady shear measurements with increasing and decreasing shear rates (hysteresis loops) were also made for each gel formulation. Each measurement consisted of three parts: a stepwise increase in shear rate from 1 s^{-1} to 100 s^{-1} with 21 measurement points, 10 measurement points with a constant shear rate of 100 s^{-1} for 5 seconds each, and finally, a stepwise decrease in shear rate from 100 s^{-1} to 1 s^{-1} with 21 points (with 5 s measurement time for each rate). The yield stress and thixotropic behavior of the gels were evaluated.

The thermodynamic stability of MEs was assessed by the three-step procedure (heating-cooling cycle, centrifugation test and the freeze-thaw cycle) as reported by Shafiq et al. [2007]. In the heating-cooling cycle, the MEs underwent 6 cycles, where they were kept at 40 ± 2 ºC and then at 4 ± 2 ºC for at least 48 hours. For the centrifugation test, the MEs underwent centrifugation at 3,500 rpm for 30 minutes and were scrutinized for any drug precipitation or phase separation or any color/consistency changes. Finally, for the freeze-thaw cycles, the formulations were stored between −25 ± 2 ºC and 25 ± 2 ºC at least for 48 hours. After each test, the MEs were examined for any drug precipitation or phase separation or any color/consistency changes.

3.5.6. Hen's egg test chorioallantoic membrane (HET-CAM)

An *ex vivo* toxicity study of the MEs was carried out as per the HET-CAM [Sahle et al., 2014]. Naturally fertilized chicken eggs (50-60) g of the New Hampshire breed being provided on the day of the laying by the Livestock Research Center of the Martin Luther University of Halle-Wittenberg were used. After transport in polystyrene-coated containers, the eggs were incubated in pallets in an incubator for 8 days at 37 ^{0}C and 55% air humidity. Every 12 hrs, the eggs were turned, except for the last 24 hrs (9th day of incubation). After the end of the breeding phase (10th day of incubation) the eggs were transferred individually into polystyrene coatings, opened and prepared micro surgically at room temperature as described below.

After candling the egg poles with a high-intensity cold light source, a nearly circular hole with a diameter of 1,5 cm was cut near the air chamber into the weaker convex pole of the eggs. The dust caused during the opening was carefully blown off the amnion without any contact using a rubber bellows, and the amnion was wetted with 37 ^{0}C warm saline (0,9% NaCl). After careful dissection with microsurgical cutlery 20-30 minutes after the opening of the eggs and a resting phase in the incubator, the outer egg membrane was removed under a laminar flow hood and the CAM was exposed. Approximately 10-30 % of the prepared eggs were not fertilized and had to be discarded. Only eggs were used for the tests, which had a well-developed vascular network on the CAM. For applications, 300 µL of each ME was administered to 6 eggs in each case not later than 30 min after preparation of eggs. Sterile water (negative control) and 1% sodium lauryl sulphate (SLS) (positive control) were applied on the CAM as reference solutions. In the collection of the scores, first, an observation of the eggs within a total period of 5 minutes (300 s) was carried out. During this period, changes in the CAM according to the following criteria regarding the time of occurrences (irritation score, IS) and their severity at the end of the observation period were documented. Occurrences of bleeding (hemorrhage), i.e., the extravasation of erythrocytes was classified as hemorrhage (H). Vessels being lysed or becoming transparent were classified as lysis of vessels (L). Stagnation of blood flow and signs of intravascular coagulation were classified as coagulation (C).

The calculation of the irritation score (IS) was performed according to the Inter-agency Coordinating Committee on the Validation of Alternative Methods (ICCVAM) criteria using the Eq. 8 [ICCVAM, 2006]:

$$IS = \left(\frac{301 - sekH}{300} x5\right) + \left(\frac{301 - sekL}{300} x7\right) + \left(\frac{301 - sekC}{300} x9\right) \quad \text{(Eq. 8)}$$

Where, IS = Irritation score, sek= seconds until the on-set of the effect, H= hemorrhage, L = Lysis and, C= Coagulation. The following threshold values were defined for the evaluation criteria: IS ≤ 1= no evidence of irritation potential, IS > 1 and ≤ 4= slight irritation potential, IS > 4 and ≤ 9 = moderate

irritation potential and IS > 9 = strong irritation potential. The severity of changes versus the end of the observation period was evaluated using the following criteria: 0= no response, 1= mild reaction, 2= moderate reaction, and 3= strong reaction. The hemorrhage (H) was assigned semi-quantitatively, according to the degree of erythrocyte extravasates, to the following categories: Single capillary bleedings in morphologically intact capillaries were classified as mild, multiple capillary bleedings in morphologically intact capillaries as moderate, and morphologically damaged capillaries with capillary bleedings or mass bleedings as heavy H. Scattered transparent capillary sections were evaluated as light, transparency of all capillaries as moderate and the incidence of complete lysis of vessels as heavy L. Coagulation (C) was assigned semi-quantitatively, according to the degree of coagulation phenomena, to the following categories: Single capillary thrombosis in morphologically intact capillaries were classified as mild, multiple capillary thrombosis in morphologically intact capillaries as moderate, and damaged capillaries with extended segments of capillary thrombosis as heavy C. After the end of the experiments all eggs, were killed during 48 hours in the freezer at -20 ^{0}C and then disposed hygienically in the hospital waste.

3.5.7. *Ex vivo* permeability study

Pig ears obtained from a local slaughterhouse in Halle (Saale), Germany were used for the *ex vivo* permeation study [Salerno et al., 2015]. The pig ears were carefully cleaned with water. The hair from the outer region of the ears was removed and then the skin was carefully separated from cartilage using a scalpel. Subsequently, adipose subcutaneous tissue was removed. Circular pieces of skin (19 mm in diameter, 1.6 mm ± 2 mm in thickness) were punched from the best areas of the separated skin, hermetically sealed in tinfoil, packed in an occlusive polyethylene bag and stored at –20 ^{0}C. Just before the experiment began, skin samples were defrosted at room temperature and the surface was dried using cotton pads, and dermatomed to nominal thickness (ca. ≥ 1 mm), using the manual dermatome or scalpel blades [OECD, 2004]. The experimentally obtained thickness was determined using a digital caliper. All prepared skin samples were punched to 19 mm disks. The outer border of the application area of the excised pig was marked. It was then mounted on unjacketed vertical Franz diffusion cells [Franz and Barker, 1977] (with 3 ml of acceptor volume, 9 mm orifice internal diameter (orifice area of 0.64 cm^2), and a 5 mL receptor volume) (SES GmbH Analysesysteme, Bechenheim, Germany). The receptor compartment was filled with phosphate-buffered saline pH 7.4 and was continuously stirred at 600 RPM throughout the experiment. The temperature of the cell was maintained at 32 ^{0}C using an incubator.

The skin mounted in the cell was allowed to rest for an hour in contact with receptor media before the application of the samples. Twenty milligram (20 mg) of each formulation was applied onto the epidermal skin side and evenly distributed within the application area (0.64 cm^2) and was allowed to permeate for 300 min. A mass balance study was conducted after the 300 min permeation period. The

apparatus was disassembled, the remaining formulation on the skin surface was thoroughly wiped with a cotton swab and transferred to a 2mL Eppendorf tube. One milliliter (1 mL) of methanol was added and the FAAs were extracted; resulting solutions were sonicated for 10 min, centrifuged at 5000 g for 10 min (Centrifuge Mega Star 3.0R, VWR International, LLC, Darmstadt, Germany). The supernatant was transferred to another 2 mL Eppendorf tube and concentrated under vacuum in an Eppendorf Concentrator (Model 5301, Eppendorf, Hamburg, Germany) at 45 °C for 45 min. This sample was labeled **"**swab**"**. After removing the remaining formulation on the surface, the SC was removed by employing the tape stripping method (D-Squame Stripping Discs (CuDerm (Dallas, TX, USA)). Application of the adhesive tape was followed by uniform pressure for a fixed time (225 g/cm^2, 10 s) [Sølberg et al., 2019]. The strips were then removed with a tweezer in a quick uniform movement, following the longitudinal axis of the skin sample. SC was sequentially removed using 30 consecutive strips [Sølberg et al., 2019] applied on the same skin area with a new tape being used for each application. Then the strips were pooled into six 2mL Eppendorf tubes (each containing 5 strips) and each was extracted with 500 µL methanol. The solutions were concentrated under vacuum in an Eppendorf Concentrator (Model 5301, Eppendorf, Hamburg, Germany) at 45 °C for 30 min and the resulting solutions were further pooled to two 2 mL Eppendorf tubes. The pooled samples were further concentrated under vacuum in an Eppendorf Concentrator at 45 °C for 45 min. The resulting solutions were labeled as SC_1 and SC_2. The excess skin around the diffusion area was removed and the viable epidermis was separated from the dermis using a heat method [Zou et al., 2017]. For this, the skin was sandwiched in aluminum foil and pressed on a slide warmer at 50 ^{0}C for 50 s. Then the viable epidermis layer was gently peeled from the dermis with dissection forceps, cut into small pieces, and transferred to a 2 mL Eppendorf tube. This sample was labeled VEP. The remaining dermal part was cut (longitudinal axis) into five equal small pieces with a thickness of about 200 µm and these were labeled DER1-DER5 from the epidermis side to the lower parts of the dermis. The skin pieces were quantitatively transferred to different 2 mL Eppendorf tubes. Five hundred microliter (500 µL) of methanol was added to each sample containing the VEP and DER1-DER5 and the skin samples were mixed thoroughly for 20 min on a vortex (JK Janke and Kunkel IKA, model IKA VIBRAX-VXR). Then a steel ball of 5 mm in diameter was inserted to each of the Eppendorf tubes and the skin samples were homogenized using a mixer mill (Model MM 301, Retsch GmbH, Germany) at 25 cycle per second for 5 min. The homogenized skin samples were centrifuged at 5000 g for 10 min. The supernatants were concentrated under vacuum in the Eppendorf Concentrator at 45 °C for 45 min. Finally, 200 uL of the receptor medium was transferred to 1.5 mL Eppendorf tube, centrifuged at 5000 x g for 10 min, and the supernatant was transferred to another 1.5 mL Eppendorf tube and this was labelled as "receptor". The FAA content in each of the samples taken from the acceptor liquid, surface of the skin, tape stripping and the skin samples were analyzed using an HPLC/DAD method. Each of the concentrated solutions (swab, SC1, SC2, EP+DER1, DER2, DER3, DER4, and DER5) were

reconstituted with 100 µL water. Then each solution (including the permeated part) was derivatized as per the procedure stated in section 3.5.8 (starting from the addition of 200 µL of 0.5 M sodium borate buffer pH 8.6) and analyzed using the HPLC/DAD method [Kahsay et al., 2022].

3.5.8. Assay content of the FAAs in the formulations

Preparation of standard solutions

Twenty milimolar (20 mM) stock solutions of each of the selected FAAs were prepared in 2mL Eppendorf tubes using water as solvent. Then, 50 µL of each stock solution was transferred to a 1.5-mL Eppendorf tube and diluted to 1,000 µL with the same solvent to obtain a stock solution of 1 mM. A series of six standard solutions having a concentration of 50, 100, 200, 400, 600, and 800 µM were then prepared by transferring appropriate volumes of the stock solution and diluting with water in separate 1.5 µL Eppendorf tubes.

Preparation of samples

A stock solution of the formulation containing about 2.5 mg/mL of the respective FAA was extracted using methanol as solvent. The resulting solutions were then filtered through Whatman filter paper No. 42 and 40 µL of the filtrate were further diluted to 200 µL with bidistilled water. Then, 100 µL of each solution was derivatized as per the procedure mentioned in the standard preparation (starting from the addition of 200 µL of 0.5 M sodium borate buffer pH 8.6).

Derivatization

Then 100 µL of each of the standard and sample solutions were transferred to 1.5 mL Eppendorf tubes. Two hundred microliters (200 µL) of 0.5 M sodium borate buffer pH 8.6 and 400 µL 6 mM Fmoc-Cl solution (in acetonitrile) were added to each solution. The resulting solutions were mixed very well and incubated for 10 min for complete derivatization. Three hundred microliters (300 µL) of 12.5 mM Adamantine HCl (in water: acetonitrile, 1:3 v/v) were added to each solution to terminate the reaction. The solutions were mixed again and incubated for another 2 min. Then they were centrifuged (Model Mega Star 3.0R, VWR International, LLC, Darmstadt, Germany) at 10,000 g for 5 min, and the supernatant was transferred to an HPLC autosampler vial.

HPLC chromatographic conditions

The chromatographic apparatus consisted of Shimadzu HPLC system (Shimadzu Corporation, Tokyo, Japan) with Solvent Delivery Module LC-40D, Auto-sampler Module SIL-40C, Diode Array Detector Module SPD-40M, Column Oven Module CTO-40C, and System Controller Module CBM-40. Chromatographic separations were carried out on an InfinityLab Poroshell 120 E.C 18 (3 x 50) mm column, with particle size of 2.7 µm (Agilent Technologies Germany GmbH & Co. KG, Waldbronn,

Germany). Solvent A and solvent B consisted of water and acetonitrile, respectively, and each contained 0.2% glacial acetic acid and 0.1% trimethylamine as pH adjusters. The gradient system was adjusted as follows (time (min), %B): 0/15, 4/15, 7/24, 16/24, 18/45, 21/45, 24/70, 25/15. The auto-sampler temperature was maintained at 4 °C; 10 µL of each sample were injected. The column temperature was maintained at 25 °C and the detection of the derivatized samples was performed using diode array detector. The total run time was set at 26 min.

Calculation

The concentration of each FAA in the different fractions was calculated from the slope and regression line of the respective calibration curves.

CHAPTER 4: RESULTS

4.1. Free amino acid contents of selected Ethiopian plant and fungi species: a search for alternative natural free amino acid sources for cosmeceutical applications

Author:	Birhanu Nigusse Kahsay, Jörg Ziegler, Peter Imming, Tsige Gebre-Mariam, Reinhard H. H. Neubert. Lucie Moeller
Source:	https://doi.org/10.1007/s00726-021-03008-5
Journal:	Amino Acids
Publisher:	Springer
Date:	July 2021
Author contributions:	RHHN, **BNK**, LM, TGM planned the experiments. **BNK** collected the samples and carried out the experiments (JZ and LM have assisted in the LC-MS/MS analysis). **BNK** calculated and analyzed the data. RHHN supervised the project. **BNK** prepared the draft manuscript; JZ, PI, TGM, RHHN, LM reviewed the draft; and **BNK** prepared the final manuscript. All authors have read and agreed to the published version of the manuscript. LM is the corresponding author.

The FAA contents of the different plant and mushroom species included in the present study are shown in Table 4. Evidently, the concentrations are significantly different, and the total FAAs found in the water extracts of the different species tested ranged from 0.86 mg/g (peal of mango, Mangifera indica L.) to 400.01 mg/g (oyster mushroom, Pleurotus ostreatus (Jacq. ex Fr.) P. Kumm.) as calculated on dry basis. All the tested 27 FAAs were found in most of the samples at varying concentrations (taurine (Tau), methionine oxide, O-acetylserine and oxyproline were analyzed but the results are not included in Table 1 as the concentrations were very low).

Oyster mushroom (Pleurotus ostreatus (Jacq. ex Fr.) P. Kumm.), had the highest total FAA concentration as compared to all the tested samples. Among the legume seeds included in the present study, dekoko (Pisum sativum var. abyssinicum (A. Braun) Berger), which obtains a premium price in local markets, contained relatively high amount of total FAAs followed by flaxseed (Linum usitatissimum L.), common bean (Phaseolus vulgaris L.), sunflower seeds (Helianthus annuus L.), soybean (Glycine max [L.] Merr.) (130.91–214.39 mg/g) (Table 4). The other legume seeds investigated were peanuts (Arachis hypogaea L.), fenugreek (Trigonella foenum-graecum L.) and sesame seed (Sesamum indicum L.) with a total FAA content of 73.62, 57.37 and 44.31 mg/g,

respectively. Seeds of Ethiopian oat (Avena abyssinica Hochst.) and teff (Eragrostis tef (Zuccagni) Trotter) were selected and investigated from the cereal products. Ethiopian oat had very low total FAA concentration (4.41 mg/g) while teff had a total FAA content of 162.84 mg/g. The dominant FAAs in teff seeds were Glu, Asp, Asn, Ala, and Lys (11.39–26.61 mg/g).

The edible parts of 14 vegetables were included in the present study and the total FAA content was highest in broccoli (Brassica oleracea var italica Plenck) followed by garlic (Allium sativum L.), Ethiopian onion (Allium spathaceum Steud. ex A.Rich), cabbage (Brassica oleracea var. capitata (L.) Metzg.), Ethiopian mustard (Brassica carinata), black mustard (Brassica nigra L.), Ethiopian potato (Plectranthus edulis (Vatke) Agnew), tomato (Solanum lycopersicum L.), lettuce (Lactuca sativa L.) and carrot (Daucus carota subsp. sativus (Hoffm.) Schübl. & G. Martens) in decreasing order (60.25–291.90 mg/g on dry basis) (Table 4). Among the vegetables, relatively low amount of total FAA was obtained in cucumber (Cucumis sativus L.), pumpkin (Cucurbita maxima Duchesne), coriander (Coriandrum Sativum) and zucchini (Cucurbita pepo subsp. pepo convar. Giromontiina) (11.67–59.89 mg/g). Most of the FAAs were greater than 7.00 mg/g and the dominant FAAs found in broccoli and cabbage were Arg, Asp, and Glu.

Among the fruits and fruit peals included in this study, avocado (Persea americana Mill.) had the highest total FAA content (60.92 mg/g), followed by pineapple (Ananas comosus (L.) Merr), watermelon (Citrullus lanatus (Thunb.) Matsum. & Nakai), papaya (Carica papaya L.), strawberry (Fragaria × ananassa DUCHESNE), banana (Musa acuminata Colla), and mango (Mangifera indica L.) with total FAA contents in the range of 1.72–54.68 mg/g. The peals of banana and mango were also tested but their FAA contents were very low (total FAA concentrations of 4.55 and 0.86 mg/g, respectively).

Spices commonly used in Ethiopian traditional dishes have also promising amounts of FAAs (Table 4). Ginger (Zingiber officinale Roscoe), a plant with diverse biological activities [Zhao et al. 2011], had total FAA content of 248.50 mg/g. The dominant FAAs were Asp, Asn, Ala, Glu and Arg (9.88–83.40 mg/g). Met was found at a very low concentration (0.04 mg/g). Cumin (Cuminum cyminum L.) and black cumin (Nigella sativa L.), which are active reservoirs of numerous bioactive compounds with various therapeutic applications, had total FAA concentrations of 164.20 and 122.07 mg/g, respectively. FAAs such as Arg, Asn, Asp, Glu, Pro, and Ala were the most abundant FAAs in both. Hot peppers (Capsicum annuum L.) and black pepper (Piper nigrum L.) contribute a major share in the Ethiopian spice scenario. The total FAA contents of these plants were 205.68 and 139.35 mg/g, respectively. Free forms of Asn, Ala, GABA, and Asp were found at high concentrations (6.94–54.06 mg/g) in both plants. The remaining spices, namely, rosemary (Salvia rosmarinus SCHLEID.), lemon

grass (Cymbopogon citratus (DC.) Stapf) and cinnamon (Cinnamomum verum J. Presl) had a total FAA contents of less than 81.00 mg/g.

The leaves of some herbs, namely, chamomile (Matricaria chamomilla L.), peppermint (Mentha × piperita L.), Mexican spice basil (Ocimum basilicum L.), rue (Ruta chalepensis L.), and thyme (Thymus vulgaris L. were also included in the present study. Highest total FAAs were found in rue, chamomile, and thyme (110.05–215.83 mg/g) (Table 4). The dominant FAAs in chamomile were Asn, Gln, Asp, Glu, Lys, Arg, and Pro. Mekmeko (Rumex abyssinicus Jacq.), another perennial herb, had a total FAA content of 47.10 mg/g. Among the seven indigenous aloe species included in this study, relatively high total FAA content was obtained in Aloe percrassa Tod., A. tewoldei M.G. Gilbert & Sebsebe and A. ankoberensis M.G. Gilbert & Sebsebe (73.06–76.70 mg/g). The leaves of other plants grown in Ethiopia were also included. Moringa (Moringa oleifera Lam.), a highly valued plant with exceptional nutritional value and array of health benefits, is widely grown in many tropical and subtropical countries. In the present study, the total FAA content of the leaf part of moringa tree was 449.71 mg/g. The dominant amino acids were Asg, Ala, Asp, Glu, Ser, and Leu. Hemp (Cannabis sativa L.) and clove (Syzygium aromaticum (L.) Merr. & L.M. Perry)) had total FAA concentration of 195.01 and 261.29 mg/g, respectively. FAAs such as Asp, Gln, Asn, Glu, Lys, and Tyr were the dominant ones in both.

Table 4: Free amino acid content of different Ethiopian plant and mushroom species

S/N	Plants	Part	Concentration (mg/g)											
			L-Ala	L-Cys	L-Citr	L-Asp	L-Glu	L-Phe	L-Gly	L-GABA	L-His	L-Ilu	L-Lys	L-Leu
1	*Allium sativum* L. (garlic)	Tubers	11.48±0.60	9.03±0.01	5.53±0.30	19.41±0.62	23.3±0.74	4.21±0.49	1.93±0.14	0.53±0.02	6.6±0.95	2.25±0.11	18.93±0.78	4.07±0.30
2	*Allium spathaceum* STEUD. EX A.RICH (Ethiopian onion)	Tubers	5.00±0.51	6.17±0.61	1.05±0.08	13.79±1.59	14.89±1.25	5.69±0.48	1.47±0.21	0.91±0.16	7.86±0.54	4.86±0.48	14.77±1.30	14.06±1.40
3	*Aloe ankoberensis* GILBERT AND SEBSEBE	Leaves	0.74±0.09	5.53±0.53	1.54±0.18	3.05±0.17	1.59±0.13	0.99±0.03	0.03±0.00	0.16±0.01	1.95±0.07	0.38±0.00	18.7±0.02	0.49±1.41
4	*Aloe benishangulana* SEBSEBE & TESFAYE	Leaves	1.08±0.05	0.46±0.04	ND [a]	0.53±0.05	0.93±0.05	0.60±0.07	0.09±0.01	0.88±0.05	0.23±0.03	0.56±0.03	1.21±0.11	0.78±0.06
5	*Aloe debrana* CHRISTIAN	Leaves	0.96±0.15	0.40±0.04	ND [a]	0.28±0.03	0.77±0.07	0.33±0.34	0.10±0.01	0.65±0.10	0.19±0.01	0.44±0.06	0.92±0.19	0.57±0.12
6	*Aloe percrassa* TOD.	Leaves	0.61±0.05	7.15±1.74	1.05±0.39	3.46±1.05	1.34±0.31	1.05±0.03	0.04±0.01	0.3±0.13	2.07±0.07	0.62±0.00	20.82±0.21	0.69±0.43
7	*Aloe pirottae* BERGER	Leaves	0.48±0.07	3.93±0.57	0.18±0.04	1.75±0.44	0.44±0.10	0.8±0.07	0.04±0.01	0.17±0.03	0.89±0.11	0.37±0.00	11.24±0.07	0.54±1.44
8	*Aloe sinana* REYNOLDS	Leaves	0.36±0.09	4.33±2.92	0.46±0.29	2.81±1.85	0.80±0.54	0.7±0.12	0.03±0.01	0.22±0.08	1.31±0.30	0.34±0.00	17.76±0.10	0.58±1.14
9	*Aloe tewoldei* GILBERT & SEBSEBE	Leaves	0.35±0.07	6.30±0.71	1.11±0.83	4.56±0.54	1.38±0.16	0.61±0.11	0.02±0.01	0.27±0.08	1.94±0.72	0.34±0.00	19.18±0.11	0.43±1.35
10	*Ananas comosus* (L.) MERR. (pineapple)	Fruit	1.04±0.46	1.12±0.19	0.06±0.02	4.64±0.26	2.85±0.19	0.83±0.27	0.17±0.00	1.07±0.32	0.62±0.15	0.38±0.15	3.46±0.84	0.85±0.16
11	*Arachis hypogaea* L. (peanut)	Seeds	4.93±0.02	0.86±0.01	0.13±0.00	2.36±0.09	2.10±0.23	7.07±0.13	0.44±0.01	3.05±0.00	0.86±0.02	1.34±0.01	1.45±0.05	3.38±0.01
12	*Avena abyssinica* HOCHST. (Ethiopian oat)	Seeds	0.14±0.23	0.06±0019	0.02±0.06	0.54±1.37	0.42±0.97	0.04±0.38	0.04±0.09	0.05±0.07	0.08±0.74	0.05±0.24	0.11±0.11	0.06±0.28
13	*Brassica carinata* A.BRAUN (Ethiopian mustard)	Seeds	9.13±0.43	4.06±0.58	0.1±0.03	26.23±0.64	26.4±0.37	6.98±0.48	2.22±0.18	16.1±0.86	1.68±0.20	5.3±0.37	3.76±0.29	3.78±0.43
14	*Brassica nigra* L. (black mustard)	Leaves	1.57±0.12	6.24±0.85	0.94±0.09	15.3±0.82	2.71±0.01	2.02±0.58	0.46±0.02	1.68±0.18	1.47±0.71	8.66±3.70	1.30±0.19	8.93±3.70
15	*Brassica oleracea* var *italica* (broccoli)	Leaves	11.79±0.08	9.10±0.42	0.27±0.01	25.06±1.94	21.01±1.73	12.53±0.10	4.61±0.05	3.09±0.05	18.03±3.56	9.78±0.12	8.40±0.21	8.37±0.20
16	*Brassica oleracea* var. *capitata* (cabbage)	Leaves	20.79±1.74	8.60±0.35	0.21±0.03	22.89±1.72	19.57±0.05	3.19±0.03	3.94±0.60	5.85±0.84	8.82±0.41	7.62±0.26	6.62±0.02	8.27±0.40
17	*Cannabis sativa* L. (hemp)	Leaves	2.51±0.18	4.90±0.65	0.73±0.09	17.47±1.7	9.82±0.14	2.89±0.12	0.40±0.02	3.13±0.10	2.13±0.33	1.88±0.32	8.77±0.22	2.57±0.14
18	*Capsicum annuum* L. (hot peppers)	Fruit	19.42±0.64	5.02±0.26	0.91±0.08	10.25±1.33	5.46±0.80	3.76±0.11	1.89±0.11	14.33±1.23	4.28±0.91	4.00±0.10	4.12±0.81	10.86±0.31
19	*Carica papaya* L. (papaya)	Fruit	3.73±0.97	0.74±0.33	0.78±0.01	3.32±0.32	2.17±0.34	0.96±0.19	1.77±0.25	2.72±0.32	0.91±0.11	1.36±0.06	1.08±0.49	1.32±0.69
20	*Cinnamomum verum* J.PRESL (cinnamon)	Bark	0.65±0.41	0.18±0.14	0.08±0.02	0.39±0.25	0.3±0.16	0.25±0.21	0.25±0.07	0.78±0.58	0.65±0.25	0.29±0.19	0.69±0.56	0.67±0.52
21	*Citrullus lanatus* (THUNB.) MATSUM. & NAKAI (watermelon)	Seeds	7.28±0.07	0.89±0.04	0.39±1.08	3.89±0.20	4.39±0.29	0.75±0.03	0.51±0.02	3.7±0.10	1.19±0.08	0.86±0.03	1.39±0.05	1.86±0.05
22	*Citrullus lanatus* (THUNB.) MATSUM. & NAKAI (watermelon)	Fruit	0.10±0.06	0.07±0.01	1.04±0.00	0.17±0.03	0.23±0.11	0.08±0.00	0.05±0.00	0.11±0.04	0.15±0.01	0.09±0.00	0.24±0.00	0.17±0.00
23	*Coriandrum sativum* L. (coriander)	Leaves	0.85±0.03	1.95±0.49	1.92±0.38	15.37±3.00	1.19±0.27	0.97±0.13	0.11±0.01	0.23±0.02	0.79±0.18	0.7±0.00	4.94±0.10	0.52±2.48
24	*Cucumis sativus* L. (cucumber)	Fruit	1.32±0.17	0.28±0.06	0.23±0.05	1.66±0.15	1.38±0.21	0.25±0.02	0.18±0.01	1.03±0.07	0.22±0.06	0.11±0.02	0.40±0.06	0.18±0.03
25	*Cucurbita maxima* Duchesne (pumpkin)	Seeds	0.21±0.07	0.42±0.13	0.09±0.06	2.26±0.81	3.14±0.91	0.39±0.06	0.07±0.02	0.21±0.11	0.54±0.14	0.12±0.00	0.55±0.10	0.13±0.03
26	*Cucurbita pepo* subsp. *pepo* convar. giromontiina (zucchini)	Fruit	2.79±0.43	0.96±0.20	1.54±0.05	10.54±4.61	3.35±1.55	0.87±0.14	0.26±0.06	3.68±0.69	0.72±0.11	0.46±0.07	0.89±0.19	0.46±0.11
27	*Cuminum cyminum* L. (cumin)	Seeds	13.21±0.54	4.40±0.15	0.26±0.02	17.45±1.27	17.44±1.64	5.71±0.29	2.85±0.19	4.69±0.48	6.34±0.24	4.42±0.29	5.09±0.01	4.85±0.74
28	*Cymbopogon citratus* (DC.) STAPF (lemon grass)	Leaves	1.36±0.41	1.97±0.56	0.16±0.09	3.13±0.44	3.52±1.06	1.52±0.24	0.14±0.06	0.74±0.27	1.57±0.61	0.36±0.08	4.13±01.67	0.64±0.14
29	*Daucus carota* subsp. *sativus* (HOFFM.) ARCANG. (carrot)	Tubers	9.33±0.08	1.14±0.46	0.46±0.09	4.7±0.72	5.36±1.30	0.87±0.13	0.58±0.03	3.87±0.39	1.08±0.20	1.01±0.10	1.14±0.02	2.15±0.34
30	*Eragrostis tef* (Zucc.) TROTTER (teff)	Seeds	14.16±0.71	4.30±0.29	0.37±0.01	20.5±1.19	23.77±1.14	4.43±0.26	4.82±0.29	1.04±0.09	5.83±0.24	3.93±0.00	11.39±0.27	4.11±0.48

Table 4 (continued)

S/N	Plants	Concentration (mg/g)											
		Part	L-Ala	L-Cys	L-Citr	L-Asp	L-Glu	L-Phe	L-Gly	L-GABA	L-His	L-Ilu	L-Lys	L-Leu
31	*Fragaria* × *ananassa* DUCHESNE (strawberry)	Fruit	1.01±0.05	0.72±0.06	0.06±0.04	2.97±0.07	1.69±0.10	0.15±0.01	0.08±0.00	0.79±0.04	0.54±0.13	0.09±0.02	0.30±0.04	0.12±0.01
32	*Glycine max* (L.) MERR. (soybean)	Seeds	5.04±0.10	1.32±0.16	0.25±0.07	14.39±1.10	17.31±2.74	2.81±0.38	1.86±	2.66±0.65	8.54±0.60	2.01±0.43	8.65±0.18	3.40±0.47
33	*Helianthus annuus* L. (sunflower)	Seeds	6.36±0.49	3.52±0.04	0.19±0.07	14.34±0.35	9.12±0.39	8.04±0.99	2.75±0.51	0.70±0.10	5.05±0.76	6.52±0.48	5.62±0.80	5.81±0.89
34	*Lactuca sativa* L. (lettuce)	Leaves	0.48±0.03	5.85±2.07	0.24±0.08	13.00±7.53	1.29±0.61	0.48±0.19	0.04±0.01	0.25±0.08	0.71±0.10	0.48±0.00	7.87±0.16	0.59±1.56
35	*Linum usitatissimum* L. (flax)	Seeds	9.92±0.29	3.77±0.20	0.08±0.02	21.47±0.78	14.61±1.19	8.41±0.64	2.92±0.08	0.33±0.09	4.28±0.33	5.68±0.30	9.78±0.57	7.14±1.63
36	*Malus domestica* BORKH. (apple)	Fruit	0.15±0.01	0.03±0.00	ND [a]	0.56±0.09	0.26±0.02	0.01±0.00	0.01±0.00	0.12±0.02	0.02±0.00	0.03±0.00	0.03±0.00	0.02±0.00
37	*Mangifera indica* L. (mango)	Fruit	0.30±0.04	0.04±0.00	0.02±0.01	0.33±0.01	0.23±0.00	0.01±0.00	0.01±0.00	0.13±0.02	0.03±0.01	0.02±0.00	0.05±0.00	0.02±0.00
38	*Mangifera indica* L. (mango)	Peal	0.09±0.00	0.02±0.02	0.01±0.01	0.11±0.00	0.07±0.01	0.01±0.01	0.01±0.00	0.06±0.01	0.02±0.04	0.01±0.01	0.02±0.00	0.01±0.02
39	*Matricaria chamomilla* L. (chamomile)	Flower	2.26±0.13	4.78±0.21	0.46±0.01	7.62±1.15	7.84±1.05	2.81±0.23	0.52±0.09	1.60±0.07	3.86±0.62	2.09±0.24	7.25±0.05	2.31±0.08
40	*Mentha* x *piperita* L. (peppermint)	Leaves	1.00±0.07	1.11±0.07	0.02±0.01	2.69±0.11	0.19±0.02	2.08±0.12	0.20±0.01	0.72±0.04	1.12±0.09	0.37±0.00	0.83±0.04	0.27±0.14
41	*Moringa oleifera* LAM. (moringa)	Leaves	17.73±0.71	14.53±0.71	0.71±0.11	21.91±0.04	18.03±1.07	14.93±1.44	3.20±0.36	10.58±1.15	7.23±0.76	12.5±0.84	13.1±0.38	13.29±1.14
42	*Musa acuminata* COLLA (banana)	Peal	0.11±0.01	0.13±0.01	ND [a]	0.50±0.05	0.23±0.05	0.01±0.00	0.05±0.00	0.29±0.03	0.73±0.18	0.03±0.00	0.12±0.03	0.17±0.01
43	*Musa acuminata* COLLA (banana)	Fruit	0.37±0.06	0.18±0.01	ND [a]	0.54±0.03	0.41±0.11	0.03±0.00	0.05±0.00	0.20±0.04	0.08±0.01	0.03±0.00	0.08±0.00	0.08±0.00
44	*Nigella sativa* L. (black cumin)	Seeds	6.66±0.49	2.41±01	0.17±0.01	9.63±0.62	20.02±0.28	7.51±0.91	1.67±0.09	1.78±0.21	2.36±0.16	2.97±0.12	5.28±0.20	3.79±0.79
45	*Ocimum basilicum* L. (Mexican spice basil)	Leaves	1.59±0.13	1.77±0.12	0.26±0.05	2.41±0.29	0.27±0.01	1.21±0.11	0.20±0.02	1.23±0.08	1.02±0.02	0.54±0.00	2.8±0.03	1.13±0.15
46	*Persea americana* MILL. (avocado)	Fruit	6.94±0.08	1.68±0.08	0.14±0.00	1.81±0.08	2.44±0.32	1.01±0.08	1.38±0.04	20.3±1.07	0.64±0.25	2.09±0.14	3.69±1.01	3.61±0.93
47	*Phaseolus vulgaris* L. (common bean)	Seeds	16.39±0.06	4.46±0.01	0.79±0.01	9.98±0.17	4.56±0.14	3.49±0.04	1.65±0.02	12.48±0.01	3.58±0.22	3.72±0.01	4.2±0.03	7.95±0.03
48	*Piper nigrum* L. (black pepper)	Fruit	6.74±0.48	1.29±0.04	0.10±0.04	54.06±4.26	2.16±0.35	0.89±0.09	0.94±0.11	10.5±0.82	0.93±0.02	0.96±0.02	1.68±0.01	1.16±0.31
49	*Pisum sativum* var. *Abyssinicum* (A. BRAUN) BERGER (decoco)	Seeds	5.79±0.45	6.51±0.07	0.72±0.05	29.74±2.38	28.38±1.23	5.09±0.29	2.79±0.04	3.96±0.46	3.59±0.31	2.88±0.47	9.15±1.16	4.88±0.23
50	*Plectranthus edulis* (VATKE) ANGEW (Ethiopian potato)	Tubers	5.45±0.98	4.26±0.53	0.18±0.03	10.87±0.26	3.31±0.63	8.10±0.86	1.35±0.19	8.88±1.42	2.53±0.26	5.55±0.73	7.13±1.17	4.27±0.66
51	*Pleurotus ostreatus* (JACQ. EX FR.) P.KUMM. (oyster mushroom)	Fruit body	18.47±0.76	23.42±0.38	0.84±0.13	20.62±9.39	35.65±6.26	19.6±0.12	4.27±0.31	1.38±0.02	26.38±2.36	13.39±0.21	26.19±02.78	17.13±0.15
52	*Ruta chalepensis* L. (rue)	Leaves	12.71±0.36	7.45±0.46	0.25±0.02	10.73±0.71	4.64±0.40	9.01±0.62	2.41±0.04	6.1±0.26	4.64±0.16	6.45±0.35	8.10±0.39	7.51±0.15
53	*Rumex abyssinicus* JACQ. (mekmako)	Leaves	1.11±0.15	1.83±0.13	0.07±0.02	2.40±0.26	4.13±0.58	1.29±0.11	0.24±0.03	5.8±0.27	2.35±0.22	1.71±0.16	2.04±0.12	1.43±0.11
54	*Salvia rosmarinus* SCHLEID. (rosemary)	Leaves	4.63±0.29	0.83±0.06	0.12±0.04	2.84±0.25	2.42±0.26	7.9±0.25	0.52±0.07	3.49±0.59	1.11±0.35	1.52±0.22	1.78±0.23	4.21±0.37
55	*Sesamum indicum* L. (sesame)	Seeds	3.61±0.02	1.06±0.01	0.35±0.01	1.88±0.06	2.98±0.07	1.19±0.02	0.47±0.00	4.34±0.01	1.18±0.04	1.04±0.01	2.37±0.02	2.65±0.03
56	*Solanum lycopersicum* L. (tomato)	Fruit	2.77±0.16	1.61±0.49	0.51±0.04	26.18±3.68	25.65±3.46	4.46±0.55	0.24±0.03	5.74±0.86	4.62±0.44	1.02±0.21	3.97±0.59	1.11±0.17
57	*Syzygium aromaticum* (L.) MERR. & L.M.PERRY (clove)	Flower	15.67±0.01	6.04±0.00	0.45±0.00	8.07±0.02	13.21±0.30	12.77±0.02	3.00±0.00	32.88±0.03	8.87±0.01	10.23±0.01	21.01±0.01	25.71±0.05
58	*Thymus vulgaris* L. (thyme)	Leaves	7.79±0.67	2.90±0.31	3.65±0.19	5.50±0.42	4.91±0.45	2.43±0.33	1.08±0.41	4.57±0.38	1.36±0.53	2.61±0.25	2.85±0.55	3.83±0.46
59	*Trigonella foenum-graceum* L. (fenugreek)	Seeds	6.29±0.06	1.69±0.04	0.21±0.02	1.79±0.06	2.56±0.30	0.96±0.11	1.25±0.03	17.97±0.04	0.79±0.14	2.02±0.03	4.02±0.13	3.95±0.24
60	*Zingiber officinale* ROSCOE (ginger)	Tubers	20.77±1.46	4.74±0.00	1.01±0.03	83.40±0.13	20.65±0.80	2.92±0.34	2.83±0.16	9.81±0.29	3.21±0.10	3.7±0.12	6.59±0.11	5.81±0.16
		Min	**0.09**	**0.02**	**0.00**	**0.11**	**0.07**	**0.00**	**0.01**	**0.05**	**0.02**	**0.00**	**0.02**	**0.01**
		Max	**20.79**	**23.42**	**5.53**	**83.4**	**35.65**	**19.6**	**4.82**	**32.88**	**26.38**	**6.26**	**26.19**	**25.71**

Table 4 (continued)

S/N	Plants	Concentration (mg/g)											Total FAA[b]
		Part analyzed	L-Met	L-Asn	L-Orn	L-Pro	L-Gln	L-Arg	L-Ser	L-Thr	L-Val	L-Try	L-Tyr	
1	*Allium sativum* L. (garlic)	Tubers	1.31±0.22	25.31±2.17	4.21±0.34	3.56±0.17	14.66±1.42	16.42±1.33	9.90±0.8	7.60±0.69	5.39±0.29	3.96±0.50	11.00±1.74	**225.09**
2	*Allium spathaceum* STEUD. EX A.RICH (Ethiopian onion)	Tubers	1.76±0.78	24.84±0.34	2.13±0.18	2.14±0.33	10.27±0.60	9.98±0.97	6.02±0.58	5.42±0.64	5.89±0.69	10.26±0.92	22.42±3.24	**188.01**
3	*Aloe ankoberensis* GILBERT AND SEBSEBE	Leaves	0.01±0.10	6.20±0.01	0.35±0.01	0.16±0.00	12.44±0.01	4.01±0.11	2.42±0.07	5.29±0.21	0.45±0.00	0.50±0.03	6.35±0.01	**73.06**
4	*Aloe benishangulana* SEBSEBE & TESFAYE	Leaves	0.02±0.01	0.52±0.01	0.02±0.00	0.50±0.04	1.47±0.10	0.58±0.02	0.35±0.01	0.44±0.03	0.63±0.04	0.20±0.02	0.71±0.05	**12.28**
5	*Aloe debrana* CHRISTIAN	Leaves	0.01±0.01	0.75±0.29	0.09±0.02	0.35±0.03	0.40±0.13	0.43±0.10	0.26±0.06	0.38±0.06	0.50±0.07	0.16±0.04	0.72±0.10	**9.27**
6	*Aloe percrassa* TOD.	Leaves	0.01±0.15	7.58±0.24	0.38±0.04	0.16±0.00	10.21±0.02	3.56±1.16	2.15±0.7	6.26±0.30	0.52±0.00	0.54±0.14	5.68±0.02	**75.91**
7	*Aloe pirottae* BERGER	Leaves	0.00±0.05	4.68±0.11	0.23±0.02	0.11±0.00	3.85±0.01	2.01±0.14	1.21±0.08	3.72±0.12	0.34±0.00	0.52±0.05	2.16±0.06	**39.40**
8	*Aloe sinana* REYNOLDS	Leaves	0.00±0.24	7.01±0.30	0.54±0.07	0.12±0.00	5.92±0.05	3.19±1.26	1.93±0.76	3.94±1.23	0.35±0.01	0.31±0.17	3.64±0.07	**56.86**
9	*Aloe tewoldei* GILBERT & SEBSEBE	Leaves	0.00±0.01	6.10±0.05	0.47±0.10	0.13±0.00	15.3±0.05	3.80±0.75	2.29±0.46	6.14±0.46	0.36±0.00	0.34±0.12	5.45±0.09	**76.70**
10	*Ananas comosus* (L.) MERR. (pineapple)	Fruit	0.19±0.07	20.14±6.48	0.12±0.01	0.28±0.09	5.04±3.65	4.55±0.98	2.74±0.59	1.30±0.42	0.54±0.14	0.15±0.03	2.72±0.50	**54.68**
11	*Arachis hypogaea* L. (peanut)	Seeds	0.03±0.01	26.75±0.18	0.48±0.00	0.60±0.02	4.80±0.02	1.89±0.02	1.14±0.01	0.84±0.01	1.65±0.01	0.74±0.01	7.84±0.01	**73.62**
12	*Avena abyssinica* HOCHST. (Ethiopian oat)	Seeds	0.00±0.04	0.80±2.81	0.01±0.13	0.09±1.09	0.26±2.96	0.11±0.58	0.07±0.35	0.04±0.28	0.05±0.44	0.25±0.76	0.22±0.69	**4.41**
13	*Brassica carinata* A.BRAUN (Ethiopian mustard)	Seeds	2.00±0.03	22.67±2.12	0.11±0.01	2.79±0.45	2.01±0.22	7.83±0.42	4.72±0.25	4.29±0.12	4.86±0.79	4.69±0.16	4.26±0.47	**161.05**
14	*Brassica nigra* L. (black mustard)	Leaves	1.75±0.39	0.77±0.43	1.33±0.71	0.01±0.00	0.53±0.08	5.28±1.64	3.19±0.99	12.69±0.03	0.03±0.01	2.93±0.44	0.70±0.06	**80.35**
15	*Brassica oleracea* var *italica* (broccoli)	Leaves	5.20±0.68	25.53±0.27	2.46±0.44	20.58±0.36	27.01±0.94	14.35±0.3	8.65±0.18	7.59±0.25	12.25±0.27	7.42±0.13	21.86±1.92	**291.90**
16	*Brassica oleracea* var. *capitata* (cabbage)	Leaves	0.92±0.32	23.08±0.31	0.60±0.03	19.4±2.89	32.10±1.47	20.5±2.57	12.37±01.55	7.75±0.88	10.16±1.28	1.89±0.43	11.24±1.07	**248.81**
17	*Cannabis sativa* L. (hemp)	Leaves	0.04±0.01	9.12±1.11	0.30±0.01	0.84±0.10	11.03±1.67	4.46±0.55	2.69±0.33	4.75±0.66	2.44±0.08	1.53±0.13	9.64±0.85	**102.33**
18	*Capsicum annuum* L. (hot peppers)	Fruit	0.12±0.09	30.38±3.08	0.98±0.24	2.92±0.08	27.22±1.7	13.37±0.02	8.07±0.01	5.59±0.52	4.79±0.06	2.11±0.03	4.06±0.81	**205.68**
19	*Carica papaya* L. (papaya)	Fruit	0.10±0.05	5.50±0.23	1.10±0.43	1.80±0.33	0.35±0.16	3.71±0.01	2.24±0.00	0.87±0.01	0.77±0.002	0.32±0.09	1.18±0.49	**37.77**
20	*Cinnamomum verum* J.PRESL (cinnamon)	Bark	ND [a]	2.14±2.47	0.46±0.08	0.17±0.07	1.00±1.09	1.11±0.48	0.67±0.29	0.24±0.15	0.16±0.14	0.12±0.10	1.02±0.57	**12.12**
21	*Citrullus lanatus* (THUNB.) MATSUM. & NAKAI (watermelon)	Seeds	0.03±0.00	8.49±0.03	0.67±0.04	0.57±0.06	6.43±0.27	2.54±0.05	1.53±0.03	0.88±0.04	1.02±0.02	0.14±0.01	1.38±0.06	**50.21**
22	*Citrullus lanatus* (THUNB.) MATSUM. & NAKAI (watermelon)	Fruit	0.01±0.00	0.26±0.37	0.03±0.00	0.07±0.00	0.52±0.06	0.26±0.04	0.16±0.03	0.07±0.02	0.08±0.00	0.05±0.02	0.19±0.00	**4.20**
23	*Coriandrum sativum* L. (coriander)	Leaves	0.01±0.14	0.90±0.07	0.35±0.02	0.12±0.00	1.58±0.02	2.34±0.37	1.41±0.22	3.62±0.27	0.89±0.00	0.46±0.14	1.94±0.08	**42.70**
24	*Cucumis sativus* L. (cucumber)	Fruit	ND [a]	0.50±0.33	0.09±0.01	0.13±0.02	0.83±0.52	0.99±0.07	0.60±0.04	0.30±0.05	0.13±0.02	0.12±0.03	0.64±0.03	**11.67**
25	*Cucurbita maxima* Duchesne (pumpkin)	Seeds	0.01±0.01	1.19±0.45	0.11±0.03	0.06±0.02	1.39±0.66	0.58±0.22	0.35±0.13	0.24±0.05	0.12±0.02	1.76±0.5	1.38±0.62	**16.11**
26	*Cucurbita pepo* subsp. *pepo* convar. giromontiina (zucchini)	Fruit	ND [a]	7.96±1.00	0.12±0.03	0.24±0.06	11.78±2.21	5.62±0.87	3.39±0.52	0.85±0.15	0.58±0.08	0.17±0.04	1.56±0.33	**59.89**
27	*Cuminum cyminum* L. (cumin)	Seeds	0.46±0.07	37.30±3.36	0.51±0.13	13.38±0.42	4.99±0.05	5.08±0.27	3.06±0.16	4.03±0.44	4.88±0.65	2.80±0.21	3.80±0.06	**164.20**
28	*Cymbopogon citratus* (DC.) STAPF (lemon grass)	Leaves	0.08±0.10	20.47±6.35	0.15±0.02	0.29±0.07	6.84±5.34	3.46±0.73	2.09±0.44	1.96±0.53	0.71±0.13	0.33±0.02	5.47±1.05	**61.76**
29	*Daucus carota* subsp. *sativus* (HOFFM.) ARCANG. (carrot)	Tubers	0.03±0.02	10.43±1.37	0.79±0.06	0.66±0.09	8.10±0.11	2.83±0.21	1.71±0.13	1.07±0.14	1.24±0.11	0.17±0.07	1.24±0.17	**60.25**
30	*Eragrostis tef* (Zucc.) TROTTER (teff)	Seeds	1.22±0.32	26.61±0.25	0.51±0.03	3.38±0.02	4.38±0.23	8.31±0.59	5.01±0.36	4.42±0.2	4.08±0.00	3.23±0.44	5.81±0.22	**162.84**

Table 4 (continued)

S/N	Plants	Concentration (mg/g)											Total FAA[b]
		Part	L-Met	L-Asn	L-Orn	L-Pro	L-Gln	L-Arg	L-Ser	L-Thr	L-Val	L-Try	L-Tyr	
31	*Fragaria* × *ananassa* DUCHESNE (strawberry)	Fruit	ND [a]	27.51±0.97	0.08±0.01	0.09±0.01	0.67±0.05	1.75±0.11	1.05±0.07	0.65±0.02	0.16±0.01	0.07±0.01	0.63±0.10	**41.20**
32	*Glycine max* (L.) MERR. (soybean)	Seeds	0.38±0.07	27.48±1.65	0.62±0.06	1.73±0.49	1.11±0.01	3.52±1.43	2.12±0.87	1.71±0.41	1.99±0.41	7.45±0.68	5.82±1.63	**130.91**
33	*Helianthus annuus* L. (sunflower)	Seeds	2.48±0.15	21.90±0.90	0.27±0.05	16.05±0.77	4.52±0.56	5.44±0.89	3.28±0.54	2.91±0.18	4.75±0.55	4.24±0.54	6.28±0.44	**134.01**
34	*Lactuca sativa* L. (lettuce)	Leaves	ND [a]	24.94±0.26	0.37±0.03	0.08±0.00	10.62±0.01	4.54±0.79	2.74±0.48	5.57±1.01	0.59±0.00	0.43±0.35	2.25±0.02	**83.51**
35	*Linum usitatissimum* L. (flax)	Seeds	2.39±0.20	20.03±0.43	0.31±0.04	5.28±0.06	4.78±0.48	5.82±0.10	3.51±0.06	3.82±0.18	4.77±0.40	6.62±0.48	7.44±0.48	**148.71**
36	*Malus domestica* BORKH. (apple)	Fruit	ND [a]	0.43±0.00	0.01±0.00	0.02±0.00	0.05±0.01	0.11±0.01	0.07±0.00	0.03±0.00	0.04±0.00	ND [a]	0.02±0.00	**2.01**
37	*Mangifera indica* L. (mango)	Fruit	ND [a]	0.06±0.01	0.01±0.00	0.05±0.01	0.10±0.00	0.16±0.01	0.10±0.01	0.03±0.00	0.01±0.00	ND [a]	0.02±0.00	**1.72**
38	*Mangifera indica* L. (mango)	Peal	ND [a]	0.20±0.01	0.01±0.01	0.01±0.00	0.05±0.00	0.07±0.02	0.04±0.01	0.01±0.01	0.01±0.01	0.02±0.02	0.01±0.05	**0.86**
39	*Matricaria chamomilla* L. (chamomile)	Flower	0.06±0.02	21.44±0.61	0.23±0.01	5.23±0.18	14.64±0.79	7.42±0.21	4.48±0.13	4.42±0.16	2.55±0.13	1.40±0.12	5.82±0.52	**110.05**
40	*Mentha* x *piperita* L. (peppermint)	Leaves	0.01±0.03	11.14±0.00	0.04±0.00	0.16±0.00	1.53±0.01	2.44±0.14	1.47±0.08	1.05±0.11	0.97±0.00	1.23±0.11	1.13±0.07	**31.41**
41	*Moringa oleifera* LAM. (moringa tree)	Leaves	2.21±0.37	32.42±6.86	0.92±0.21	7.82±0.46	7.83±1.08	19.02±3.17	11.47±1.91	10.93±1.63	10.08±1.98	11.69±1.17	16.2±1.06	**266.90**
42	*Musa acuminata* COLLA (banana)	Peal	ND [a]	0.42±0.02	0.02±0.00	0.08±0.00	0.40±0.01	0.48±0.03	0.29±0.02	0.10±0.01	0.09±0.01	0.02±0.00	0.25±0.20	**4.55**
43	*Musa acuminata* COLLA (banana)	Fruit	ND [a]	3.34±0.37	0.01±0.00	0.04±0.00	0.41±0.06	0.41±0.04	0.25±0.03	0.17±0.02	0.05±0.00	0.10±0.02	0.07±0.00	**6.99**
44	*Nigella sativa* L. (black cumin)	Seeds	0.69±0.02	16.19±1.49	0.43±0.02	8.37±1.11	2.66±0.36	3.87±0.43	2.33±0.26	2.04±0.13	2.58±0.23	15.05±1.02	6.30±0.69	**122.07**
45	*Ocimum basilicum* L. (Mexican spice basil)	Leaves	0.12±0.07	10.13±0.00	0.12±0.00	0.21±0.00	9.61±0.02	1.90±0.18	1.15±0.11	1.52±0.06	0.84±0.00	0.50±0.07	2.37±0.01	**42.37**
46	*Persea americana* MILL. (avocado)	Fruit	ND [a]	2.63±0.13	0.85±0.16	2.74±0.08	0.50±0.01	2.93±0.21	1.77±0.13	1.66±0.04	2.29±0.05	0.20±0.01	1.39±0.40	**60.92**
47	*Phaseolus vulgaris* L. (common bean)	Seeds	0.09±0.00	25.81±0.28	0.81±0.04	2.53±0.03	23.92±0.01	14.02±0.05	8.46±0.03	4.95±0.02	4.30±0.02	1.89±0.05	4.92±0.07	**181.36**
48	*Piper nigrum* L. (black pepper)	Seeds	0.01±0.00	48.37±1.75	0.28±0.03	1.46±0.12	0.24±0.03	2.82±0.35	1.70±0.21	1.03±0.03	0.99±0.09	0.50±0.11	1.15±0.08	**139.35**
49	*Pisum sativum* var. *Abyssinicum* (A. BRAUN) BERGER (decoco)	Seeds	0.63±0.04	35.27±7.84	1.39±0.18	11.79±2.38	2.58±0.56	4.39±0.65	2.65±0.39	6.12±0.34	3.62±0.67	3.02±0.22	7.17±1.35	**214.39**
50	*Plectranthus edulis* (VATKE) ANGEW (Ethiopian potato)	Tubers	5.46±0.73	27.13±2.82	0.76±0.20	3.90±0.57	22.82±1.96	5.74±0.56	3.46±0.34	4.46±0.33	7.84±0.83	2.27±0.32	2.48±0.25	**153.29**
51	*Pleurotus ostreatus* (JACQ. EX FR.) P.KUMM. (oyster mushroom)	Fruit body	22.2±9.95	15.69±1.09	5.06±0.68	3.64±0.01	34.59±5.33	28.69±0.42	17.31±0.25	22.63±0.6	15.20±0.13	8.56±0.47	26.05±3.86	**400.01**
52	*Ruta chalepensis* L. (rue)	Leaves	0.68±0.23	27.25±0.06	0.96±0.38	30.10±0.66	7.10±0.37	7.73±0.71	4.67±0.43	6.70±0.24	7.32±0.62	8.03±0.31	14.48±0.93	**215.83**
53	*Rumex abyssinicus* JACQ. (mekmako)	Leaves	0.01±0.00	2.45±0.22	0.11±0.01	0.97±0.40	6.52±0.49	3.58±0.13	2.16±0.08	1.84±0.05	1.72±0.07	0.60±0.18	3.91±0.26	**47.13**
54	*Salvia rosmarinus* SCHLEID. (rosemary)	Leaves	0.04±0.01	28.13±0.26	0.57±0.08	0.71±0.11	5.85±0.92	2.28±0.44	1.38±0.27	1.00±0.14	1.88±0.15	0.84±0.10	8.21±0.06	**80.97**
55	*Sesamum indicum* L. (sesame)	Seeds	0.01±0.01	7.67±0.23	0.43±0.01	0.74±0.00	5.18±0.01	2.30±0.02	1.39±0.01	0.95±0.01	0.91±0.01	0.74±0.01	1.85±0.02	**44.31**
56	*Solanum lycopersicum* L. (tomato)	Fruit	0.03±0.01	18.74±2.64	0.25±0.02	0.38±0.04	20.51±3.10	3.29±0.67	1.98±0.40	1.43±0.37	0.74±0.08	1.12±0.12	8.37±1.64	**137.15**
57	*Syzygium aromaticum* (L.) MERR. & L.M.PERRY (clove)	Flower	0.21±0.00	18.69±0.15	1.52±0.00	5.19±0.01	46.87±0.00	6.78±0.01	4.09±0.01	6.05±0.00	8.02±0.01	4.83±0.00	11.23±0.02	**261.19**
58	*Thymus vulgaris* L. (thyme)	Leaves	0.01±0.01	18.54±1.59	1.16±0.98	7.54±2.58	12.51±0.70	5.64±1.13	3.40±0.68	2.78±0.33	3.28±0.34	2.70±0.22	4.96±0.28	**111.83**
59	*Trigonella foenum-graceum* L. (fenugreek)	Seeds	0.03±0.02	2.64±0.14	0.70±0.04	2.42±0.04	0.58±0.35	2.61±0.10	1.57±0.06	1.51±0.05	2.15±0.06	0.25±0.04	1.11±0.16	**57.37**
60	*Zingiber officinale* ROSCOE (ginger)	Tubers	0.04±0.01	21.05±1.22	2.40±0.29	6.95±0.14	1.34±0.16	9.88±0.27	5.96±0.16	4.97±0.06	5.47±0.31	2.00±0.04	4.82±0.32	**248.50**
		Min	**0.00**	**0.06**	**0.01**	**0.01**	**0.05**	**0.07**	**0.04**	**0.01**	**0.01**	**0.00**	**0.01**	
		Max	**22.2**	**48.37**	**5.06**	**30.1**	**64.59**	**28.69**	**17.31**	**22.63**	**15.2**	**15.05**	**26.25**	

a ND= Not detected, **b** Total FAA= Total free amino acid content

4.2. Development and validation of a simple, selective, and accurate reversed-phase liquid chromatographic method with diode array detection (RP-HPLC/DAD) for the simultaneous analysis of 18 free amino acids in topical formulations.

Author:	Birhanu Nigusse Kahsay, Lucie Moeller, Peter Imming, Reinhard H. H. Neubert* & Tsige Gebre-Mariam
Source:	https://doi.org/10.1007/s10337-022-04160-0
Journal:	Chromatographia
Publisher:	Springer
Date:	March 2022
Author contributions:	RHHN and **BNK** planned the experiments. **BNK** carried out the method development and validation and data analysis. RHHN supervised the project. **BNK** prepared the draft manuscript; LM, PI, TGM, and RHHN reviewed the draft; and **BNK** prepared the final manuscript. All authors have read and agreed to the published version of the manuscript. RHHN and TGM are the corresponding authors.

4.2.1. Sample pretreatment and optimization of derivatization condition

Before performing the validation activities, a preliminary study (method development) was conducted to optimize the sample pretreatment, derivatization process, and chromatographic conditions. Acetone and acetonitrile were compared as derivatizing reagents and better results were obtained when the later reagent was used. Preparing the Fmoc-Cl in acetone resulted in a broad and big interfering peak as compared to that of acetonitrile. The removal of unreacted Fmoc-Cl with adamantanamine (ADAM) gave better results than that of n-pentane. The results obtained after extraction of the excess Fmoc-Cl with *n*-pentane were not consistent. Moreover, the concentrations obtained were lower than that obtained after reaction with ADAM, maybe due to considerable loss of the derivatized FAAs during the removal of excesss *n*-pentane. Further, relatively longer extraction time is needed as it requires extracting the excess Fmoc-Cl solution at least three times with 500 µL of *n*-pentane. On the other hand, the reaction of the unused Fmoc with excess ADAM resulted in the spectacular decrease of the reagent peak, without any loss of the hydrophobic Fmoc derivatives. The extent of formation of Fmoc-OH was greatly decreased, and the excess Fmoc Cl was eliminated completely. The resulting Fmoc-OH peak was sufficiently resolved from the FAA derivatives and didn't interfere with the peaks of the analyte of interest. The response of the amino acid derivatives was independent of the ADAM

concentration within the tested concentration range. Hence, acetonitrile and ADAM were used to prepare the Fmoc-Cl solution and to remove the excess Fmoc-Cl respectively. For Fmoc-Cl derivatization borate buffer was used. Different concentrations of borate buffer (20, 200, 500 mM) were tested. Derivatization was effective at the highest concentration (500 mM). Therefore, this concentration of buffer was selected and used. The effect of the buffer pH on derivatization yields was investigated in the pH range of 7–10 using borate buffer solution (0.5 M). Among the tested pH range, buffer solution at pH 8.6 was selected for the derivatization. A reaction time of 10 min was sufficient for complete reaction between the FAAs and Fmoc-Cl in borate buffer maintained at pH 8.6.

4.2.2. Optimization of chromatographic conditions

Of the two analytical columns (Lichrosphere C18, 150 mm x 4.6 mm, 5 µm particle size and Agilent InfinityLab Poroshell 120 E.C 18 (3 x 50) mm, 2.7 µm), better resolution, peak shape and shorter retention time were obtained with the latter one. For mobile phase optimization, the effect of mobile phase concentration of organic modifier, mobile phase pH, and flow rate were investigated. As the content of the organic modifier was decreased, the resolution was improved, and the end time was prolonged (common feature for RP HPLC). The peak resolution and shape were improved when glacial acetic acid and trimethylamine were added. Among the different mobile phases tested, a gradient elution consisting of solvent A (water) and B (acetonitrile) each containing 0.2% glacial acetic acid and 0.1% trimethylamine showed a better resolution and peak shape. A decrease in pH increased the retention of all tested FAAs. The retention time of the Fmoc-OH was only slightly affected by the pH of the eluent. When the pH was increased, L-Arg, L-Asn, L-Gln and L-Ser were not fully resolved. Mobile phase flow rates ranging from 0.5-1.0 mL/min were investigated. Optimum results (in terms of resolution and end time) were obtained at a flow rate of 0.70 mL/min, which gave a total run time of about 30 min and resolution of > 2.0 for most of the investigated FAAs. With the longer column (Lichrosphere C18, 150 mm x 4.6 mm) the end time was about 50 min.

The effect of column temperature on resolution and peak shape was also investigated. As the temperature increased, the resolution between successive peaks was poor. The best resolution was obtained at 25 ^{0}C followed by 30 ^{0}C and some of the peaks overlapped at 40 ^{0}C (for example the peaks due to L-Thr and L-Gly). Consistent results were obtained at 25 ^{0}C and this temperature was selected for the oven temperature. The maximum detection for the derivatized compounds was at 263 nm and this was evidenced from spectral analysis. The effect of the presence of other FAAs such as L-cysteine HCl (L-Cys), L-tryptophan (L-Trp), and L-tyrosine (L-Tyr) was also investigated. Care should be taken as they could overlap with the other FAAs. Under the mentioned experimental conditions, L-Trp elutes just before L-Phe, L-Tyr elutes next to L-Ala while L-Cys elutes at the end next to L-Lys. Solvent B should be reduced at the respective retention times to attain the required resolution.

4.2.3. Robustness

The results on robustness indicate that small changes in pH of mobile phase (solvent A), flow rate, and column temperature in the range 3.7 ± 0.2, 0.7 mL/min ± 5%, and 25 ± 3 ^{0}C respectively had no significant effect on the chromatographic performance. The repeatability of peak area and retention time, tailing factor, theoretical plate numbers, and resolution were not significantly affected under such small changes. Moreover, the percentage of solvent B can be varied within ± 2 % in the gradient program. We used this method for more than a year and consistent results were obtained in both new and aged analytical columns. Solution stability was also investigated against freshly prepared standard solutions. The stock solutions were stable for two weeks at -20 ^{0}C before derivatization and for 24 hrs after derivatization in HPLC auto-sampler at 4 ^{0}C.

4.2.4. System suitability

System suitability testing (SST) was studied by performing the experiment and looking for changes in retention times, separation, and asymmetry of the peaks. The retention time, peak area, theoretical plate's values, height equivalent to theoretical plate (HETP), tailing factor and resolution were recorded and the results obtained are given in Table 5.

As can be seen from Table 5, the theoretical plate numbers for all the analytes were above 18,000 and the HETP was very low (not more than 2). The tailing factor was below 2 and this is within the pharmacopeial requirements. The resolutions among the different analytes were above 2.0 for most of the FAAs. Even though the resolution between L-Asn & L-Gln and L-His & L-Orn was below 2.0, the peaks were baseline separated (with a resolution of greater than 1.5) and there was no problem in the quantification. The peaks due to L-Ile & L-Leu were sufficiently resolved in the present work. Hence this method has improved resolution as compared to previously reported methods. The % RSD of each set of parameters (retention time, peak area, tailing factor, efficiency, and HETP) was less than 2% indicating the reproducibility of RP-HPLC/DAD system for quantitative analysis of the eighteen FAAs. Hence, the method fulfills the acceptance criteria for the mentioned SST parameters. The chromatograms of 6 replicates of the standard solution are shown in Fig. 3 and they were consistent in peak area, peak shape, and retention time.

Table 5: Results of the system suitability test for the simultaneous analysis of 18 free amino acids by HPLC/DAD using Agilent InfinityLab Poroshell 120 E.C 18 (3 x 50 mm, 2.7 µm) column (n=6)**.**

FAA	Ret. time (min)		Peak area (µV. min)		N. of theoretical plates		HETP		Tailing factor		Resolution	
	Average	% RSD	Average	% RSD	Average	% RSD	Average	% RSD	Average	% RSD	Average	% RSD
L-Arg	9.60	0.11	1084669.17	0.43	42067.50	0.47	1.19	0.47	1.02	1.32	-----	-----
L-Asn	10.54	0.12	624859.50	0.42	37194.83	0.42	1.34	0.42	1.04	0.54	4.00	0.82
L-Gln	10.95	0.13	1625946.50	0.86	29501.17	1.07	1.69	1.07	1.24	1.37	1.96	0.85
L-Ser	11.93	0.13	1614815.50	0.24	26605.50	1.28	1.88	1.29	1.16	0.29	3.21	0.60
L-Asp	12.93	0.14	585814.00	0.46	29619.67	0.95	1.69	0.94	1.23	0.94	2.84	0.77
L-Glu	14.27	0.16	754136.17	0.55	28415.00	0.96	1.76	0.96	1.10	0.80	3.64	0.54
L-Thr	15.57	0.18	1245178.67	1.12	29540.17	0.67	1.69	0.67	1.11	0.35	2.91	0.33
L-Gly	16.53	0.17	1638611.17	0.88	25670.33	1.32	1.95	1.34	1.00	0.23	2.89	1.17
L-Ala	18.81	0.04	1193973.81	4.20	194777.66	1.51	0.26	1.51	1.29	1.03	6.45	1.15
L-Pro	19.51	0.04	1138373.50	0.25	136283.50	1.64	0.37	1.65	1.15	1.28	3.66	1.27
L-Met	20.42	0.05	1253059.83	0.67	195740.16	0.89	0.25	0.89	1.22	0.74	4.60	1.09
L-Val	21.02	0.06	1168886.67	0.98	154665.17	1.26	0.32	1.25	1.17	1.32	2.98	1.47
L-Phe	22.75	0.07	932631.33	1.14	153655.50	1.15	0.32	1.16	1.20	1.48	17.19	1.23
L-Ile	23.27	0.05	1030549.67	0.31	196941.67	1.39	0.25	1.39	1.11	0.40	10.48	0.70
L-Leu	23.54	0.04	1133970.33	0.69	200119.00	1.56	0.25	1.55	1.07	0.44	2.01	0.22
L-His	26.38	0.02	1651545.17	1.23	356321.33	1.07	0.145	1.09	1.12	1.25	20.91	1.02
L-Orn	26.55	0.03	2649649.50	0.42	381551.33	1.62	0.13	1.62	1.21	0.16	1.64	0.72
L-Lys	27.12	0.03	2530910.17	1.11	334841.30	0.66	0.15	0.67	1.31	0.23	4.10	1.59

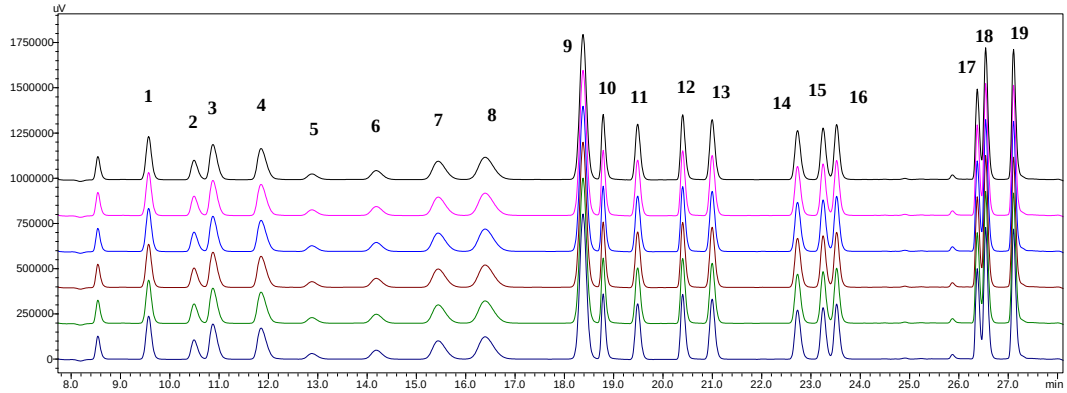

Fig. 3: Chromatograms of six replicates of the 20 µM standard solution (1: L-Arg, 2: L-Asn, 3: L-Gln, 4: L-Ser, 5: L-Asp, 6: L-Glu, 7: L-Thr, 8: L-Gly, 9: Fmoc-OH, 10: L-Ala, 11: L-Pro, 12: L-Met, 13: L-Val, 14: L-Phe, 15:L-Ile, 16: L-Leu, 17: L-His, 18: L-Orn, 19:L-Lys).

4.2.5. Method validation

Specificity

Specificity was determined by comparing the chromatograms of the individual FAA working standards, FAA-loaded formulations, and placebo formulations. As can be seen in Fig. 4, there are no interfering peaks at the retention time of the respective analytes from the placebo solution. Moreover, there were minimal differences between retention times and peak area (% difference of less than 0.5 %) in case of the standard and sample solutions.

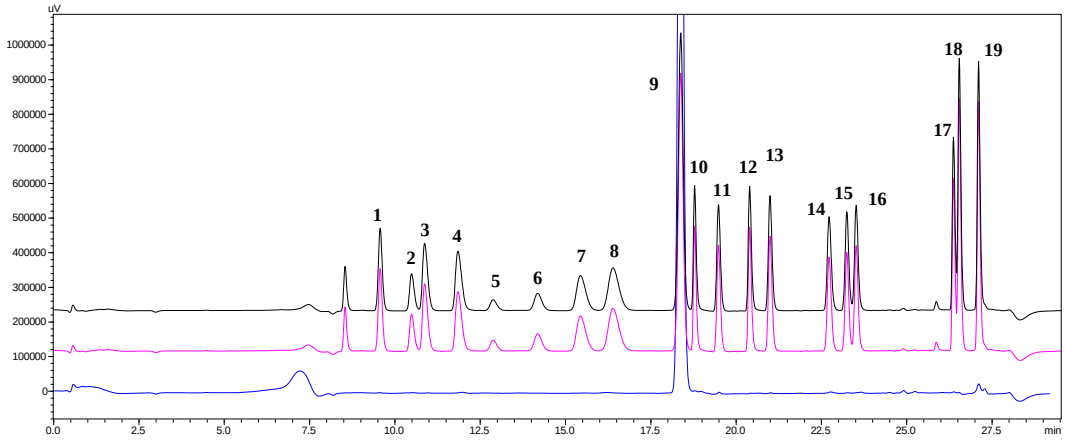

Fig. 4: Chromatograms of the placebo solution (blue), standard solution (violet), and sample solution (black) (1: L-Arg, 2: L-Asn, 3: L-Gln, 4: L-Ser, 5: L-Asp, 6: L-Glu, 7: L-Thr, 8: L-Gly, 9: Fmoc-OH, 10: L-Ala, 11: L-Pro, 12: L-Met, 13: L-Val, 14: L-Phe, 15:L-Ile, 16: L-Leu, 17: L-His, 18: L-Orn, 19:L-Lys)

Linearity, Limit of Detection and Limit of Quantification

The calibration curve was constructed within the linear concentration range of 5-80 µM. Each concentration was made into five independent replicates. Linearity was assessed using the correlation coefficient (R^2) of the regression line. The results in Table 6 show that R^2 were in the range of 0.9954–0.9991. The LOD and LOQ values were in the range of 0.13 to 1.36 µM and 0.42 µM to 4.54 µM, respectively (Table 6). This estimate was further confirmed by the independent analysis of real samples prepared at the detection and quantification limit and the results were not significantly different from those reported in Table 6.

Table 6: Results of Linearity, LOD, LOQ (n=5) for the simultaneous analysis of 18 free amino acids by HPLC/DAD using Agilent InfinityLab Poroshell 120 E.C 18 (3 x 50 mm, 2.7 µm) column

Analyte	Linearity range	Linearity equation	R^2	S.D of Y-int	Mean Slope	LOD (µM)	LOQ (µM)
L-Arg	(5-80) µM	Y=37077.90X + 12437.73	0.9975	11532.85	37077.90	0.93	3.11
L-Asn	(5-80) µM	Y=20179.30X + 6848.57	0.9987	6156.32	20179.30	0.92	3.05
L-Gln	(5-80) µM	Y=41283.27X + 9426.13	0.9991	4281.03	41283.27	0.31	1.04
L-Ser	(5-80) µM	Y=50221.40X + 26200.47	0.9973	9292.66	50221.40	0.56	1.85
L-Asp	(5-80) µM	Y=73157.17X + 74215.60	0.9986	13538.17	73157.17	0.56	1.85
L-Glu	(5-80) µM	Y=59628.57X + 51925.20	0.9968	11124.60	59628.57	0.56	1.87
L-Thr	(5-80) µM	Y=41665.73X + 28593.10	0.9978	17082.63	41665.73	1.23	4.11
L-Gly	(5-80) µM	Y=51145:00X + 21811.17	0.9975	13134.49	51145.00	0.77	2.57
L-Ala	(5-80) µM	Y=41042.80X + 22072.10	0.9973	6306.74	41042.80	0.46	1.54
L-Pro	(5-80) µM	Y=40138.33X + 567758.30	0.9974	6306.74	40138.33	0.47	1.57
L-Met	(5-80) µM	Y=47051.37X + 11466.230	0.9976	2296.22	47051.37	0.15	0.49
L-Val	(5-80) µM	Y=43894.10X + 13274.730	0.9968	14242.17	43894.10	0.97	3.24
L-Phe	(5-80) µM	Y=24227.33X + 3694.03	0.9986	1956.81	24227.33	0.24	0.81
L-Ile	(5-80) µM	Y=42090.03X + 15931.10	0.9984	8597.02	42090.03	0.61	2.04
L-Leu	(5-80) µM	Y=49001.73X + 24230.40	0.9972	15178.85	49001.73	0.93	3.10
L-His	(5-80) µM	Y=21074.23X + 26618.03	0.9954	9560.45	21074.23	1.36	4.54
L-Orn	(5-80) µM	Y=59201.90X + 47779.87	0.9981	3400.02	59201.90	0.17	0.57
L-Lys	(5-80) µM	Y=76389.53X + 69674.90	0.9970	3213.82	76389.53	0.13	0.42

Precision

The results of the precision, precision intermediate and accuracy are shown in Table 7 and Table 8, and Table 9 respectively. The %RSD and overall %RSD were < 2.0 for the precision and precision intermediate respectively and the % recovery at all the three concentrations were within the acceptance criteria (90-110 %) for the accuracy (Table 7-9).

Table 7: Results of precision in the simultaneous analysis of 18 free amino acids by HPLC/DAD using Agilent InfinityLab Poroshell 120 E.C 18 (3 x 50 mm, 2.7 µm) column.

Sample	Concentration (µM)								
	1	2	3	4	5	6	Average	SD	%RSD
L-Arg	20.09	20.08	20.07	20.09	19.84	19.83	19.99	0.13	0.64
L-Asn	20.05	19.89	19.92	19.95	20.12	20.06	20.00	0.09	0.47
L-Gln	20.05	19.87	19.94	19.89	19.85	20.39	20.00	0.20	1.02
L-Ser	19.85	20.06	19.96	19.83	20.00	20.29	20.00	0.17	0.85
L-Asp	19.85	20.13	20.11	20.11	20.10	19.70	20.00	0.18	0.90
L-Glu	20.11	20.11	19.95	19.79	19.95	20.09	20.00	0.13	0.63
L-Thr	20.03	20.26	20.17	20.15	19.86	19.52	20.00	0.27	1.35
L-Gly	20.06	20.05	20.02	20.25	19.64	19.97	20.00	0.20	0.98

Table 7 (continued)

Sample	Concentration (μM)								
	1	2	3	4	5	6	Average	SD	%RSD
L-Ala	19.99	19.85	19.82	20.16	20.05	20.10	20.00	0.13	0.67
L-Pro	19.96	20.15	19.96	19.79	19.89	20.25	20.00	0.17	0.86
L-Met	20.08	19.61	20.04	20.19	19.92	20.15	20.00	0.21	1.06
L-Val	20.07	19.75	19.92	20.26	20.34	19.66	20.00	0.27	1.35
L-Phe	19.95	19.99	20.17	19.98	19.90	19.98	20.00	0.09	0.46
L-Ile	19.62	19.90	20.39	19.68	20.37	20.03	20.00	0.33	1.66
L-Leu	19.99	20.02	19.79	19.89	20.22	20.07	20.00	0.14	0.72
L-His	20.00	20.19	19.97	19.87	19.93	20.03	20.00	0.11	0.55
L-Orn	20.27	20.08	20.02	19.90	19.81	19.92	20.00	0.17	0.81
L-Lys	20.14	19.99	19.84	19.96	20.24	19.83	20.00	0.16	0.82

Table 8: Results of intermediate precision in the simultaneous analysis of 18 free amino acids by HPLC/DAD using Agilent InfinityLab Poroshell 120 E.C 18 (3 x 50 mm, 2.7 μm) column

Sample	Concentration (μM)														
	Day 1						Day 2						Overall		
	1	2	3	4	5	6	1	2	3	4	5	6	Mean	SD	%RSD
L-Arg	20.09	20.08	20.07	20.09	19.84	19.83	20.01	20.01	20.12	19.88	19.86	19.94	20.01	0.15	0.76
L-Asn	20.05	19.89	19.92	19.95	20.12	20.06	20.01	19.95	19.87	19.94	20.09	19.96	19.98	0.08	0.40
L-Gln	20.05	19.87	19.94	19.89	19.85	20.39	19.68	19.89	20.12	19.94	19.85	20.07	19.94	0.18	0.89
L-Ser	19.85	20.06	19.96	19.83	20.00	20.29	19.79	20.01	20.11	19.97	20.14	19.88	20.01	0.16	0.82
L-Asp	19.85	20.13	20.11	20.11	20.10	19.70	19.89	19.97	19.85	20.09	19.84	20.16	19.97	0.17	0.83
L-Glu	20.11	20.11	19.95	19.79	19.95	20.09	20.10	20.14	19.96	19.86	19.96	19.97	20.03	0.18	0.91
L-Thr	20.03	20.26	20.17	20.15	19.86	19.52	20.13	19.97	20.08	20.14	19.86	19.77	19.99	0.21	1.05
L-Gly	20.06	20.05	20.02	20.25	19.64	19.97	19.79	19.95	20.11	20.31	19.76	19.81	19.98	0.20	1.00
L-Ala	19.99	19.85	19.82	20.16	20.05	20.10	19.76	19.87	19.91	19.82	20.04	20.14	19.94	0.16	0.81
L-Pro	19.96	20.15	19.96	19.79	19.89	20.25	19.95	20.08	19.93	19.86	19.79	19.76	19.98	0.18	0.92
L-Met	20.08	19.61	20.04	20.19	19.92	20.15	19.87	19.95	20.02	20.17	19.97	19.49	19.95	0.21	1.08
L-Val	20.07	19.75	19.92	20.26	20.34	19.66	20.08	19.79	19.93	20.16	19.98	19.97	19.98	0.16	0.81
L-Phe	19.95	19.99	20.17	19.98	19.90	19.98	20.42	20.06	19.97	19.86	20.04	20.11	20.06	0.19	0.95
L-Ile	19.62	19.90	20.39	19.68	20.37	20.03	19.30	19.94	20.13	19.74	20.21	20.08	19.90	0.29	1.46
L-Leu	19.99	20.02	19.79	19.89	20.22	20.07	19.85	19.94	20.11	19.83	19.96	19.97	19.95	0.13	0.65
L-His	20.00	20.19	19.97	19.87	19.93	20.03	19.67	20.21	20.09	19.97	20.16	20.03	19.98	0.18	0.91
L-Orn	20.27	20.08	20.02	19.90	19.81	19.92	20.05	20.04	19.99	19.81	20.17	19.94	19.93	0.19	0.95
L-Lys	20.14	19.99	19.84	19.96	20.24	19.83	19.87	20.14	19.87	19.92	19.87	19.97	19.93	0.12	0.62

Accuracy

The results of accuracy are shown in Table 9. The % recovery at all the three concentrations were within the acceptance criteria (90-110 %).

Table 9: Results of recovery in analysis of the spiked free amino acid samples at three concentration levels by RP-HPLC/DAD using Agilent InfinityLab Poroshell 120 E.C 18 (3 x 50 mm, 2.7 µm) column (n = 3).

Analyte	Recovery (%) at different concentrations (means ± SD, n=3)			
	50% (10 µM)	100% (20 µM)	200% (40 µM)	Overall recovery
L-Arg	99.10 ± 1.53	99.70 ± 0.38	97.30 ± 0.13	98.70 ± 1.25
L-Asn	98.03 ± 1.42	99.65 ± 1.07	98.79 ± 0.61	98.83 ± 0.81
L-Gln	97.87 ± 1.49	99.05 ± 0.77	96.21 ± 1.16	97.71 ± 1.43
L-Ser	98.37 ± 1.74	99.48 ± 1.46	96.65 ± 0.09	98.16 ± 1.42
L-Asp	96.90 ± 0.47	99.02 ± 0.78	96.82 ± 0.32	97.56 ± 1.24
L-Glu	97.93 ± 0.59	98.87 ± 0.46	96.99 ± 0.75	97.93 ± 0.94
L-Thr	98.17 ± 0.69	98.00 ± 0.32	96.85 ± 0.16	97.67 ± 0.72
L-Gly	98.40 ± 0.53	98.40 ± 1.33	98.23 ± 0.82	98.34 ± 0.10
L-Ala	99.57 ± 1.56	98.03 ± 0.65	99.14 ± 0.28	98.91 ± 0.79
L-Pro	100.63 ± 0.90	96.27 ± 0.49	96.53 ± 0.16	97.81 ± 2.44
L-Met	99.23 ± 1.57	97.87 ± 0.53	97.04 ± 0.47	98.05 ± 1.11
L-Val	97.50 ± 1.61	99.63 ± 0.54	98.32 ± 0.49	98.48 ± 1.07
L-Phe	99.40 ± 1.21	98.90 ± 0.72	98.15 ± 1.19	98.82 ± 0.63
L-Ile	99.80 ± 0.97	99.05 ± 0.91	97.30 ± 0.51	98.72 ± 1.28
L-Leu	99.77 ± 1.02	98.38 ± 0.56	97.98 ± 0.91	98.71 ± 0.94
L-His	98.83 ± 0.41	98.35 ± 0.56	96.31 ± 1.26	97.83 ± 1.34
L-Orn	100.80 ± 0.10	99.03 ± 0.31	99.23 ± 1.00	99.69 ± 0.97
L-Lys	99.30 ± 0.56	98.15 ± 0.98	98.09 ± 0.93	98.51 ± 0.68

4.2.6. Application of the method in routine quality control test

The applicability of the method in routine quality control testing was confirmed by conducting assay determinations on topical preparations. In addition to the microemulsion, the method was applied on microemulsion-based hydrogels (the additional ingredients included in the hydrogels did not interfere with the analyte peaks and the selectivity of the method was same as that of the microemulsion (Fig 4). The content of the selected FAAs was determined by analyzing the assay content of the final finished products (microemulsions and microemulsion-based hydrogels). As can be seen in Table 10, the assay values were within the range of 95-105 % which is within the pharmacopoeia assay requirements (90-110%).

Table 10: Assay values of different topical preparations as determined by HPLC/DAD using Agilent InfinityLab Poroshell 120 E.C 18 (3 x 50 mm, 2.7 µm) column

Sample	Assay content (%) (means ± SD, n=3)		
	Microemulsion	Carbopol® 934 based hydrogel	Poloxamer® 407 based hydrogel
L-Arg	99.67 ± 0.68	98.73 ± 1.29	99.82 ± 1.77
L-Asn	100.08 ± 0.33	98.42 ± 0.38	98.80 ± 1.35
L-Gln	98.63 ± 1.17	99.11 ± 0.86	97.67 ± 1.50
L-Ser	99.18 ± 1.13	97.90 ± 1.12	98.82 ± 2.10
L-Asp	99.40 ± 0.98	97.65 ± 1.41	99.68 ± 1.19
L-Glu	97.90 ± 0.96	98.72 ± 0.67	97.10 ± 0.69
L-Thr	99.48 ± 1.65	97.66 ± 0.73	99.86 ± 1.98
L-Gly	101.56 ± 0.88	99.65 ± 2.33	98.22 ± 3.18
L-Ala	99.85 ± 0.71	99.23 ± 0.56	99.62 ± 0.76
L-Pro	97.92 ± 1.01	98.51 ± 2.08	98.76 ± 2.30
L-Met	100.67 ± 0.23	97.98 ± 1.15	99.88 ± 1.59
L-Val	99.81 ± 1.33	98.49 ± 1.10	99.28 ± 1.33
L-Phe	99.65 ± 0.31	99.05 ± 0.79	99.72 ± 0.36
L-Ile	98.98 ± 1.05	98.72 ± 1.31	99.45 ± 0.73
L-Leu	97.82 ± 0.61	98.71 ± 0.95	99.87 ± 0.63
L-His	99.00 ± 0.15	97.83 ± 1.37	97.32 ± 0.56
L-Orn	102.00 ± 1.20	99.69 ± 0.97	99.68 ± 0.67
L-Lys	99.82 ± 0.79	98.51 ± 0.69	99.56 ± 0.40

4.3. Corneocytary pathway across the stratum corneum: Identification of model systems and parameters to study dermal delivery of free amino acids

Author:	Birhanu Nigusse Kahsay, Lucie Moeller, Johannes Wohlrab, Reinhard H.H. Neubert, Tsige Gebre-Mariam
Status	Revised version submitted to Skin Pharmacology and Physiology
Publisher:	S. Karger AG
Author contributions:	RHHN, **BNK,** and JW designed the concept and study plan. **BNK** conducted experiments and data analysis. RHHN supervised the project. **BNK** prepared the draft manuscript. LM, JW, TGM, RHHN reviewed the draft manuscript. **BNK** prepared the final manuscript. All authors have read and agreed to the final version of the manuscript. RHHN is the corresponding author.

4.3.1. Uptake of FAAs into different skin models

$K_{COR/W}$ values for each of the 18 FAAs in the three different dried skin models (PHSC, SC of pig ear skin, and isolated keratin particles obtained from chicken feathers) are shown in Table 11. There was a significant difference in the uptake of FAAs between the three different skin models. The highest uptake was seen in the pig ear skin followed by PHSC. This ranking of $K_{COR/W}$ (pig skin > human skin > keratin particles) was consistent for all the FAAs. Even though the $K_{COR/W}$ values were higher in pig ear skin than that of PHSC, the differences were not significant for most of the FAAs ($p > 0.05$) except for some of the FAAs such as L-Arg, L-Glu, L-Met, L-His, and L-Lys ($p < 0.005$).

Table 11: Corneocyte-water uptake coefficient ($K_{COR/W}$) of 18 FAAs in different skin models (n=6, means ± SD)

S/N	Amino acids	$K_{COR/W}$		
		Human skin	Pig ear skin	Keratin particles
1	L-Arg	1.04 ± 0.06	1.52 ± 0.04	0.27 ± 0.15
2	L-Asn	0.71 ± 0.25	0.96 ± 0.31	0.37 ±0.05
3	L-Gln	1.60 ± 0.10	1.74 ± 0.07	0.27 ±0.11
4	L-Ser	1.08 ± 0.14	1.16 ± 0.08	0.31 ±0.12
5	L-Asp	1.55 ± 0.22	1.67 ± 0.28	0.36 ±0.03
6	L-Glu	1.06 ± 0.18	1.42 ± 0.27	0.61 ±0.10
7	L-Thr	0.88 ± 0.28	1.09 ± 0.14	0.31 ±0.09
8	L-Gly	0.98 ± 0.51	1.06 ± 0.06	0.30 ±0.02
9	L-Ala	0.96 ± 0.31	0.99 ± 0.03	0.31 ±0.04
10	L-Pro	1.28 ± 0.30	1.34 ± 0.25	0.24 ±0.02
11	L-Met	0.93 ± 0.28	1.33 ± 0.28	0.27 ±0.03
12	L-Val	1.03 ± 0.18	1.13 ± 0.13	0.28 ±0.02
13	L-Phe	1.54 ± 0.26	1.77 ± 0.17	0.23 ±0.01
14	L-Ile	0.66 ± 0.20	0.88 ± 0.05	0.23 ±0.03
15	L-Leu	0.95 ± 0.28	1.18 ± 0.15	0.25 ±0.08
16	L-His	1.03 ± 0.01	1.45 ± 0.24	0.53 ±0.11
17	L-Orn	0.77 ± 0.16	0.98 ± 0.06	0.31 ±0.14
18	L-Lys	0.91 ± 0.33	1.34 ± 0.18	0.29 ±0.02

4.3.2. Effect of separation technique on $K_{COR/W}$

The effect of four SC separation techniques namely, heat treatment in water, heat treatment on metal, enzymatic (dispase II) and chemical methods *on* $K_{COR/W}$ values were analyzed and compared. As can be seen from Table 12, the different SC separation techniques employed did not influence the subsequently determined $K_{COR/W}$ values of the FAAs ($p > 0.05$).

Table 12: Effect of separation technique on corneocyte-water uptake coefficients (KCOR/W) using pig ear skin (n=3, means ± SD)

S/N	Amino acids	$K_{COR/W}$			
		Heat treatment on water	Heat treatment on metal	Dispase II	EDTA
1	L-Arg	1.52 ± 0.04	1.53 ± 0.03	1.58 ± 0.05	1.51 ± 0.03
2	L-Asn	0.57 ± 0.03	0.58 ± 0.04	0.59 ± 0.04	0.61 ± 0.01
3	L-Gln	1.74 ± 0.07	1.75 ± 0.01	1.76 ± 0.02	1.76 ± 0.02
4	L-Ser	1.16 ± 0.08	1.23 ± 0.21	1.15 ± 0.05	1.16 ± 0.06
5	L-Asp	1.88 ± 0.07	1.86 ± 0.03	1.85 ± 0.03	1.85 ± 0.11
6	L-Glu	1.42 ± 0.27	1.28 ± 0.21	1.32 ± 0.27	1.38 ± 0.23
7	L-Thr	1.09 ± 0.14	1.04 ± 0.09	1.11 ± 0.04	1.11 ± 0.04
8	L-Gly	1.06 ± 0.06	1.10 ± 0.06	1.10 ± 0.02	1.14 ± 0.05
9	L-Ala	0.99 ± 0.03	1.07 ± 0.14	1.12 ± 0.15	1.19 ± 0.15
10	L-Pro	1.34 ± 0.25	1.22 ± 0.12	1.23 ± 0.09	1.32 ± 0.03
11	L-Met	1.33 ± 0.28	1.32 ± 0.17	1.37 ± 0.21	1.44 ± 0.05
12	L-Val	1.14 ± 0.14	1.13 ± 0.18	1.12 ± 0.16	1.11 ± 0.02
13	L-Phe	1.77 ± 0.13	1.72 ± 0.11	1.74 ± 0.13	1.73 ± 0.12
14	L-Ile	0.88 ± 0.05	0.94 ± 0.05	0.96 ± 0.06	0.98 ± 0.03
15	L-Leu	1.18 ± 0.15	1.06 ± 0.06	1.08 ± 0.12	1.08 ± 0.05
16	L-His	1.45 ± 0.24	1.44 ± 0.14	1.44 ± 0.16	1.56 ± 0.15
17	L-Orn	0.98 ± 0.07	1.05 ± 0.16	1.14 ± 0.13	1.09 ± 0.07
18	L-Lys	1.34 ± 0.19	1.39 ± 0.16	1.46 ± 0.15	1.42 ± 0.03

4.3.3. Effect of initial concentration of the drug on $K_{COR/W}$

The effect of varying the initial aqueous phase drug concentration (C_i) on the $K_{COR/W}$ of the FAAs is presented in Table 13. The $K_{COR/W}$ values tend to decrease with increasing C_i.

Table 13: Effect of initial aqueous phase concentration Ci on corneocyte- water partition coefficient ($K_{COR/W}$) (means ± SD, n=3)

S/N	Amino acids	$K_{COR/W}$		
		C_i= 0.1 mM	C_i= 1 mM	C_i= 10 mM
1	L-Arg	1.23 ± 0.10	1.04 ± 0.07	0.94 ± 0.08
2	L-Asn	0.45 ± 0.06	0.41 ± 0.02	0.32 ± 0.02
3	L-Gln	1.93 ± 0.03	1.60 ± 0.11	1.39 ± 0.16
4	L-Ser	1.33 ± 0.10	1.08 ± 0.14	0.95 ± 0.08
5	L-Asp	2.04 ± 0.09	1.60 ± 0.11	1.31 ± 0.12
6	L-Glu	1.55 ± 0.09	1.05 ± 0.18	0.89 ± 0.13
7	L-Thr	0.89 ± 0.07	0.77 ± 0.09	0.75 ± 0.18
8	L-Gly	1.29 ± 0.05	0.96 ± 0.09	0.61 ± 0.17
9	L-Ala	1.03 ± 0.16	0.81 ± 0.04	0.65 ± 0.09
10	L-Pro	1.37 ± 0.05	1.23 ± 0.10	1.23 ± 0.08
11	L-Met	1.00 ± 0.18	0.95 ± 0.13	0.77 ± 0.13
12	L-Val	1.14 ± 0.17	1.03 ± 0.17	0.88 ± 0.09
13	L-Phe	1.76 ± 0.11	1.57 ± 0.10	1.19 ± 0.10
14	L-Ile	0.92 ± 0.08	0.82 ± 0.05	0.65 ± 0.09
15	L-Leu	1.20 ± 0.05	1.01 ± 0.19	0.89 ± 0.11
16	L-His	1.54 ± 0.08	1.25 ± 0.04	0.96 ± 0.09
17	L-Orn	0.93 ± 0.06	0.77 ± 0.16	0.63 ± 0.17
18	L-Lys	1.01 ± 0.28	0.91 ± 0.33	0.80 ± 0.08

4.3.4. Effect of delipidization of the SC on $K_{COR/W}$ (comparison of $K_{SC/W}$ and $K_{COR/W}$)

The effect of the lipid content of the SC on $K_{COR/W}$ was investigated and the results are reported in Fig. 5. The results indicate that the presence of the lipid content in the SC slightly affects the $K_{COR/W}$ of the FAAs. The $K_{COR/W}$ was lower in the intact SC as compared to the data obtained for delipidated SC ($K_{COR/W}$).

4.3.5. Effect of permeation enhancers on $K_{COR/W}$

The effect of different permeation enhancers was investigated using the PHSC as a skin model. As can be seen from Table 14, all the selected diffusion enhancers have a significant effect on the FAA uptake by isolated corneocytes.

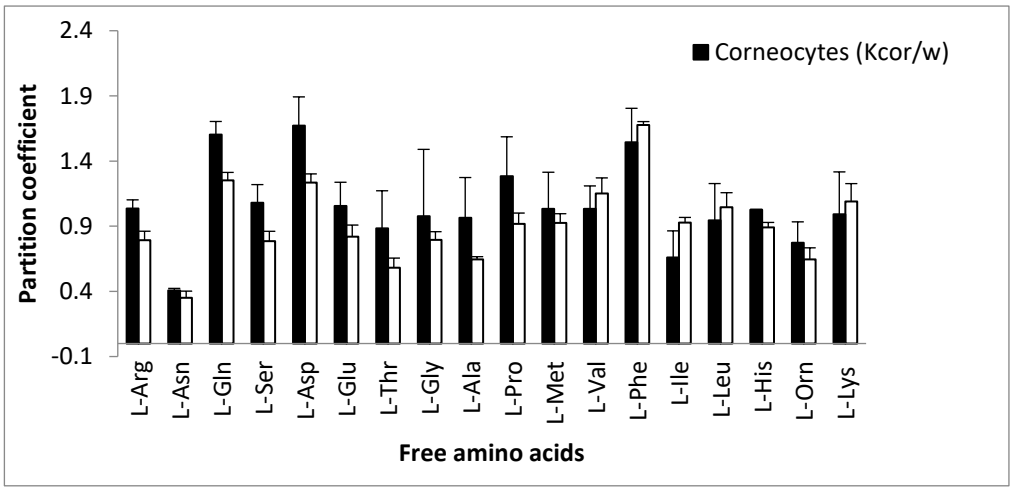

Fig. 5: Effect of delipidization of SC on Corneocyte-water partition coefficients ($K_{COR/W}$) of 18 free amino acids

Table 14: Effect of chemical permeation enhancers on the corneocyte-water uptake coefficients ($K_{COR/W}$) of 18 FAAs (n=3, means ± SD).

S/N	FAAs	$K_{COR/W}$					
		Water	PG	NMP	2-P	DMSO	Transcutol
1	L-Arg	1.04 ± 0.06	1.09±0.14	1.64±0.07	1.32±0.06	1.42±0.05	1.68±0.16
2	L-Asn	0.41 ± 0.02	0.85±0.05	1.19±0.13	1.11±0.06	1.19±0.06	1.54±0.05
3	L-Gln	1.60 ± 0.10	0.96±0.03	1.78±0.02	1.65±0.04	1.37±0.08	1.75±0.17
4	L-Ser	1.08 ± 0.14	0.98±0.08	1.43±0.06	1.21±0.04	1.49±0.17	1.78±0.17
5	L-Asp	1.67 ± 0.22	1.35±0.02	1.76±0.04	1.61±0.06	1.48±0.08	1.57±0.05
6	L-Glu	1.06 ± 0.18	1.36±0.05	1.43±0.15	1.20±0.03	1.56±0.08	1.63±0.16
7	L-Thr	0.88 ± 0.28	1.09±0.04	1.21±0.09	1.21±0.04	1.51±0.09	1.83±0.17
8	L-Gly	0.98 ± 0.51	1.01±0.04	1.18±0.10	1.16±0.06	1.48±0.06	1.56±0.15
9	L-Ala	0.96 ± 0.31	1.17±0.03	1.06±0.05	1.88±0.08	1.36±0.08	1.72±0.19
10	L-Pro	1.28 ± 0.30	1.35±0.03	1.55±0.03	1.48±0.06	1.49±0.15	1.71±0.15
11	L-Met	0.93 ± 0.28	1.16±0.02	1.26±0.08	1.22±0.06	1.81±0.07	1.73±0.17
12	L-Val	1.03 ± 0.18	1.13±0.04	1.36±0.06	1.30±0.09	1.50±0.11	1.66±0.16
13	L-Phe	1.54 ± 0.26	1.40±0.03	1.71±0.06	1.44±0.08	1.41±0.15	1.67±0.17
14	L-Ile	0.66 ± 0.20	1.11±0.02	1.15±0.07	1.18±0.05	1.35±0.08	1.44±0.16
15	L-Leu	0.95 ± 0.28	1.11±0.02	1.16±0.05	1.29±0.06	1.44±0.06	1.57±0.16
16	L-His	1.03 ± 0.01	1.39±0.04	1.50±0.05	1.56±0.03	1.30±0.04	1.63±0.14
17	L-Orn	0.77 ± 0.16	1.03±0.02	1.10±0.08	1.28±0.09	1.28±0.04	1.65±0.16
18	L-Lys	0.91 ± 0.33	1.13±0.04	1.21±0.08	1.37±0.07	1.44±0.09	1.80±0.18

PG: propylene glycol, NMP: N-methyl-2-pyrrolidone, 2-P: 2-pyrrolidone, DMSO: dimethylsulphoxide

4.3.6. *In vitro* skin permeation of FAAs

The log Kp value of experimental results were compared with results predicted using four mathematical models (**Table 15)** for the 18 FAAs. The R^2 and MAE values were 0.7420 - 0.7559 and 0.023 - 0.182 respectively.

Table 15: Comparison of experimental skin permeation coefficients (KP) with data predicted using four mathematical models for 18 FAAs

S/N	FAA	MW (g/mol)	Log KOW	Exp'tal Log Kp (cm/h)	Predicted Log Kp (cm/h)			
					Potts & Guy	Bunge & Cleek	Modified Robinson	Mitragotri
1	L-Arg	174.2	-3.79	-6.59	-6.49	-6.65	-4.87	-5.56
2	L-Asn	132	-3.48	-5.91	-6.01	-6.17	-4.73	-4.55
3	L-Gln	147	-3.11	-5.65	-5.84	-5.98	-4.70	-4.94
4	L-Ser	105	-3.00	-5.58	-5.51	-5.65	-4.50	-4.52
5	L-Asp	133	-3.61	-5.98	-6.11	-6.27	-4.75	-4.55
6	L-Glu	147	-3.51	-6.16	-6.13	-6.28	-4.78	-4.93
7	L-Thr	119	-2.83	-5.88	-5.47	-5.61	-4.51	-4.73
8	L-Gly	75	-3.00	-4.26	-5.33	-5.47	-4.32	-3.59
9	L-Ala	89	-2.77	-5.05	-5.25	-5.38	-4.32	-4.52
10	L-Pro	115	-2.62	-4.96	-5.3	-5.43	-4.41	-4.27
11	L-Met	149	-2.10	-5.14	-5.14	-5.25	-4.37	-4.83
12	L-Val	117	-2.29	-5.91	-5.08	-5.20	-4.28	-5.23
13	L-Phe	165	-1.44	-4.69	-4.77	-4.85	-4.14	-4.17
14	L-Ile	131	-1.82	-4.74	-4.83	-4.93	-4.14	-4.48
15	L-Leu	131	-1.72	-4.70	-4.76	-4.86	-4.09	-4.38
16	L-His	155	-2.85	-5.70	-5.71	-5.84	-4.66	-5.01
17	L-Orn	169	-3.6	-6.53	-6.32	-6.47	-4.84	-5.18
18	L-Lys	182	-3.77	-6.92	-6.53	-6.68	-4.88	-5.49
			Regression coefficient (R^2)		**0.7477**	**0.7420**	**0.7559**	**0.7524**
			Mean absolute error (MAE)		**0.045**	**0.023**	**0.182**	**0.149**

4.4. Delivery of free amino acids into and through the stratum corneum of the skin using microemulsions and microemulsion-based hydrogels: Formulation, characterization, and *ex-vivo* permeation studies

Author:	Birhanu Nigusse Kahsay,Sophie Luise Meiser, Johannes Wohlrab, Reinhard H.H. Neubert, Peter Langguth
Status	Submitted to “die Pharmazie”
Publisher:	Govi-Verlag Pharmazautischer Verlag
Author contributions:	RHHN, PL, JW and **BNK** designed the concept and study plan. **BNK** prepared and characterized the colloidal formulations (JW assisted in the toxicity study, and PL & SLM assisted in the rheology study). PL and RHHN supervised the project. **BNK** prepared the draft manuscript. PL, RHHN, ZW, SLM reviewed the draft manuscript. All authors have read and agreed to the final version of the manuscript. PL is the corresponding author.

4.4.1. Formulation and characterization of MEs containing FAAs

After selecting the desired formulation ingredients, the MEs were prepared and characterized as per the procedure outlined in the experimental section. The physico-chemical and particle properties of the MEs are shown in Table 16. The droplet size and polydispersity index (PDI) for all formulations was in the range of 17.43 to 37.40 nm and 0.0.04 to 0.18 respectively. The zeta potentials ranged from -0.53 to -3.51 and the viscosity was in the range of 44.40 to 66.23 cp. While the refractive index and the pH for the four MEs were not significantly different ($p > 0.05$), the globule size and viscosity of the three MEs (ME1, ME2, ME3) were significantly different ($p < 0.05$). ME1 and ME4 had the same formulation components (except for the source of the FAAs) and they had almost similar characteristics.

Table 16: Physico-chemical and particle properties of the different formulations (n=3, means ± SD)

Parameter	Formulation code			
	ME1	ME2	ME3	ME4
Globule size (nm)	17.43 ± 0.26	25.65 ± 0.40	37.40 ± 0.24	20.51 ± 0.09
Polydispersibility index (PDI)	0.18 ± 0.02	0.13 ± 0.01	0.14 ± 0.03	0.04 ± 0.01
Zeta potential (mV)	-0.53 ± 0.09	-3.51± 0.13	-3.01± 0.18	-1.51 ± 0.22
Refractive index	1.42 ± 0.01	1.43 ± 0.03	1.42 ± 0.02	1.43 ± 0.01
Viscosity (cp)	44.40 ± 0.82	53.61 ± 0.99	66.23 ± 1.49	47.01 ± 0.45
pH	6.67 ± 0.31	6.72 ± 0.14	6.77 ± 0.23	6.68 ± 0.20
Thermodynamic stability	Stable	Stable	Stable	Stable
Physical stability (months)	> 12	> 12	> 12	> 12

There was no drug precipitation, phase separation or any color change after the MEs were subjected to the three stress tests (heating cooling cycle, centrifugation, and freeze thaw cycle) indicating that the MEs were thermodynamically stable. Moreover, all the MEs were stable over a period of one year (no evidence of precipitation, crystallization, color change and phase separation were found at room temperature).

4.4.2. Rheology test of the MEBHGs

In the rheology test for the gel formulations strain sweep measurements were made. The formulations showed linear deformation behavior (i.e., moduli were independent of the strain amplitude) below ca. 10 % and a strong decrease in modulus (shear thinning behavior) above the critical strain level (non-linear range). Below the critical strain level, the structure of the gel formulations was intact, they behave solid-like, and storage modulus G' was greater than loss modulus G''. Based on this preliminary test, a deformation amplitude of 1 % was selected for the next frequency sweep (i.e., measurement with varying frequency at fixed amplitude) in the linear viscoelastic range (LVR) from which the storage modulus G' and loss modulus G'' were obtained as shown in Fig. 6.

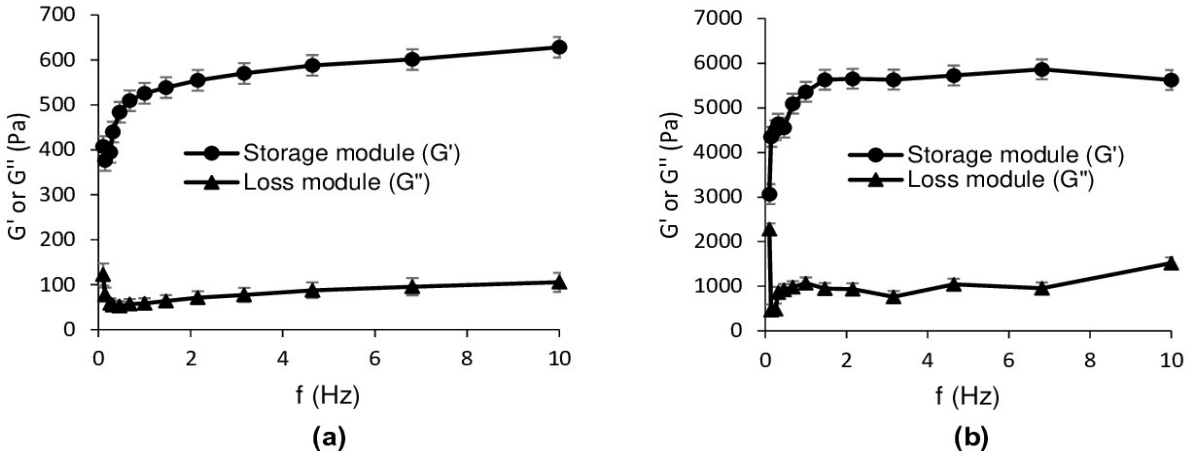

Fig. 6: Frequency sweep for the gel formulations (G’ and G’’ as a function of angular frequency at 1% strain measured at 32 ^{o}C ((a) MEBHG1, (b) MEBHG2).

The results of the shear stress and viscosity at different shear rates are shown in Fig. 7. The viscosity of the hydrogels decreases with increasing shear rate and the shear stress grows slower than linearly with shear rate. At the initial stage, the viscosity of MEBHG2 was higher than MEBHG1, but both decreased to zero at the end of the test. The thixotropic behavior of MEBHG1 was slightly higher than that of MEBHG2. The yield stress for MEBHG1 and MEBHG2 were 118.03 ± 6 Pa and 99.56 ± 4 Pa respectively.

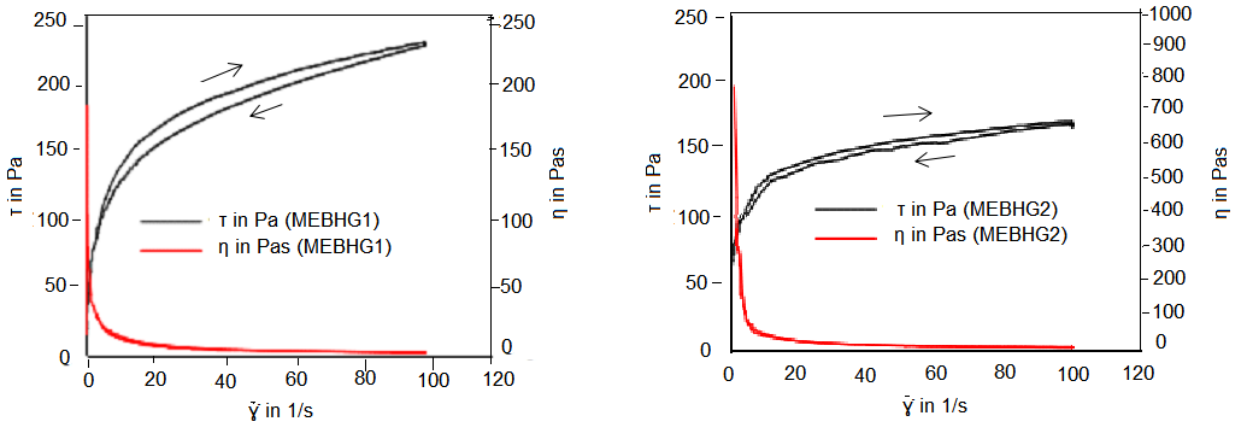

(a) (b)

Fig. 7: Hysteresis loop of the gel formulations (shear stress as a function of controlled shear rate) and viscosity as a function of shear rate measured at 32 °C ((a) MEBHG1, (b) MEBHG2).

4.4.3. Skin irritation study

The irritation scores (ISs) of different MEs and MEBHGs were determined to evaluate the skin irritation or corrosion potential of formulations (Table 17) using HET-CAM. The test was conducted according to the principles of Good Laboratory Practices (GLP). Moreover, the controls carried along with the test prove the validity and integrity of the test and meet the criteria defined accordingly. The results indicate that all the tested formulations show no evidence for irritation potential. 1% SLS had higher IS values, which is classified as strongly irritant.

Table 17: Results of cytotoxicity study

Test sample	Irritation score (IS)	Severity			Irritation potential
		Hemorrhage	Lysis	Coagulation	
Sterile water (n=12)	0	0	0	0	No
1% SLS (n=12)	10.81 ± 0.52	1.50 ± 0.48	0.30 ± 0.65	2.80 ± 0.00	Strong
ME1 (n=6)	0	0	0	0	No
ME2 (n=6)	0	0	0	0	No
ME3 (n=6)	0	0	0	0	No
MEBHG1	0	0	0	0	No
MEBHG2	0	0	0	0	No
MEBHG3	0	0	0	0	No

4.4.4. Ex vivo permeation study

The degree of permeability of the FAAs from the formulations into the different layers of the pig ear skin was determined after 300 min (Fig. 8). In general, the FAAs from the MEs show greater permeation as compared to the H-Cream.

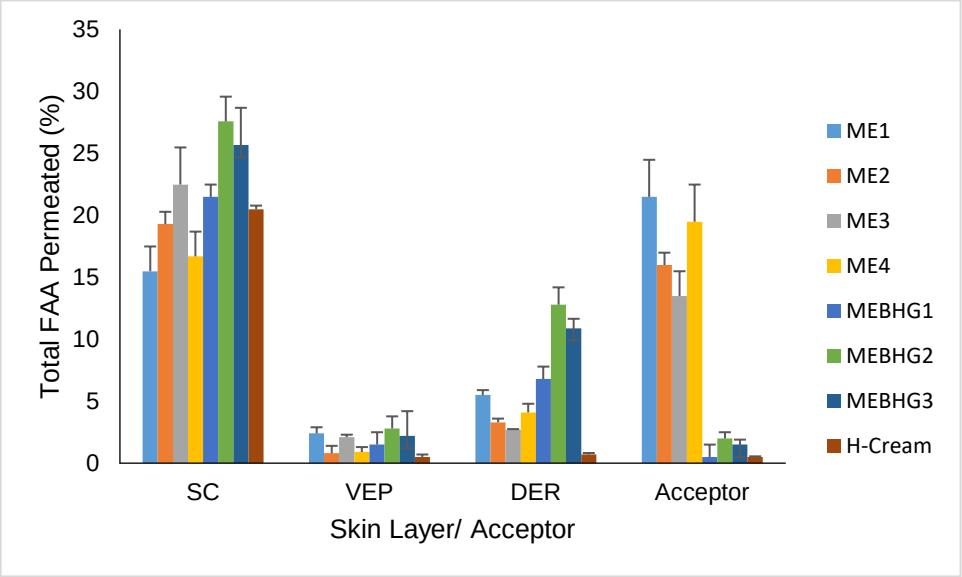

Fig. 8: Percentage of total free amino acids (FAAs) permeated into different layers of the skin from the various formulations (SC: stratum corneum, VEP: viable epidermis, DER: dermis) (n=3, mean ± SD).

The different MEs show also slightly different permeation behavior. For example, at the end of the experiment, the flux of ME1 was higher than that of ME3, even though the latter had a higher content of surfactant/co-surfactant. The permeation of the FAAs to the deeper layers (acceptor chamber) of the skin decreases as the viscosity increases (permeation from MEs was much better and deeper than the MEBHGs). Comparing the two polymers, Poloxamer® 407 based MEBHG2 and MEBHG3 permeated to the different layers of the skin as compared to Carbopol® 934 containing MEBHG1.

4.4.5. Assay content

The assay content of the FAAs loaded into the different formulations were investigated using a validated HPLC/DAD analytical method [Kahsay et al., 2022]. The assay value for all the formulations is shown in Table 18.

Table 18: Assay content of the FAAs in the different formulations (n=3, mean ± SD)

FAA	Assay (%)					
	ME1	ME2	ME3	MEBHG1	MEBHG2	MEBHG3
L-Arg	94.60 ± 1.49	92.67 ± 1.04	94.73 ± 1.97	95.50 ± 1.32	94.80 ± 1.93	97.20 ± 1.64
L-Asn	95.52 ± 1.27	95.90 ± 1.47	95.90 ± 1.92	96.33 ± 1.15	97.47 ± 1.29	95.43 ± 1.25
L-Gln	96.50 ± 1.32	96.40 ±1.64	96.60 ± 0.53	96.73 ± 1.27	95.57 ± 1.69	96.20 ± 1.39
L-Ser	96.73 ± 1.21	96.93 ± 1.30	96.83 ± 1.61	94.40 ± 1.64	96.03 ± 1.27	97.80 ± 0.92
L-Asp	94.93 ± 1.90	93.73 ± 1.03	96.43 ± 1.40	97.47 ± 0.50	97.47 ± 0.92	95.53 ± 0.50
L-Glu	94.83 ± 2.02	97.17 ± 1.66	95.60 ± 1.64	95.60 ± 1.44	96.20 ± 0.72	96.20 ± 1.71
L-Thr	96.13 ± 1.72	95.03 ± 1.54	95.63 ± 0.64	96.27 ± 0.64	94.53 ± 1.29	96.73 ± 1.62
L-Gly	96.70 ± 1.70	94.33 ± 1.14	95.13 ± 1.72	96.57 ± 1.40	95.30 ± 1.47	94.53 ± 1.36
L-Ala	94.30 ± 1.13	93.37 ± 0.64	96.13 ± 1.68	96.83 ± 1.04	96.77 ± 0.97	96.77 ± 1.69
L-Pro	96.47 ± 1.36	95.73 ± 1.55	96.57 ± 1.34	96.33 ± 0.56	94.13 ± 1.47	96.03 ± 1.75
L-Met	97.83 ± 1.32	94.83 ± 1.04	96.17 ± 1.89	96.83 ± 1.61	97.57 ± 1.44	96.47 ± 1.42
L-Val	93.30 ± 1.54	94.67 ± 1.92	95.43 ± 1.83	97.93 ± 1.10	97.03 ± 2.12	97.47 ± 1.36
L-Phe	95.20 ± 1.71	94.53 ± 1.75	96.70 ± 1.21	95.10 ± 1.65	95.87 ± 1.21	94.37 ± 1.98
L-Ile	96.67 ± 1.33	93.83 ± 1.26	99.03 ± 1.70	95.60 ± 1.44	98.17 ± 0.29	95.73 ± 1.62
L-Leu	92.17 ± 1.04	94.60 ± 1.04	96.20 ± 0.72	95.93 ± 1.01	96.87 ± 0.81	95.90 ± 1.28
L-lHis	96.87 ± 1.48	93.70 ± 1.81	97.37 ± 1.02	97.33 ± 1.15	96.73 ± 0.64	95.13 ± 1.21
L-Orn	97.23 ± 0.68	94.47 ± 1.40	94.87 ± 1.03	97.63 ± 1.58	94.27 ± 1.42	95.71 ± 0.61
L-Lys	95.23 ± 1.08	94.57 ± 1.91	97.07 ± 1.10	97.67 ± 1.15	96.83 ±1.61	95.81 ± 0.86

CHAPTER 5: DISCUSSION

5.1. Free amino acid contents of selected Ethiopian plant and fungi species: a search for alternative natural free amino acid sources for cosmeceutical applications

As shown in section 3.1, the FAA contents of the different plant and mushroom species were different from each other. Even though the content of the total FAA could differ from one source to the other, there were consistent findings with regard to the dominant FAAs in most of the investigated materials. Among the tested materials, oyster mushroom (Pleurotus ostreatus) had the highest total FAA content (400.01 mg/g) found in the present study (Table 4). The presence of such molecules may contribute to its characteristic flavor [Mau et al., 1998]. A total FAA content of 161.09 mg/g was reported by Kim et al [2009] after HPLC analysis on this type of mushroom which originated from Korea, and this was lower than the value obtained in the present study. The literature also reveals that there is a significant difference in the total FAA content of different mushroom species [Sun et al., 2017] and this could be due to the difference in the harvesting time, growth condition, geographical origin in addition to the differences in extraction, derivatization, or quantification methods. Oyster mushroom is also reported as a healthy food rich in protein, chitin, vitamins, and minerals which contains many bioactive molecules [Khan and Tania, 2012]. It is ranked second among the important cultivated mushrooms in the world [Jose and Janardhanan, 2000]. The legume plants which are expected to contain high amounts of amino acids had different FAA profiles (Table 4). The dominant FAAs in most of the legume plants were Arg, Asp, Glu, Asn, Gln, and Leu. Previous studies on some of these plants, namely flax seeds [Panaite et al., 2017], common bean [Fukuji et al., 2019; Saboori-Robat et al., 2019], and sunflower seeds [Robinson, 1975] also indicated that the stated FAAs were found at relatively higher concentration as compared to the other FAAs. However, the concentrations obtained were different possibly due to the difference in testing methodology and source of the materials. It is also mentioned in the literature that soybean seeds can store nitrogen mostly in the form of either proteins or FAAs [Takahashi et al., 2003].

There were also some studies done on the FAA content of some vegetables. In a study by Gomes and Rosa [2001], 17 FAAs were detected in different broccoli cultivars and the dominant amino acids were Gln and Glu. A study by Oliveira [2008], reported the total FAA content ranged from 3.30 to 14.40 mg/g after HPLC/UV analysis, indicated that the dominant FAAs in cabbage were Arg, Pro, and Thr. In the present study, the dominant FAAs found in broccoli and cabbage were Arg, Asp, and Glu. Garlic and Ethiopian onion were dominated by FAAs such as Arg, Glu, Lys, Asn, Gln, Asp, Leu, Gln, Try, and Ala (Table 4). A study by Lee and Harnly [2005] indicated that 18 FAAs were present in garlic and Gln, Asn, Glu, Lys, Pro, and Ser were reported as the dominant FAAs. Ethiopian potato and tomato were also dominated with free form Gln, Asn, and Asp. Investigation on other potato species also indicated that FAAs of high concentration were obtained after extracting with hot water [Furudate and

Meguro, 2001]. Even though it is mentioned in the literature that Cit occurs most abundantly in Cucurbitaceous plants [Joshi and Fernie, 2017], zucchini and cucumber had low concentration of this compound (Table 4).

The dominant FAAs in most of the fruit samples were Asn, GABA, Asp, Glu, Gln, Ala, Ser, and Lys and this was consistent with a previous study done by Zeng et al [2015]. Among the common Ethiopian spices, ginger had the highest total FAA (248.50 mg/g). While the content of Asp, Asn, Ala, Glu and Arg were relatively higher than the other FAAs, the Met content was found at a very low concentration (0.04 mg/g). Ogbuewu et al. [2014] who tested 17 amino acids in ginger reported a total amino acid content of 256.10 mg/g, also indicated Arg as the most dominant amino acid and Met at relatively lower concentration compared to the other FAAs. Reports on cumin also indicate that the seeds of this plant are rich in FAAs [Badr and Georgiev, 1990; Toghrol and Daneshpejouh, 1974]. Moreover, a study by Yimer et al. [2019] revealed that Glu, Arg, and Asp are the major amino acids found in black cumin which is consistent with the present study. A study on hot pepper seeds grown in China, where 18 amino acids were detected, showed that the main amino acids were Glu and Asp (both of which had concentrations of above 20.00 mg/g) [Zou et al., 2015].

Chamomile, which is often referred to as the “star among medicinal species”, is a well-known medicinal plant species from the Asteraceae family [Singh et al., 2011]. The dominant FAAs in chamomile were Asn, Gln, Asp, Glu, Lys, Arg, and Pro. Very close findings were reported by Ma et al. [2015] in which 15 FAAs were detected and analyzed by HPLC. Oleo species have been commonly used in the cosmetics industry. In this study, the total FAA content and the types of the dominant FAAs were different among the species. In previous study by Kim et al. [2013], a total of 24, 23 and 17 amino acids were detected in three species of aloe, namely, Aleo vera (L.) Burm.f., A. saponaria (Aiton) Haw., and Aleo arborescens Mill., respectively, indicating that different species can have different composition. Among the herbs, hemp is reported in many research areas. In the present study, it had total FAA content of 195.01 mg/g. Previous studies on protein isolates of hemp also revealed that the plant had high amounts of amino acids [Tang et al., 2006]

In general, the present study revealed that FAAs for cosmeceutical applications can be obtained from several nature-based resources. As reported by Hussain et al [2019], the concentration of each FAA in the stratum corneum of healthy human skin is less than 10.00 nmol/mg indicating that only very low amounts of these bioactive molecules are required in formulations pertaining to replacement therapies for the treatment of dry skin conditions. As can be seen from the results in Table 1, the concentration of most of the FAAs was greater than 15.00 mg/g which is enough for dermatological preparations for the management of dry skin condition. Natural sources including but not limited to oyster mushroom, broccoli, garlic, Ethiopian onion, ginger, cabbage, cumin, and decoco contain a significant amount of

most of the FAAs. Among the tested FAAs, free Asp, Asn, Glu, Arg, Gln, GABA, His, Ala, Ser, Thr, Tyr, Try, Leu, Ile, Val, Pro, Phe, Gly, Pro, and Lys were dominantly found in these and other plants. Even though the remaining FAAs, namely, Tau, Cit, Orn, oxyproline, O-acetylserine, and methionine oxide were found at low concentrations, they were found in sufficient quantity in some of the plants and in the mushroom. For example, oyster mushroom can be considered as source of Met, Cys and Orn. Moreover, sufficient amount of Tau and O-acetylserine were obtained in black mustard; and reasonable content of Cit was obtained in garlic. Hence, a crude extract of some of the stated plants have all the required FAAs and use of such resources for cosmeceutical applications has a great advantage over other sources (synthetic, enzymatic, and fermentation) in terms of economic benefits besides other nature-related advantages.

The natural products that had the highest amounts of FAAs as per the current study have also been used in many cosmeceutical preparations. For example, “Birch Water Purifying Essence”, “Larecea™ Extract”. and “Onion Juice Cream” are some examples of commercially available cosmeceutical preparations which contain extracts from mushroom, broccoli, and onion as their main components. Despite the few commercial moisturizers that contain nature-based extracts, to our knowledge, much research work has not been done on topical formulations loaded with plant or mushroom-based FAAs. The current study gives a clear insight to the natural products with high amounts of FAAs and will help to fill the research gap in topical preparations loaded with plant or mushroom-based FAA.

5.2. Development and validation of a simple, selective, and accurate reversed-phase liquid chromatographic method with diode array detection (RP-HPLC/DAD) for the simultaneous analysis of 18 free amino acids in topical formulations

Before conducting the validation work, some preliminary study (method validation) was done to optimize the sample pre-treatment, derivatization, and chromatographic conditions as highlighted in section 3.2.1 to 3.2.2. One common disadvantage of using Fmoc-Cl as derivatizing reagent in the HPLC analysis of FAAs is its reactivity towards water: Following hydrolysis and decarboxylation, Fmoc-OH is formed and its peak interferes with the peak area of some of the FAAs. Hence, an appropriate reagent should be selected to prepare the derivatizing reagent and remove the excess of Fmoc-Cl. As stated in section 3.2.1, preparing the Fmoc-Cl in acetone resulted in a broad and big interfering peak as compared to that of acetonitrile. With regard to the removal of the unconsumed Fmoc-Cl reagent, *n*-pentane is reported as the most common reagent [Bank et al., 1996]. Other reagents such as adamantanamine [Fabiani et al., 2006] or heptylamine [Kirschbaum et al., 1994] are also reported in the literature. In this study, compared to *n*-pentane, better results were obtained when ADAM was used in terms of time, effectiveness of removal of the excess reagent, resolution (of the interfering peak to that of the FAAs), and peak shape. Moreover, the concentrations obtained after

extraction with *n*-pentane were lower than that obtained after reaction with ADAM, maybe due to considerable loss of the derivatized FAAs during the removal of excess *n*-pentane. Hence, acetonitrile and ADAM were used to prepare the Fmoc-Cl solution and to remove the excess Fmoc-Cl, respectively.

For Fmoc-Cl derivatization, most commonly used is borate buffer [López-Cervantes et al., 2006; You et al., 2007; Lozanov et al., 2004; Gustavsson and Betnér, 1990] and hence, this buffer was used in the present study. The higher the concentration of the derivatizing reagent, the more effective the derivatization. This could be due to the promotion of reactivity of amine functional groups with the derivatization reagent at the highest concentration of borate buffer. In the literature, it is reported that borate buffer is used in a wide concentration ranging, from 0.20 M [You et al., 2007], to 0.325 M [Lozanov et al., 2004], and up to 0.5 M [Gustavsson and Betnér, 1990]. The derivatization yield was also dependent on the pH of the borate buffer. The derivatization capacity of the buffer was good at higher pH. Despite this fact, performing derivatizations in reaction media at pH $\geq$ 10.0 had several disadvantages including increased hydrolysis rate of the reagent, the need of high Fmoc concentration to ensure its excess, and the appearance of a huge Fmoc-OH peak. Hence, a lower pH of 8.6 was selected for the derivatization. In the literature, buffer-pH values in the range 6 to 11.4 are reported, most of which are in the range of pH 8.0-9.0 [Haynes et al., 1991, Lozanov et al., 2004], and this is consistent with the present work.

Once the derivatization technique was optimized, some experiments were done to select an appropriate analytical column and to optimize the chromatographic conditions. As outlined in section 3.2.3, an Agilent InfinityLab Poroshell 120 E.C 18 (3 x 50) mm, 2.7 µm was used for the validation activity. Such columns are based on superficially porous particle technology, which features a solid silica core and a porous outer layer. Compared to traditional totally porous particles of the same (or similar) size, Poroshell particles deliver exceptional efficiency and reliability enabling fast and high-resolution separations. It provides superior peak shapes for faster, more accurate results due to high-purity silica and advanced bonding chemistry. This column is known for its excellent lot-to-lot reproducibility giving confidence in chromatographic separations [Agilent Technologies, 2020] and was used for the validation activity. The composition and pH of the mobile phase, column temperature and flow rate were optimized based on experimental results as stated in section 3.2.2.

Finally, before performing the validation work, the robustness of the analytical method and system suitability test were investigated. The robustness of an analytical procedure is a measure of its capacity to remain unaffected by small, but deliberate variations in method parameters and provides an indication of its reliability during normal usage. In the present study, small changes in pH of mobile phase (solvent A), flow rate, and column temperature had no significant effect on the chromatographic

performance. The stock solutions were also stable for two weeks at -20 ^{0}C before derivatization and for 24 h after derivatization in an HPLC auto-sampler at 4 ^{0}C. Hence, the method conditions can be considered robust.

System suitability testing (SST) is an integral part of many analytical procedures. In this study, such a test was done, and the results are shown in Table 5 and Fig. 3. The higher the plate number N, the greater the efficiency of the column. The lower the HETP, the better the resolution and the more efficient the separation. Efficiency is optimized when N is maximized and HETP is minimized. As can be seen from Table 5, the theoretical plate numbers for all the analytes were above 18,000 and the HETP was very low (not more than 2). The tailing factor was within the pharmacopeial requirements (< 2.0). The resolutions among the different analytes were above 2.0 for most of the FAAs indicating sufficient resolution between successive peaks. The % RSD of each set of parameters (retention time, peak area, tailing factor, efficiency, and HETP) was less than 2% indicating the reproducibility of RP-HPLC/DAD system for quantitative analysis of the eighteen FAAs. Hence, the method fulfills the acceptance criteria for the mentioned SST parameters.

After optimizing the derivatization and chromatographic conditions, the full validation work was done. All validation parameters including specificity/selectivity, linearity, LOD, LOQ, accuracy, and precision were investigated. The specificity of an analytical method is the ability to assess unequivocally the analyte in the presence of components which may be expected to be present. As can be seen in Fig. 4, the validated method is specific for the selected FAAs. Moreover, the minimal differences between retention times and peak area (% difference of less than 0.5 %) in case of the standard and sample solutions allow confident and highly specific peak identification.

The linearity of an analytical procedure is the ability of the analytical method to obtain test results which are directly proportional to the concentration of analyte in the sample. The results in Table 6 show that R^2 were greater than 0.995 indicating excellent linearity, which implies the reliable quantitation of FAAs. From the LOD and LOQ values (Table 6), the developed method can be considered sensitive enough to detect low concentrations of the FAAs. In the literature, it is stated that Fmoc based derivatization of FAAs had better sensitivity than the other derivatizing reagents. López-Cervantes et al. [2006] reported detection limits in the range of 23-72 ng/mL. LOD values in the range of 3 to 6 µM were obtained by the work of Fabiani et al. [2002]. Garside et al. [1988] also reported a detection limit of 0.5 µM with fluorescence detection system and this was very close to the sensitivity of the current method.

The precision of an analytical procedure expresses the closeness of agreement (degree of scatter) between a series of measurements obtained from multiple sampling of the same homogeneous sample under the prescribed conditions. Repeatability, also called intra-day precision, expresses the

precision under the same operating conditions over a short interval of time. It was determined on six determinations at 100% concentration of the test solution (20 µM). The results in Table 7 show that the validated method fulfills the requirements for precision (the % RSD was < 2%). Intermediate precision expresses within-laboratories variations: different days, different analysts, different equipment, etc. As shown in Table 8, the method fulfills the requirements for intermediate precision (the overall % RSD was < 2 %). Hence, the validated analytical method is precise.

The accuracy of an analytical procedure expresses the closeness of agreement between the value which is accepted either as a conventional true value or an accepted reference value and the value found. As can be seen from the results (Table 9), the values were within the acceptance criteria (90-110 %) stated in the ICH guideline [ICH, 2005] indicating the accuracy of the analytical method.

Finally, the applicability of the method in routine quality control testing was confirmed by conducting assay determinations on topical preparations. The results (Table 10) confirm that the developed method can be applied to any liquid and/or semisolid topical dosage forms without any further modification or after simple method verification. In summary, the results indicate that this new method fulfills all the validation requirements of an analytical method as stated in the ICH Q2 (R1) guideline and can be applied to liquid and semi-solid preparations.

5.3. Corneocytary pathway across the stratum corneum: Identification of model systems and parameters to study dermal delivery of free amino acids

The aim of this section was to identify alternative skin models/types (by studying $K_{COR/W}$) to study the corneocytary diffusion pathway of the FAAs and to study the skin permeation coefficient (K_P) values of selected FAAs. As reported in Table 11, there was a difference in the uptake of FAAs among the three different skin models (PHSC, pig ear skin and keratin particles). Even though the $K_{COR/W}$ values were higher in pig ear skin than that of PHSC, the differences were not significant for most of the FAAs ($p > 0.05$) except for some of the FAAs such as L-Arg, L-Glu, L-Met, L-His, and L-Lys ($p < 0.005$). There are contradicting reports on the similarity of human and pig skin in terms of permeation. Some studies indicated that the permeation of human and pig ear skin is close to each other [Dick and Scott, 1992; Singh et al., 2002; Moniz et al., 2021], while others indicate that animal skin (including pig skin) shows differences in permeation from human skin and is often more permeable [Feldmann and Maibach, 1970; Bronaugh and Stewart, 1985]. To avoid the overestimation of the human percutaneous skin absorption by using the pig skin as a substitute, the $K_{SC/V}$ value of PHSC was plotted against that of the pig ear skin. As shown in Eq. 8, a good $K_{COR/W}$ correlation was obtained between the PHSC and that of pig ear skin with an R^2 value of 0.9784. Hence, when the pig skin ear is used such correlation should be considered.

$$K_{COR/W}\,(\text{pig ear SC}) = 1.0101\ K_{COR/W}\,(\text{PHSC}) + 0.1834 \qquad \text{(Eq 8)}$$

Many factors including SC separation technique, initial concentration of the FAAs, delipidization of the SC, and permeaton enhancers can affect the $K_{COR/W}$ value of the FAAs. Each of these factors were investigated and the results are as stated in section 3.3.2-3.3.4. The epidermal-dermal junction (EDJ) is mainly maintained by groups of cell surface protein complexes [Briggaman, 1982]. The breakdown of such complexes is a critical step in dermal-epidermal separation. In the present work, the SC was separated from the other underlying layers of the skin using four techniques of the skin and the effect of such separation techniques on the $K_{COR/W}$ was insignificant (Table 12). Among the tested techniques, the "heat treatment in water" was the most rapid and facile. Even though the applied heat does not modify fibrous proteins within the isolated epidermis [Baden and Gifford, 1970], some practical problems arose when using a hot plate. There was an uneven separation of the epidermis over the complete skin surface, and this may be due to gradual thermal diffusion which required additional time to fully separate the two layers. It is also known that heat-separated epidermis and dermis significantly lose viability [Wester et al., 1998]. Despite these drawbacks, the $K_{COR/W}$ values were not significantly different from those obtained in the other techniques. The enzyme treatment method for the separation of the epidermis from the dermis involves the use various proteases including dispase, pancreatin, trypsin, pronase, collagenase, and elastase [Becker et al., 1952; Einbinder et al., 1966; Walzer et al., 1989; Zou and Maibach, 2018]. In the current study, dispase II, a neutral protease found in Bacillus polymyxa capable of digesting lamina densa by cleaving the extracellular matrix components such as type IV collagen and fibronectin [Stenn et al., 1989], was selected. The epidermis-dermis separation using this enzyme was gentle but effective which was in agreement with previous reports [Kitano and Okada, 1983; Stenn et al., 1989]. This proteolytic enzyme can cleave the basement membrane zone region while preserving the viability of the epithelial cells. Relatively intact epidermal sheets were obtained with this technique. The use of EDTA was problematic because incomplete epidermal-dermal separation frequently occurred, reducing substantially the SC yield.

As shown in Table 13, the $K_{COR/W}$ values tend to decrease with increasing C_i. This type of behavior has been previously reported [Chandrasekaran et al., 1980; Surber et al., 1990] in which the existence of bound and freely diffusible molecules within the SC is postulated. As the number of molecules available for partitioning into the SC increases, the immobilized fraction becomes saturated while the unbound compound can continue to rise. Hence, the measured $K_{COR/W}$ may not be consistent with increasing concentration until the binding sites in the SC are saturated.

Before conducting the study on the effect of the lipid content of the SC on $K_{COR/W}$, the lipid content was determined after separating the SC sheets from the rest of the epidermal sheets to confirm its values with the reported data. The total lipid content of the SC of pig ear was 9.08 ± 0.75 % and this was consistent with data reported by Gray and Yardley (8.0%) [Gray and Yardley, 1975]. As can be

seen from Fig 5, the presence of the lipid content in the SC slightly affects the $K_{COR/W}$ of the FAAs. The $K_{COR/W}$ was lower in the intact SC as compared to the data obtained for delipidated SC ($K_{COR/W}$). In intact SC a fraction of the volume is made up by lipids. The partition coefficient of FAA into the lipids would be lower, i.e., the partition coefficient into the same volume of lipids + CORs would be lower than into CORs.

The permeation enhancers were carefully selected based on their enhancing mechanism (i.e those enhancers that can enhance permeation by increasing partitioning property of the drug to the skin and/or the interaction of drug with the CORs or keratin were selected). As can be seen from Table 14, the permeation enhancers increased the uptake of the FAAs by isolated corneocytes. Relatively higher $K_{COR/W}$ was obtained in the presence of transcutol® P followed by N-methyl-2-pyrrolidone and 2-pyrrolidone. Hence, the inclusion of these permeation enhancers will increase the partitioning of the FAAs to the corneocyte part of the SC.

From the above COR-water partitioning studies, it is clear that the FAAs have high partitioning behaviour to the CORs in aqueous vehicle suggesting their suitability for the corneocytary pathway. This was consistent with some studies conducted by other authors. Chen et al, [2010, 2013] proposed transcellular diffusion of hydrophilic molecules through highly resistive CORs. Hussain et al., [2019 (a)] showed that urea, taurine and amino acids are able to diffuse into isolated CORs. Furthermore, it was found that hydrophilic permeation enhancer molecules such as urea and taurine do not influence the nanostructure of the SC lipids [Mueller et al., 2016] showing that hydrophilic permeation enhancers do not influence the nanostructure of the SC lipids. Water is also able to diffuse easily into the CORs [von Hal et al., 1996; Nakazawa et al., 2012] indicating that the passage through the CORs is substantial for small hydrophilic molecules such as amino acids, urea and small peptides. Hence, the corneocytary pathway (via COR and the corneodesmosomes) could allow the diffusion of hydrophilic drugs to pass through the SC [Barry, 1987; Moser et al., 2001]

In addition to the $K_{COR/W}$, the permeability coefficient (K_P) is very important parameter in the literature. The KP values of the 18 FAAs is as shown in Table 15. The KP values were very low, as expected, due to the hydrophilic nature of the FAAs. An attempt was also done if the available mathematical models could predict the skin permeation of these compounds by comparing the experimental K_P values with the predictive values (Table 15). The most frequently quoted models, in particular simple mathematical models of quantitative structure permeability relationships (QSPR), assume SC lipid as the main pathway for skin permeation and their applicability for hydrophilic molecules could have some limitations [Chen et al., 2013]. This indicates the need for polar pathway. Hence, the four models were selected to represent both the SC polar and lipid pathways. As seen from the predictive K_P values in

Table 15, the lipid barrier models (Potts & Guy, Bunge & Cleek) provide relatively reasonable fits to the data as compared to the models that include a polar pathway (modified Robinson and Mitragotri). The later over-predicts the Kp value. The over-prediction by the modified Robinson model could be due to the assumption of water-like diffusivity in the polar pathway. The FAAs could penetrate more poorly than the modified Robinson model predicts. The Mitragotri model considers four possible skin permeation pathways, namely, (1) free-volume diffusion through lipid bilayers, (2) lateral diffusion along lipid bilayers, (3) diffusion through aqueous pores in lipid bilayers and (4) diffusion through shunts. Being polar solutes, there could be hindered diffusion of the FAAs through the two polar pathways (shunts and pores) [Kasting et al., 2019] and this could result in the over prediction of the Kp values.

The mathematical models did not consider the corneocytary pathway and the possible entrapment of the FAAs by the CORs in their calculations. Theoretically, this was expected to result in different permeation ability than what was predicted from the mathematical models. Despite this fact, the models gave good prediction (from a water vehicle) without considering a possible corneocytary pathway. Hence, even though further study could be required to develop more accurate models (that considers the corneocytary pathway), the stated models are able to reasonably predict the skin permeation of the FAAs.

5.4. Delivery of free amino acids into and through the stratum corneum of the skin using microemulsions and microemulsion-based hydrogels: Formulation, characterization, and *ex-vivo* permeation studies

FAAs are assumed to follow the corneocytary pathway (diffusion into the corneocytes) when they are applied to the skin. The delivery of these compounds to the desired sites of the skin is challenging due to their hydrophilic nature. In the present study, colloidal preparations (in the form of MEs and MEBHGs) were prepared to overcome the barrier function of the SC for these FAAs. As shown in Table 1, the prepared MEs had very small (nano-size internal droplets) and uniform droplet size (PDI very close to zero) indicating their desired particle properties [Souto et al., 2022]. The small droplet size of the MEs might be due to the lowering of the interfacial tension by the surfactant mixture. The surfactant mixture reduces the curvature of nano-droplets, therefore providing them a very low globule size [Tenjarla, 1999]. The particle size of ME3 was highest among all the MEs and this could be due to the higher concentration of oil in this formulation. The prepared MEs had low viscosity implying that they can spread easily on the skin. The viscosity increased with increasing surfactant concentration (viscosity of ME1 < ME2 < ME3) and this might be due to the intrinsic viscosity of surfactants [Roohinejad et al., 2015]. The refractive index of all MEs was consistent and was close to that of water (1.33) confirming that the MEs were oil-in-water type. The pH value for all the MEs was around neutral

and this is generally acceptable for products that are meant for topical application [Martinez-Pla et al., 2004]. All the MEs were also stable over a period of 12 months indicating the suitability of the formulation design and the selected formulation ingredients.

The low viscosity of MEs is often considered a limitation for application to the skin. To overcome this problem, their viscosity was increased by addition of polymers Carbopol® 934 (MEHG1) and Poloxamer® 407 (MEBHG2 and MEBHG3). The rheological properties of these two polymers were investigated and compared (MEBHG2 and MEBHG3 had similar rheological properties and hence only MEBHG1 and MEBHG2 were compared). As shown in the frequency sweep experiment (Fig. 6), the storage modulus G' was higher than the loss modulus G'' in both gelling agents. This indicates that the elastic properties prevailed over the viscous behavior and hence structural stability in the tested range. Over the range of angular frequencies from 100 to 0.1 rad/s the G' values showed a weak frequency dependence indicating that both formulations are within the gel state. Comparing the two polymers, those thickened with Poloxamer 407 (MEBHG2) were characterized by enhanced toughness (higher values of G′ modulus) in the presence of shearing forces than that of Carbopol based hydrogel (MEBHG1). This shows the formation of an extended three-dimensional network and hence strong elastic behavior when Poloxamer 407 was used as gelling agent. The lower G' value of the Carbopol based hydrogel (MEBHG1) might indicate the weak interactions between polymer chains resulting also in weakening of elastic properties [Froelich et al., 2015]. In the hysteresis loop (Fig. 7) the upward ramp shows a higher shear stress compared to the downwards ramp indicating that the sample's behavior is time-dependent under shear load. Furthermore, the viscosity of the hydrogels decreases with increasing shear rate. These indicate that the preparations have non-Newtonian shear-thinning behavior. Thixotropic properties are very important for the topical application of pharmaceutical semi-solid formulations [Lee et al., 2009]. As shown in Fig. 7, the traces of shear stress for increasing and decreasing shear rate overlap with only minor difference and both formulations have thixotropic behavior. The yield stress values of the prepared hydrogels were within the range of typical semisolid formulations (yield stress value greater than 20 Pa) [Dragicevic-Curic et al., 2009].

The surfactant(s) used in the preparation of MEs might irritate tissues [Zhong et al., 2009]. Moreover, the co-surfactants and oils used might irritate the skin when used at higher concentrations. Therefore, it is recommended to investigate the irritation and corrosive potential of the MEs and MEBHGs. Even though there are some established animal *in vivo* methods designed to conduct skin irritation and toxicity studies [Chen et al., 2007; Gannu et al., 2010], they need exploitation of experimental animals. Since recent years, Hen's egg test chorioallantoic membrane (HET-CAM) test was developed as a sound alternative to the animal *in vivo* tests used to investigate the corrosive potential of

pharmaceutical preparations on the skin and mucus membrane [Moniruzzaman et al., 2010; Goebel et al., 2010]. Hence, this method was used to evaluate the compatibility of the preparations with the skin. The results clearly showed that all the MEs and MEBHGs were non-irritant with all MEs with IS values zero (same result as that of water) (Table 17). This shows neither the surfactants mixture nor the oil phase cause skin irritation and corrosion. This could be due to the smaller amount of these components in the formulations.

As shown in Fig. 8, the FAA loaded formulations have different skin permeability. The MEs ensure better permeation for the FAAs as compared to the H-Cream vehicle since FAAs did not permeate into the deeper layers of the SC and other skin layers even after 300 min from the hydrophilic cream. This difference might be due to the small droplet size and large surface area to volume ratio of the ME [Schwarz et al., 1995, Zhou et al., 2009]. Similar trends were reported in the literature [Friedman et al., 1995; Schwarz et al., 1995; Otto et al., 2009; Sahle et al., 2013]. In addition to the droplet size, the thermodynamic activity of the FAAs in the ME might also have been modified to favor partitioning into the SC [Kreilgaard, 2002]. The surfactant and co-surfactant in the MEs may also reduce the diffusional barrier of the SC by acting as penetration enhancers [Rhee et al., 2001]. Moreover, the permeation enhancers could contribute to this phenomenon. There was also a slight difference within the permeation behavior of the MEs. For example, the flux of FAAs from ME1 was higher than that of ME3, even though the latter had a higher content of surfactant/co-surfactant. This might be due to the lower droplet size in ME1. It could also be the effect of the water on the ME internal structure, which in turn influences drug delivery to the skin. As water itself is seen as a permeation enhancer for hydrophilic compounds, the permeation of the FAAs could increase due to a hydration effect on the SC if the water content in ME is sufficiently high. Similar trends were reported by [Delgado-Charro et al., 1997; Araujo et al., 2010; Zhang and Michniak-Kohn, 2011; Cichewicz et al., 2013]. The incorporation of the polymers Carbopol® 934 and Poloxamer 407 significantly controlled the permeation of the FAAs into deeper layers of the skin (Fig. 8). The permeation decreases as the viscosity increases (permeation from MEs was more rapid and deeper into the skin than the MEBHGs ($p < 0.05$). This could be due to slower FAA diffusion and partitioning that could occur to a smaller extent in viscous formulations limiting drug transport across the SC. Similar findings were reported for other compounds in the literature [Huang et al., 2008; Rozman et al.,2009]. Comparing the two polymers, Poloxamer® 407 based MEBHG2 and MEBHG3 permeated to the different layers of the skin as compared to Carbopol® 934 containing MEBHG1. This could be due to the temperature dependent gelling property of Poloxamer® 407. MEBHG2 is liquid at room temperature and some part of the FAAs might permeate before the in-situ gel on the skin surface has formed. Finally, as indicated in Table 18, the assay values were within the range of (90-110 %) and fulfill the common pharmacopoeia requirements for drug content. This indicated that the FAAs were uniformly distributed throughout the formulations and

their loss was minimum during preparation of MEs and MEBHGs. As seen from the results section, the ME prepared from the standard FAAs (ME1) and that prepared from the mushroom extract (ME4) had similar characteristics. Similarly, MEBHG2 and MEBHG3 had almost similar physico-chemical and permeation properties. This indicates that FAAs extracted from nature-based sources can be used as alternative sources in resource constraint conditions.

CHAPTER 6: CONCLUSIONS

FAAs, the major components of the so called NMFs, not only act as humectants in the skin but are also responsible to maintain the acidic pH of the skin. Decreased amounts of FAAs have been reported in pathological dry skin conditions associated with AD, psoriasis (PS) and in ageing skin. The treatment option for disease conditions such as the dry skin condition is to reconstruct the natural chemical composition of the skin by topical application of these compounds. However, much research has not been done on the dermal delivery of the most important FAAs. The present work, therefore, aimed at the preparation and characterization of colloidal and standard preparations loaded with FAAs for dermal delivery.

The FAAs used for such formulations were obtained from extraction of plants and from synthetic routes and both formulations were compared. In finding the best source of FAAs, the FAA profile of about 59 plants and fungi were investigated. After collection, the FAAs were extracted, derivatized using FMOC Cl and then quantified using a sensitive and selective LC-ESI-MS/MS method. The results indicate that most of the investigated plants and mushroom have all the 27 investigated FAAs. Among the tested plant and fungus materials, those with very short harvesting period (such as broccoli, oyster mushroom, ginger, garlic, pepper, and cabbage) can be considered as sources of the FAAs. This indicates that most of the FAAs can be extracted and purified from a single natural resource. Use of such nature-based molecules for cosmeceutical purpose in biodiversity-rich countries like Ethiopia could have economic advantages in addition to its therepeautic benefit. It also helps in fulfilling customer satisfactions by fostering modern natural remedial approaches. 18 FAAs, which are also the major components of the FAAs of the NMFs, were obtained in the crude extract after the bulk extraction and purification of oyster mushroom.

After the appropriate FAAs for topical application were selected, a new, rapid, reliable, and accurate RP-HPLC/DAD method was developed and validated according to the ICH guideline. The method was able to simultaneously analyze 18 FAAs in topical formulations. The developed method offers excellent selectivity, sensitivity, linearity, precision, and accuracy. The most common drawbacks of FMOC-Cl based chromatographic systems for the FAAs (such as poor chromatogram due to lack of resolution and peak shape) were fully resolved. Compared to other reported methods, the current method involves a simple sample preparation and derivatization method, a very short analysis time, and is very economical with respect to the consumption of reagents. The validated method can be adapted by official pharmacopoeias and can be used in pharmaceutical and/or cosmeceutical quality control laboratories.

The results of the $K_{COR/W}$ of the FAA indicated that the three skin models (keratin particles, pig ear skin and PHSC) exhibited different skin partitioning properties. A relatively closer correlation was obtained between COR isolated from PHSC and pig ears as compared to keratin particles isolated from chicken feather. Most of the FAAs have high uptake into the CORs. This suggests the possible use of the corneocytary pathway for dermal delivery of FAAs. Even though good correlation was obtained from the investigated mathematical models, the skin permeation behavior of the FAAs could better be predicted using other mathematical models. The models didn't consider the effect of corneocytary pathway in their calculations suggesting for the need of new models that could give more accurate predictions. As the permeation of the FAAs is very low, permeation enhancers should be included in formulations involving these compounds. Hence, the findings of the current study should be considered while formulating FAA- loaded dosage forms for dermal delivery.

After identifying appropriate sources of the FAAs and studying their partitioning and permeation characteristics, appropriate formulations can be designed to deliver the FAAs into and through the SC. Accordingly, different MEs, MEBHGs and a H-cream containing FAAs were formulated and characterized. From the permeability studies, MEs significantly enhanced the permeability of FAAs into and across the SC. Even though Poloxamer® 407-based MEs had higher viscosity at skin temperature, they permeated into deeper skin layers than Carbopol® 934-based MEs. Oil-in-water MEs with smaller droplet sizes permeated more into the deeper skin layers than MEs with larger droplet sizes. As compared to the MEs, penetration from MEBHGs was slower. This indicates that preparation of gels of oil-in-water MEs can be used as a means of directing the MEs to the desired site within the skin. The particle and permeation properties of the MEs and MEBHGs prepared from the mushroom extracts were close to that of the formulation prepared using standard FAAs suggesting the possible use of nature-based sources for this purpose. In general, even though further evaluation is needed to elucidate the clinical efficacy of such topical dosage forms, it can be concluded that colloidal carrier systems, namely MES and MEBHGs, are effective in the delivery of FAAs to the targeted site of the skin.

REFERENCES

- Abdulmajed, K., Heard, C.M., McGuigan, C., & Pugh, W.J. (2004). Topical delivery of retinyl ascorbate co-drug. 2. Comparative skin tissue and keratin binding studies. *Skin Pharmacol. Physiol,* ***17***, 274–282.
- Agilent Technologies (2020). Agilent InfinityLab Poroshell 120 columns for HPLC and UHPLC. https://www.agilent.com/cs/library/brochures/5991-8750EN_InfinityLab_Poroshell120_brochure.pdf. Accessed on 20 December 2021.
- Akomeah, F., Nazir, T., Martin, G.P., & Brown, M.B. (2004). Effect of heat on the percutaneous absorption and skin retention of 3 model penetrants. *Eur J Pharm Sci,* ***21***, 337–345
- Albaugh, V.L., Mukherjee, K., & Barbul, A. (2017). Proline precursors and collagen synthesis: biochemical challenges of nutrient supplementation and wound healing. J Nutr, ***147***, 2011–2017.
- Anderson, B.D., Higuchi, W.I., & Raykar, P.V. (1988). Heterogeneity effects on permeability-partition coefficient relationships in human stratum corneum. *Pharm Res,* ***5***, 566-573.
- Anderson, R.L. & Cassidy, J.M. (1973). Variation in physical dimensions and chemical composition of human stratum corneum. *J. Invest. Dermatol,* ***61***, 30–32.
- Anderson, R.R., & Parrish, J.A. (1982). Optical Properties of Human Skin. In Regan, J.D., Parrish, J.A. (eds), the Science of Photomedicine. Photobiology. Springer, Boston, MA.
- Araujo, L.M., Thomazine, J.A., & Lopez, R.F. (2010). Development of micro emulsions to topically deliver 5-aminolevulinic acid in photodynamic therapy. *Eur. J. Pharm. Biopharm,* ***75***, 48–55.
- Arezki, N.R., Williams, A.C., Cobb, J.A., & Brown, M.B. (2017). Design, synthesis, and characterization of linear unnatural amino acids for skin moisturization. *Int J Cosmet Sci,* ***39***, 72–82.
- Attwood, D. (1994). Microemulsions. In: Kreuter, J., (Ed.), Colloidal Drug Delivery Systems, Drugs and the Pharmaceutical Sciences, Marcel Dekker, New York, pp 31-71.
- Azmir, J., Zaidul, I.S.M., Rahman, M.M., Sharif, K.M., Mohamed, A., Sahena, F., Jahurul, M.H.A., Ghafoor, K., Norulaini, N.A.N., Omar, A.K.M. (2013). Techniques for extraction of bioactive compounds from plant materials: a review. *J Food Eng,* ***117***, 426–436
- Baden, H.P. & Gifford, A.M. (1970). Isometric contraction of epidermis and stratum corneum with heating. *J. Invest. Dermatol,* ***54***, 298-303.
- Badiu, D.L., Luque, R., Dumitrescu, E., Craciun, A., Dinca, D. (2010). Amino acids from Mytilus galloprovincialis (L.) and Rapana venosa molluscs accelerate skin wounds healing via enhancement of dermal and epidermal neoformation. *Protein J,* ***29,*** 81–92.

- Badr, F.H. & Georgiev, E.V (1990). Amino acid composition of cumin seed (Cuminum cyminum L.). *Food Chem, **38***, 273–278
- Bandaranayake, W.M. (2006). Quality control, screening, toxicity, and regulation of herbal drugs. Modern phytomedicine: turning medicinal plants into drugs. Wiley-VCH Verlag GmbH & Co. KGaA, pp. 25–57.
- Bank, R.A., Jansen, E.J., Beekman, B., & Koppele, J.M. (1996). Amino acid analysis by reverse-phase high-performance liquid chromatography: improved derivatization and detection conditions with 9-fluorenylmethyl chloroformate. *Anal. Biochem, **240***, 167-176.
- Banning, T.P. & Heard, C.M. (2002). Binding of doxycycline to keratin, melanin and human epidermal tissue. *Int. J. Pharm, **235**,* 219–227.
- Barresi, C., Stremnitzer, C., Mlitz, V., Kezik, S., Kammeyer, A., Ghannadan, M., et al (2010). Increased sensitivity of histidinemic mice to UVB radiation suggests a crucial role of endogenous urocanic acid in photoprotection. *J Invest Dermatol, **131***,188–194.
- Barry, B. (1987). Mode of action of penetration enhancers in human skin. *J Control Release, **6***, 85–97.
- Barry, B.W. (1983). Structure, function, diseases, and topical treatment of human skin. In Barry, B.W. (ed.), Dermatological Formulations: Percutaneous Absorption (pp. 1–48). Marcel Dekker: New York.
- Barry, B.W. (1987). Mode of action of penetration enhancers in human skin. *J Control Release, **6***, 85–97.
- Barry, B.W. (2002). Drug delivery routes in skin: A novel approach. *Adv. Drug Deliv. Rev, **54***, S31–40.
- Becker, S.W., Fitzpatrick, T.B., & Montgomery, H (1952). Human melanogenesis; cytology and histology of pigment cells (melanodendrocytes). *AMA Arch Derm Syphilol, **65***, 511–523.
- Bellon, G., Chaqour, B., Wegrowski, Y., Monboisse, J.C., & Borel, J.P. (1995). Glutamine increases collagen gene transcription in cultured human fibroblasts. *Biochim Biophys Acta, **1268***, 311–323.
- Bellon, G., Monboisse, J.C., Randoux, A., & Borel. J.P. (1987). Effects of preformed proline and proline amino acid precursors (including glutamine) on collagen synthesis in human fibroblast cultures. *Biochim Biophys Acta, **930***, 39–47.
- Berhan, T., & Egziabher, G. (2009). Diversity of the Ethiopian fora. Plant genetic resources of Ethiopia. Cambridge University Press, London, pp 75–81.
- Bidlingmeyer, B.A., Cohen, S.A., & Tarvin, T.L. (1984). Rapid analysis of amino acids using pre-column derivatization. *J. Chromatogr. B Biomed. Appl, **336***, 93–104.

- Blank, I., Meloney, J., Emslie, A.G., Simon, I., & Apt, C. (1984). The diffusion of water across the stratum corneum as a function of its water content. *J Invest Dermatol,* ***82***,188-194.
- Boddé, H.E., van den Brink, I., Koerten, H.K., & de Haan, F.H.N. (1991). Visualization of in vitro percutaneous penetration of mercuric chlorite; transport through intercellular space versus cellular uptake through desmosomes. *J. Control. Release,* ***15***, 227– 236.
- Bouwstra, J.A., de Graaff, A., Gooris, G.S., Nijsse, J., Wiechers, J.W. & van Aelst, A.C. (2003). Water distribution and related morphology in human stratum corneum at different hydration levels. *J. Invest. Dermatol,* ***120***, 750–758.
- Brenner, M. & Hearing, V.J. (2008). The protective role of melanin against UV damage in human skin. *Photochem Photobiol,* ***84***, 539–549.
- Breternitz, M., Flach, M., Prassler, J., Elsner, P., & Fluhr, J.W. (2007). Acute barrier disruption by adhesive tapes is influenced by pressure, time and anatomical location: integrity and cohesion assessed by sequential tape stripping. A randomized, controlled study. *Br. J. Dermatol,* ***156***, 231–240.
- Briggaman, R.A. (1982). Biochemical composition of the epidermal-dermal junction and other basement membrane. *J Invest Dermatol,* ***78,*** 1–6.
- Bronaugh, R.L., & Stewart, R.F. (1985). Methods for in vitro percutaneous absorption studies IV: the flow-through diffusion cell. *J. Pharm. Sci,* ***74,*** 64–67.
- Bunge, A.L., & Cleek, R.L. (1995). A new method for estimating dermal absorption from chemical-exposure. 2. Effect of molecular weight and octanol-water partitioning. *Pharm. Res,* ***12***, 88-95.
- Burke, R.C., Lee, T.H., & Buettner-Janusch, V. (1966). Free amino acids and water-soluble peptides in stratum corneum and skin surface film in human beings. *Yale J Biol Med,* ***38***, 355–373.
- Burnett, C.L., Heldreth, B., Bergfeld, W.F., Belsito, D.V., Hill, R.A, Klaassen, C.D. et al (2013). Safety Assessment of -Amino Acids as Used in Cosmetics. *Int. J. Toxicol,* ***32***, 41S–64S.
- Calixto, J.B. (2019) The role of natural products in modern drug discovery. *An Acad Bras Ciencias,* ***91***, 1–7
- Caspers, P.J., Lucassen, G.W., Bruining, H.A., & Puppels, G.J. (2000). Automated depth-scanning confocal microspectrometer for rapid in-vivo determination of water concentration profiles in human skin. *J. Raman Spectrosc,* ***31***, 813–818.
- Caspers, P.J., Lucassen, G.W., Carter, E.A., Bruining, H.A., & Puppels, G.J. (2001). In vivo confocal raman microspectroscopy of the skin: Noninvasive determination of molecular concentration profiles. *J Invest Dermatol,* ***116***, 434–442.
- Catrinck, T.C.P.G., Dias, A., Aguiar, M.C.S., Silvério, F.O., Fidêncio, P.H., Pinho, G.P. (2014). A Simple and Efficient Method for Derivatization of Glyphosate and AMPA Using 9-

Fluorenylmethyl Chloroformate and Spectrophotometric Analysis. *J. Braz. Chem. Soc,* ***25***, 1194-1199.

- Chandrasekaran, S.K., Campbell, P.S., & Watanabe, T. (1980). Application of the dual sorption model to drug transport through skin. Polym. *Eng. Sci,* ***20***, 36-39.
- Chen, G., Wang, Y., Song, W., Zhao, B., Dou, Y. (2012). Rapid and selective quantification of l-theanine in ready-to-drink teas from Chinese market using SPE and UPLC-UV. *Food Chem,* ***135***, 402-7.
- Chen, H., Mou, D., Du, X., Chang, D., Zhu, J., Liu, H., Xu, X., Yang, X. (2007). Hydrogel thickened micro emulsion for topical administration of drug molecule at an extremely low concentration, *Int. J. Pharm,* ***341***, 78–84.
- Chen, L., Han, L., & Lian, G. (2010). Modelling transdermal permeation. Part I. Predicting skin permeability of both hydrophobic and hydrophilic solutes. *Am Inst Chem Eng. J,* ***56***, 1136–1146.
- Chen, L., Han, L., & Lian, G. (2013). Recent advances in predicting skin permeability of hydrophilic solutes. *Adv. Drug Deliv. Rev,* ***65***, 295-305.
- Chen, Y., Quan, P., Liu, X., Wang, M., & Fang, L. (2014). Novel chemical permeation enhancers for transdermal drug delivery. *Asian J Pharm Sci,* ***9***, 51–64
- Chikezie, P.C., Ibegbulem, C.O., & Mbagwu, F.N. (2015). Bioactive principles from medicinal plants. *Res J Phytochem,* ***9***, 88–115
- Cichewicz, A., Pacleb, C., Connors, A., Hass, M.A., & Lopes, L.B. (2013) Cutaneous delivery of α-tocopherol and lipoic acid using micro emulsions: Influence of composition and charge. *J. Pharm. Pharmacol,* ***65***, 817–826.
- Clausen, M.L., Slotved, H.C., Krogfelt, K.A., & Agner, T. (2018). Measurements of AMPs in stratum corneum of atopic dermatitis and healthy skin-tape stripping technique. *Sci. Rep,* ***8,*** 1666.
- Corsetti, G., D'Antona, G., Dioguardi, F.S., & Rezzani, R. (2010). Topical application of dressing with amino acids improves cutaneous wound healing in aged rats. *Acta Histochem,* ***112***, 497–507
- Dai, Z., Wu. Z., Jia, S., & Wu, G. (2014). Analysis of amino acid composition in proteins of animal tissues and foods as pre-column o-phthaldialdehyde derivatives by HPLC with fluorescence detection. *J Chromatogr B Analyt Technol Biomed Life Sci,* ***964***,116-27.
- Danzberger, J., Donovan, M., Rankl, C., Zhu, R., Vicic, S., Baltenneck, C., Enea, R., Hinterdorfer, P., & Luengo, G.S. (2018). Glycan distribution and density in native skin's stratum corneum. *Skin Res Tech,* ***24***, 450–458.
- De Gennes, P.G., & Taupin, C. (1982). Microemulsions and the flexibility of oil/water interfaces. *J Phys Chem,* ***86***, 2294–2304.

- De Jongh, C.M., Verberk, M.M., Spiekstra, S.W., Gibbs, S., Kezic, S. (2007). Cytokines at different stratum corneum levels in normal and sodium lauryl sulphate-irritated skin. Skin Res. *Technol,* ***13***, 390–398.
- Dejaegher, B., Heyden, Y.V. (2007). Ruggedness and robustness testing. *J. Chromatogr A,* ***1158***, 138–157.
- Delgado-Charro, M.B., Iglesias-Vilas, G., Blanco-Mendez, J., Lopez-Quintela, M.A., Marty, J.P., & Guy, R.H. (1997). Delivery of a hydrophobic solute through the skin from novel micro emulsion systems. *Eur. J. Pharm. Biopharm,* ***43***, 37–42.
- Demain, A.L. (2000). Microbial biotechnology. *Trends Biotechnol,* ***18***, 26–31.
- Denda, M., Hori, J., Koyama, J., Yoshida, S., Nanba, R., Takahashi, M., Horii, I., & Yamamoto, A. (1992). Stratum corneum sphingolipids and free amino acids in experimentally-induced scaly skin. *Arch Dermatol Res,* ***284***, 363-7
- Dick, I.P., & Scott, R.C. (1992). Pig ear skin as an in-vitro model for human skin permeability. *J Pharm Pharmacol,* ***44***, 640–645.
- Dragicevic-Curic, N., Winter, S., Stupar, M., et al. (2009). Temoporfin-loaded liposomal gels: viscoelastic properties and in vitro skin penetration. *Int J Pharm,* ***373***, 77–84.
- Durden, D.L. (2016). Asparaginase and treating diseases associated with asparagine dependence. *US Patent,* ***9*****,** 353-366.
- Einbinder, J.M., Walzer, R.A., & Mandl, I. (1966). Epidermal-dermal separation with proteolytic enzymes. *J Invest Dermatol,* ***46***, 492–504.
- Ellison, C.A., Tankersley, K.O., Obringer, C.M., Carr, G.J., Manwaring, J., Rothe, H., et al. (2020). Partition coefficient and diffusion coefficient determinations of 50 compounds in human intact skin, isolated skin layers and isolated stratum corneum lipids. *Toxicol In Vitro,* ***69***, 104990:1-14.
- Fabiani, A., Versari, A., Parpinello, G.P., Castellari, M., & Galassi, S. (2002). High-Performance Liquid Chromatographic Analysis of Free Amino Acids in Fruit Juices Using Derivatization with 9-Fluorenylmethyl-Chloroformate. *J. Chromatogr. Sci,* ***40***, 14–18.
- Fajuyigbe, D., Lwin, S.M., Diffey, B.L., Baker, R., Tobin, D.J., Sarkany, R.P.E., & Young, A.R. (2018). Melanin distribution in human epidermis affords localized protection against DNA photodamage and concurs with skin cancer incidence difference in extreme phototypes. *FASEB J,* ***32***, 3700–3706.
- Feldmann, R.J., & Maibach, H.I. (1970). Absorption of some organic compounds through the skin in man. *J. Invest. Dermatol,* ***54***, 399–404.
- Fowler, J. (2012). Understanding the Role of NMF in Skin Hydration. *Pract Dermatology,* ***2012***, 36-40.

- Franz, T.J., & Barker, E.A. (1977). Finite dose technique as a valid in vitro model for study of percutaneous absorption in man. *Clin Res,* ***25***, A198.
- Friedman, D., Schwarz, J.S., & Weisspapir, M. (1995). Submicron emulsion vehicle for enhanced transdermal delivery of steroidal and nonsteroidal antiinflammatory drugs. *J. Pharm. Sci,* ***84***, 324–329.
- Froelich, A., Osmałek, T., Kunstman, P., Roszak, R., & Białas, W. (2015). Rheological and textural properties of microemulsion-based polymer gels with indomethacin. *Drug Dev Ind Pharm, Early Online,* 1–8.
- Fukuji, A.Y.S., Constantino, L.V., Zefa, D.M., de Andrade, F.A., da Silva, M.B., & Gonçalves, L.S.A. (2019). Amino acid concentration, total phenolic compound content and antioxidant activity of snap bean genotypes. *Braz J Food Technol,* ***22:e2018069***, 1–6.
- Furudate, A., & Meguro T (2001). Free amino acids in potato tubers and their extraction by boiling water. *J Home Econ Japan,* ***52***, 71–74.
- Furuishi, T., Kunimasu, K., Fukushima, K., Ogino, T., Okamato, K., Yonemochi, E., Tomono, K., & Suzuki, T. (2019). Formulation design and evaluation of a transdermal drug delivery system containing a novel eptazocine salt with the Eudragit® E adhesive. *J Drug Deliv Sci Technol,* ***54***, 101289.
- Gannu, R.C.R., Palem, V.V., Yamsani, S.K., Yamsani, M.R., & Yamsani R (2010). Enhanced bioavailability of lacidipine via micro emulsion based transdermal gels: formulation optimization, ex vivo and in vivo characterization. *Int. J. Pharm,* ***388***, 231–241.
- Garg, R.P., Qian, X.L., Alemany, L.B., Moran, S., & Parry, R.J. (2008). Investigations of valanimycin biosynthesis: elucidation of the role of seryltRNA. *Proc Natl Acad Sci,* ***105***, 6543–6547.
- Garside, D.M., Monteiro, P.M.S., & Orren, M.J. (1988). A critical evaluation for the determination of amino acids in the marine environment by derivatization using 9- fluorenylmethyl chloroformate (FMOC-Cl) and reversed phase HPLC separation. *Afr. J. Mar. Sci,* ***6***, 47-53.
- Getie, M., Wohlrab, J., & Neubert, R.H.H. (2005). Dermal delivery of desmopressin acetate using colloidal carrier systems. *J. Pharm. Pharmacol,* ***57***, 423-427.
- Gittler, J.K., Krueger, J.G., & Guttman-Yassky, E. (2013). Atopic dermatitis results in intrinsic barrier and immune abnormalities: implications for contact dermatitis. *J Allergy Clin Immunol,* ***131***, 300–313.
- Goebel, A., & Neubert, R.H.H. (2008). Dermal Peptide Delivery Using Colloidal Carrier Systems. *Skin Pharmacol Physiol,* ***21***, 3–9.
- Goebel, A.S., Knie, U., Abels, C., Wohlrab, J., & Neubert, R.H. (2010). Dermal targeting using colloidal carrier systems with linoleic acid. *Eur. J. Pharm. Biopharm,* ***75***, 162–172.

- Goebel, A.S.B., Schmaus, G., & Neubert, R.H.H., & Wohlrab, J. (2012). Dermal Peptide Delivery Using Enhancer Molecules and Colloidal Carrier Systems. Part I: Carnosine. *Skin Pharmacol Physiol, **25***, 281–287.
- Gomes, M.H., & Rosa, E. (2001). Free amino acid composition in primary and secondary inforescences of 11 broccoli (Brassica oleracea var italica) cultivars and its variation between growing seasons. *J Sci Food Agric, **81***, 295–299
- González-Castro, M., López-Hernández, J., Simal-Lozano, J., & Oruna-Concha, M. (1997). Determination of amino acids in green beans by derivatization with phenylisothiocianate and high-performance liquid chromatography with ultraviolet detection. *J. Chromatogr. Sci, **35***, 181–185.
- Gray, G., & Yardley, H. (1975). Lipid compositions of cells isolated from pig, human, and rat epidermis. *J Lipid Res, **16***, 434–440.
- Gruber, R., Elias, P.M., Crumrine, D., Lin, T.K., Brandner, J.M., Hachem, J.P., Presland, R.B., et al. (2011). Filaggrin genotype in ichthyosis vulgaris predicts abnormalities in epidermal structure and function. *Am J Pathol, **178***, 2252–2263.
- Gustavsson, B., & Betnér, I. (1990). Fully automated amino acid analysis for protein and peptide hydrolysates by precolumn derivatization with 9-fluorenyl methylchloroformate and 1-aminoadamantane. *J. of Chromatogr A, **507***, 67–77.
- Hansen, J.R., & Yellin, W. (1972). NMR infrared spectroscopic studies of stratum corneum hydration. In Jellinck HHG, (ed.), Water Structure at the Water-Polymer Interface. New York, Plenum Press, pp 19-28.
- Hansen, S., Selzer, D., Schaefer, U.F., & Kasting, G.B. (2011). An extended database of keratin binding. *J. Pharm. Sci, **100***, 1712– 1726.
- Hansen, S., Henning, A., & Naegel, A. (2008). In-silico model of skin penetration based on experimentally determined input parameters. Part I: Experimental determination of partition and diffusion coefficients. *Eur. J. Pharm. Biopharm, **68***, 352– 367.
- Haque, T., Talukder, M.U. (2018). Chemical Enhancer: A Simplistic Way to Modulate Barrier Function of the Stratum Corneum. *Advanced Pharmaceutical Bulletin, **8***, 169–179.
- Harding, C. (2004). The stratum corneum: structure and function in health and disease. *Dermatol. Ther, **17***, 6–15.
- Harding, C.R., Watkinson, A., Rawlings, A.V., Scott, I.R. (2000). Dry skin, moisturization and corneodesmolysis. *Int J Cosmet Sci, **22***, 21-52.
- Haynes, P.A., Sheumack, D., Greig, L.G., Kibby, J., Redmond, J.W. (1991). Applications of automated amino acid analysis using 9-fluorenylmethyl chloroformate. *J Chromatogr, **588***, 107-14.

- Heard, C.M., Monk, B.V., & Modley, A.J. (2003). Binding of primaquine to epidermal membranes and keratin. *Int. J. Pharm,* ***257***, 237–244.
- Heuschkel, S., Goebel, A., & Neubert, R.H.H. (2008). Microemulsions- modern colloidal carrier for dermal and transdermal drug delivery. *J. Pharm. Sci, US* ***97***, 603-631.
- Heuschkel, S., Wohlrab, J., & Neubert, R.H.H. (2009). Dermal and transdermal targeting of dihydroavenanthramide D using enhancer molecules and novel microemulsions. *Eur. J. Pharm. Biopharm,* ***72***, 552-560.
- Hitoshi, M., Kazutaka, S., Yoshiko, I., Yoshinobu, T., Hisamine, K. (2012). Importance of amino acid composition to improve skin collagen protein synthesis rates in UV-irradiated mice. *Amino Acids,* ***42***, 2481–2489.
- Horii, I., Nakayama, Y., Obata, M., & Tagami, H. (1989). Stratum corneum hydration and amino acid content in xerotic skin. *Br J Dermatol,* ***121***, 587–592.
- Hsieh, M.M., Chen, S.M. (2007). Determination of amino acids in tea leaves and beverages using capillary electrophoresis with light-emitting diode-induced fluorescence detection. *Talanta,* ***73***, 326–331.
- Hsu, C.Y., Henry, J., Raymond, A.A., Mechin, M.C., Pendaries, V., Nassar, D., et. al. (2011). Deimination of human filaggrin-2 promotes its proteolysis by calpain 1. *J Biol Chem,* ***286***, 23222–23233.
- Huang, Y.B., Lin, Y.H., Lu, T.M., Wang, R.J., Tsai, Y.H., & Wu, P.C. (2008). Transdermal delivery of capsaicin derivative-sodium nonivamide acetate using micro emulsions as vehicles. *Int. J. Pharm,* ***349***, 206–211.
- Hui, X., Lamel, S., Qiao, P., & Maibach, H.I. (2013(a)). Isolated human/animal stratum corneum as a partial model for 15 steps in percutaneous absorption: emphasizing decontamination, part I. *J Appl Toxicol,* ***33***, 157–172.
- Hui, X., Lamel, S., Qiao, P., & Maibach, H.I. (2013(b). Isolated human and animal stratum corneum as a partial model for the 15 steps in percutaneous absorption: emphasizing decontamination, part II. *J Appl Toxicol,* ***33***, 173–82.
- Hui, X., Wester, R.C., Magee, P., & Maibach, H.I. (1995). Partitioning of chemicals from water into powdered human stratum corneum (callus): a model study. *In Vitro Toxicol,* ***8***, 159–167.
- Hui, X., Wester, R.C., Magee, P., Maibach, H.I. (2001). Partitioning of chemicals from water into powdered human stratum corneum (callus). In Hayes, A., Thomas, J., Maibach, H.I. (eds.), Toxicology of Skin (pp. 159–178). Taylor &Francis, Philadelphia.
- Hui, X., Wester, R.C., Zhai, H., Cashmore, A.K., Barbadillo, S., & Maibach, H.I. (2008). Chemical partitioning into powdered human stratum corneum: a useful in vitro model for studying interactions of chemicals and human skin. In Zhai, H., Wilhelm, K.P., Maibach, H.I. (eds),

Marzulli and Maibach's Dermatotoxicology (7th edn, pp. 87–94). CRC Press, Taylor and Francis Group: Boca Raton.

- Hussain, H., Ziegler, J., Hause, G., Wohlrab, J., & Neubert, R.H.H. (2019 (a)). Quantitative Analysis of Free Amino Acids and Urea Derived from Isolated Corneocytes of Healthy Young, Healthy Aged, and Diseased Skin. *Skin Pharmacol and Physio,* ***32***, 94–100.
- Hussain, H., Ziegler, J., Mrestani, Y., & Neubert, R.H.H. (2019 (b)). Studies of the conreocytary pathway across the stratum corneum. Part I: Diffusion of amino acids into the isolated corneocytes. *Pharmazie,* ***74***, 340-344.
- ICCVAM-Test (2006). ICCVAM Recommended Protocol for Future Studies Using the Hen's Egg Test-Chorioallantoic Membrane (HET-CAM) Test Method.
- Ikeda, M. (2003). Amino acid production processes. *Adv Biochem Eng Biotechnol,* ***79***, 1–35.
- International Conference on Harmonisation of Technical Requirements for Registration of Pharmaceuticals for Human Use ICH Q2 (R1) (2005). Validation of analytical procedures: text and methodology.
- Irvine, A.D., McLean, W.H.I., & Leung, D.Y.M. (2011). Filaggrin mutations associated with skin and allergic diseases. *N Engl J Med,* ***365***, 1315–1327.
- Ishikawa, M., Kawase, I., & Fumio, I. (2007). Combination of Amino Acids Reduces Pigmentation in B16F0 Melanoma Cells. *Biol. Pharm. Bull,* ***30***, 677—681.
- Jacobi, U., Tassopoulos, T., Surber, C., & Lademann, J. (2006). Cutaneous distribution and localization of dyes affected by vehicles all with different lipophilicity. *Arch. Dermatol. Res,* ***297***, 303–310.
- Jacobson, T.M., Yuksel, Y.U., Geesin, J.C., Gordon, J.S., Lane, A.T., & Gracy, R.W. (1990). Effects of aging and Xerosis on the amino acid composition of human skin. *J Invest Dermatol,* ***95***, 296–300.
- Jain, A.K., Thomas, N.S., & Panchagnula, R. (2002). Transdermal drug delivery of imipramine hydrochloride. I. Effect of terpenes. *J. Control. Release,* ***79***, 93–101.
- Ji, S., Fattahi, A., Rafel, N., Hofmann, I., Beckmann, M.W., Dittrich, R., Schrauder, M. (2017). Antioxidant efect of aqueous extract of four plants with therapeutic potential on gynecological diseases; Semen persicae, Leonurus cardiaca, Hedyotis difusa, and Curcuma zedoaria. *Eur J Med Res,* ***22***, 1–8.
- Jian, L., Cao, Y., & Zou, Y. (2019 (b)). Dermal-Epidermal Separation by Enzyme. In Turksen, K. (eds) Epidermal Cells. Methods in Molecular Biology (ed. *2019*, pp. 27-30). *Humana, New York.*
- Jian, L., Cao, Y., Zou, Y. (2019 (a)). Dermal-Epidermal Separation by Heat. In: Turksen, K. (eds) Epidermal Cells. Methods in Molecular Biology (ed. *2019*, pp. 23-25). *Humana, New York*.

- Jian, L., Cao, Y., Zou, Y. (2019 (c)). Dermal-Epidermal Separation by Chemical. In: Turksen K. (eds) Epidermal Cells. Methods in Molecular Biology (ed. 2019, pp. 31-33). *Humana, New York*.
- Jiravanichanun, N., Mizuno, K., Peter, B.H., Okuyama, K. (2006). Threonine in Collagen Triple-helical Structure. *Polymer Journal, **38***, 400–403.
- Jokura, Y., Ishikawa, S., Tokuda, H., Imokawa, G. (1995). Molecular analysis of elastic properties of the stratum corneum by solid-state 13C-nuclear magnetic resonance spectroscopy. *J Invest Dermatol, **104**,* 806–812.
- Jose, N., & Janardhanan, K.K. (2000). Antioxidant and antitumour activity of Pleurotus forida. *Curr Sci, **79***, 941–943.
- Joshi, V., & Fernie, A.R. (2017). Citrulline metabolism in plants. *Amino Acids, **49***, 1543–1559.
- Jungersted, J.M., Bomholt, J., Bajraktari, N., et al. (2013): In vivo studies of aquaporins 3 and 10 in human stratum corneum. *Arch Dermatol Res, **305***, 699–704.
- Jungersted, J.M., Hogh, J.K., Hellgren, L.I., Jemec, G.B., Agner, T. (2010). Skin barrier response to occlusion of healthy and irritated skin: differences in trans-epidermal water loss, erythema and stratum corneum lipids. *Contact Dermatitis, **63***, 313–319.
- Kahsay, B.N., Moeller, L., Imming, P., Neubert, R.H.H., Gebre-Mariam, T. (2022). Development and Validation of a Simple, Selective, and Accurate Reversed-Phase Liquid Chromatographic Method with Diode Array Detection (RP-HPLC/DAD) for the Simultaneous Analysis of 18 Free Amino Acids in Topical Formulations. *Chromatographia, **85***, 665–676.
- Kahsay, B.N., Ziegler, J., Imming, P., Gebre-Mariam, T., Neubert, R.H.H., & Moeller, L. (2021). Free amino acid contents of selected Ethiopian plant and fungi species: a search for alternative natural free amino acid sources for cosmeceutical applications. *Amino Acids, **53***, 1105–1122.
- Kalia, Y.N., & Guy, R.H. (2001). Modeling transdermal drug release. *Adv Drug Deliv Rev.; **48***, 159-172.
- Kalinin, E., Kajava, A.V., Steinert, P.M. (2002). Epithelial barrier function: asembly and structural features of the cornified cell envelope. *BioEssays, **24***, 789–800.
- Kang, X., Xiao, J., Huang, X., & Gu, Z. (2006). Optimization of dansyl derivatization and chromatographic conditions in the determination of neuroactive amino acids of biological samples. *Clin. Chim. Acta, **366***, 352–356.
- Kantaria, S., Rees, G.D., & Lawrence, M.J. (2003). Formulation of electrically conducting microemulsion-based Organogels. *Int J Pharm, **250***, 65–83.
- Karande, P., Jain, A., Ergun, K., Kispersky, V., & Mitragotri, S. (2005). Design principles of chemical penetration enhancers for transdermal drug delivery. *Proc Natl Acad Sci USA, **102***, 4688–93.

- Karna, E., Miltyk, W., Wolczynski, S., & Palka, J. (2001). A The potential mechanism for glutamine-induced collagen biosynthesis in cultured human skin fibroblasts. *Comp Biochem Physiol B Biochem Mol Biol,* ***130***, 23–32.
- Kasting, G.B. & Barai, N.D. (2003). Equilibrium water sorption in human stratum corneum. *J. Pharm. Sci,* ***92***, 1624–1631.
- Kasting, G.B., Miller, M.A., LaCount, T.D., & Jaworska, J. (2019). A composite model for the transport of hydrophilic and lipophilic compounds across the skin. *J. Pharm. Sci,* ***108***, 337-349.
- Katagiri, C., Sato, J., Nomura, J., & Denda, M. (2003). Changes in environmental humidity affect the water-holding property of the stratum corneum and its free amino acid content, and the expression of filaggrin in the epidermis of hairless mice. *J Dermatol Sci,* ***31***, 29–35.
- Kawashima, M., Yokose, U., Hachiya, A., Fujimura, T., Tsukahara, K., Kawada, H. et al. (2013) Improvement of crow's feet lines by topical application of 1-carbamimidoyl-Lproline(CLP). *Eur J Dermatol,* ***23***, 195–201.
- Kezic, S., O'Regan, G.M., Yau, N., Sandilands, A., Chen, H., Campbell, L.E. , et al (2011). Levels of filaggrin degradation products are influenced by both filaggrin genotype and atopic dermatitis severity. *Allergy,* ***66***, 934-40.
- Khan, M.A., & Tania, M. (2012). Nutritional and medicinal importance of Pleurotus mushrooms: an overview. *Food Rev Int,* ***28***, 313–329.
- Kim, B., Cho, H.E., Moon, S.H., Ahn, H.J., Bae, S., Cho, H.D., & An, S. (2020). Transdermal delivery systems in cosmetics. *Biomed. Dermatol. 4,* ***10***, 1-12.
- Kim, H, Lim YJ, Park JH, & Cho Y (2012). Dietary silk protein, sericin, improves epidermal hydration with increased levels of filaggrins and free amino acids in NC/Nga mice. *Br. J. Nutr,* ***108***, 1726–1735.
- Kim, M.Y., Chung, I.M., Lee, S.J., Ahn, J.K., Kim, E.H., Kim, M.J., Kim, S.L. et al. (2009). Comparison of free amino acid, carbohydrates concentrations in Korean edible and medicinal mushrooms. *Food Chem,* ***113***, 386–393.
- Kim, Y.K., Suh, S.Y., Uddin, M.R., Kim, Y.B., Kim, H.H., Lee, S.W., & Park, S.U. (2013). Variation in amino acid content among three Aloe species. *Asian J Chem,* ***25***, 6346–6348.
- Kirisako, T., Morita, Y., Hatta, S., & Tazumi, K. (2012). The effect of ornithine ingestion on skin condition. *Ther. Res,* ***33***, 1265-1281.
- Kirschbaum, J., Luckas, B., & Beinert, W.D. (1994). Pre-column derivatization of biogenic amines and amino acids with 9-fluorenylmethyl chloroformate and heptylamine. *J. of Chromatogr A,* ***661***, 193–199.
- Kitano, Y., & Okada, N. (1983). Separation of the epidermal sheet by dispase. *British Journal of Dermatology,* ***108***, 555-560.

- Koppes, S.A., Brans, R., Ljubojevic, H.S., Frings-Dresen, M.H.W., & Rustemeyer, T.K.S. (2016). Stratum Corneum Tape Stripping: Monitoring of Inflammatory Mediators in Atopic Dermatitis Patients Using Topical Therapy. *Int. Arch. Allergy Immunol,**170***, 187–193.
- Koyama, J., Horii, I., Kawasaki, K., Nakayama, Y., Morikawa, Y., Mitsui, T., & Kumagai, H. (1984). Free amino acids of stratum corneum as a biochemical marker to evaluate dry skin. *J Soc Cosm Chem, **35***, 183–195.
- Kreilgaard, M. (2002). Influence of microemulsions on cutaneous drug delivery. *Adv Drug Deliv Rev, **54***, S77-98.
- Kriukova, A., Vladymyrova, I.M., Levashova, O.L., & Tishako, T.S. (2018). Determination of Amino Acid Composition in the Harpagophytum procumbens Root. *J. Pharm. Sci, **18***, 85-91.
- Kwan, P., Sills, G.J., & Brodie, M.J. (2012). Understanding the role of NMF in skin hydration. *Pract Dermatol.; **2012***, 21–34
- Lademann, J., Jacobi, U., Surber, C., Weigmann, H.J., & Fluhrl, J.W. (2009) The tape stripping procedure – evaluation of some critical parameters. *Eur J Pharm Biopharm, **72***, 317–323.
- Lademann, J., Richter, H., Teichmann, A., Otberg, N., BlumePeytavi, U., Luengo, J., et al. (2007). Nanoparticles—an efficient carrier for drug delivery into the hair follicles. *Eur. J. Pharm. Biopharm, **66***,159–164.
- Lane, M.E. (2013). Skin penetration enhancers. *Int J Pharm, **447**, 12–21*.
- Lane, M.E., Santos, P., Watkinson, A.C., Hadgraft, J. (2012). Passive skin permeation enhancement. In Benson, H.E., Watkinson, A.C. (eds) Topical and transdermal drug delivery (pp. 23–42). Wiley, Hoboken.
- Law, R.M.. Ngo, M.A., & Maibach, H.I. (2020). Twenty Clinically Pertinent Factors/Observations for Percutaneous Absorption in Humans. *Am J Clin Dermatol, **21***, 85-95.
- Lee, C.H., Moturi, V., Lee, Y. (2009). Thixotropic property in pharmaceutical formulations. *J Control Release, **136***, 88–98.
- Lee, D.Y.,& Kim, E.H. (2019). Therapeutic efects of amino acids in liver diseases: current studies and future perspectives. *J Cancer Prev, **24***, 72–78.
- Lee, J., & Harnly, J.M. (2005). Free amino acid and cysteine sulfoxide composition of 11 garlic (Allium sativum L.) cultivars by gas chromatography with fame ionization and mass selective detection. *J Agric Food Chem, **53***, 9100–9104.
- Leopold, C.S., & Lippold, B.C. (1995). An attempt to clarify the mechanism of the penetration enhancing effects of lipophilic vehicles with differential scanning calorimetry (DSC). *J Pharm Pharmacol, **47***, 276–281.
- Leuchtenberger, W., Huthmacher, K., & Drauz, K. (2005). Biotechnological production of amino acids and derivatives: current status and prospects. *Appl Microbiol Biotechnol, **69***, 1–8

- Li, B.S., Ngo, M.A., & Maibach, H.I. (2017). Clinical relevance of complex factors of percutaneous penetration in man. *Curr Top Pharmacol,* ***21***, 85–107.
- Lian, G., Chen, L., & Han, L. (2008). An evaluation of mathematical models for predicting skin permeability. *J. Pharm. Sci,* ***97***, 584–598.
- Liron, Z., & Cohen S (1984). Percutaneous absorption of alkanoic acids ii: Application of regular solution theory. *J Pharm Sci,* ***73***, 538–42
- López-Cervantes, J., Sánchez-Machado, D.I., Rosas-Rodríguez, J.A. (2006). Analysis of free amino acids in fermented shrimp waste by high-performance liquid chromatography. *J Chromatogr A,* ***1105***, 106–110.
- Louard, R.J., Barrett, E.J., & Gelfand, R.A. (1990). Effect of infused branched chain amino acids on muscle and whole-body amino acid metabolism in man. *Clin Sci,* ***79***, 457–466.
- Lozanov, V., Petrov, S., & Mitev, V. (2004). Simultaneous analysis of amino acid and biogenic polyamines by high-performance liquid chromatography after pre-column derivatization with N-(9-fluorenylmethoxycarbonyloxy) succinimide. *J. Chromatogr A,* ***1025***, 201–208.
- Ma, X., Zhao, D., Li, X., & Meng, L. (2015). Chromatographic method for determination of the free amino acid content of chamomile fowers. *Pharmacogn Mag,* ***11***, 176–179.
- Manica, D.P., Lapos, J.A., Daniel, J.A., & Ewing, A.G. (2003). Analysis of the stability of amino acids derivatized with naphthalene-2, 3-dicarboxaldehyde using high-performance liquid chromatography and mass spectrometry. *Anal. Biochem,* ***322***, 68–78.
- Marstein, S., Jellum, E., & Eldjarn, L. (1973). The concentration of pyroglutamic acid (2-pyrrolidone-5-carboxylic acid) in normal and psoriatic epidermis, determined on a microgram scale by gas chromatography. *Clin Chim Acta,* ***49***, 389-95.
- Martinez-Pla, J.J., Martin-Biosca, Y., Sagrado, S., Villanueva-Camanas, R.M., Medina-Hernandez, M.J. (2004) Evaluation of the pH effect of formulations on the skin permeability of drugs by biopartitioning micellar chromatography. *J Chromatogr A,* ***1047***, 255-62.
- Mau, J.L., Lin, Y.P., Chen, P.T., Wu, Y.H., & Peng, J.T. (1998). Flavor compounds in king oyster mushrooms Pleurotus eryngii. *J Agric Food Chem,* ***46***, 4587–4591.
- Mayer, H.K., & Fiechter, G. (2013). Application of UHPLC for the determination of free amino acids in different cheese varieties. *Anal. Bioanal. Chem,* ***405***, 8053–8061.
- Meletis, C.D., & Barker, J.E. (2005). Therapeutic uses of amino acids. *Altern Complement Ther,* ***11***, 24–28.
- Miniaci, M.C., Irace, C., Capuozzo, A., Piccolo, M., Di Pascale, A., Russo, A., & Santamaria, R. (2016). Cysteine prevents the reduction in keratin synthesis induced by iron deficiency in human keratinocytes. *J Cell Biochem,* ***117***, 402–412.

- Mitragotri, S. (2002). A theoretical analysis of permeation of small hydrophobic solutes across the stratum corneum based on scaled particle theory. *J. Pharm. Sci,* ***91***, 744–752.
- Mitragotri, S. (2003). Modeling skin permeability to hydrophilic and hydrophobic solutes based on four permeation pathways. *J Control Release,* ***86***, 69–92.
- Moniruzzaman, M., Tamura, M., Tahara, Y., Kamiya, N., & Goto, M. (2010). Ionic liquid-inoil micro emulsion as a potential carrier of sparingly soluble drug: characterization and cytotoxicity evaluation. *Int. J. Pharm,* ***400***, 243– 250.
- Moniz, T., Lima, S.A.C., & Reis, S. (2021). Protocol for the Isolation of Stratum Corneum from Pig Ear Skin: Evaluation of the Trypsin Digestion Conditions. *Methods Protoc,* ***80***, 1-14.
- Moser, K., Kriwet, K., Naik, A., Kalia, Y.N., & Guy, R.H. (2001). Passive skin penetration enhancement and its quantification in vitro. *Eur J Pharm Biopharm,* ***52***, 103–112.
- Mueller, J., Oliveira, J.S.L., Barker, R., Trapp, M., Schroeter, A., Brezesinski, G., & Neubert, R.H.H. (2016). The effect of urea and taurine as hydrophilic penetration enhancers on stratum corneum lipid models. *BBA,****1858***, 2006–2018.
- Mueller, J., Trapp, M., & Neubert, R.H.H. (2019). The effect of hydrophilic penetration/diffusion enhancer on stratum corneum lipid models: Part II: DMSO. *Chem. Phys. Lipids,* ***104816***, 1-8.
- Mueller, U., & Huebner, S. (2003). Economic aspects of amino acids production. *Adv Biochem Eng Biotechnol,* ***79***, 137–170.
- Murakami, H., Shimbo, K., Inoue, Y., Takino, Y., & Kobayashi, H. (2012). Importance of amino acid composition to improve skin collagen protein synthesis rates in UV-irradiated mice. *Amino Acids,* ***42***, 2481–2489.
- Mustafa, A., Åman, P., Andersson, R., & Kamal-Eldin, A. (2007). Analysis of free amino acids in cereal products. *Food Chem,* ***105***, 317–324.
- Nagalingam, A. (2017). Drug delivery aspects of herbal medicines. In Japanese Kampo medicines for the treatment of common diseases: focus on infammation. Elsevier, pp 143–164.
- Nakazawa, H., Ohta, N., & Hatta, I. (2012). A possible regulation mechanism of water content in human stratum corneum via intercellular matrix. *Chem Phys Lipids,****165***, 238-243.
- Narasimha, S.M., & Shivakumar, H.N. (2010). Topical and Transdermal Drug Delivery. Editor(s): Vitthal S. Kulkarni, In Personal Care & Cosmetic Technology, Handbook of Non-Invasive Drug Delivery Systems, pp 1-36.
- Naylor, C.D., O'Rourke, K., Detsky, A.S., Baker, J.P. (1989). Parenteral nutrition with branched-chain amino acids in hepatic encephalopathy. A meta-analysis. *J. Gastroenterol,* ***97***, 1033–1042.

- Neubert, R.H.H., Sommer, E., Schölzel, M., Tuchscherer, B., Mrestani, Y., & Wohlrab, J. (2018). Dermal peptide delivery using enhancer moleculs and colloidal carrier systems. Part II: tetrapeptide PKEK. *Eur J Pharm Biopharm,* ***124***, 28–33.
- Newman, D.J., Cragg, G.M. (2012). Natural products as sources of new drugs over the 30 years from 1981 to 2010. *J Nat Prod,* ***75***, 311–335.
- Newsholme, E.A., Crabtree, B., & Ardawi, M.S. (1985). Glutamine metabolism in lymphocytes: its biochemical, physiological and clinical importance. *J Exp Physiol,* ***70***, 473–489.
- Ngo, M.A., & Maibach, H.I. (2012). Chapter 6: 15 factors of percutaneous penetration of pesticides. In: Knaak JB, Timchalk C, TorneroVelez R, editors. Parameters for pesticide QSAR and PBPK/PD models for human risk assessment. ACS Symposium Series. Washington, DC: J. Am. Chem. Soc, pp. 67–86.
- Nina, D., Jelena, P.A. & Howard, I.M. (2015). Chemical Penetration Enhancers: Classification and Mode of Action. In Nina, H.I.M (eds.), Percutaneous Penetration Enhancers Chemical Methods in Penetration Enhancement: Modification of the Stratum Corneum (pp. 11-27). Springer-Verlag Berlin Heidelberg.
- Nitsche, J.M., Wang, T.F., Kasting, G.B. (2006). A two-phase analysis of solute partitioning into the stratum corneum. *J. Pharm. Sci,* ***95***, 649– 666.
- OECD. (2004). Skin Absorption: In Vivo Method. Test Guideline No. 427; Series on Testing and Assessment. No. 428; OECD: Paris, France.
- Ogbuewu, I.P., Iwuji, T.C., Etuk, I.F., Ezeokeke, C.T., Okoli, I.C., & Iloeje, M.U. (2014). Responses of pubertal rabbits to dietary supplementation of ginger (Zingiber officinale rosc) rhizome powder. Niger. *J. Anim. Prod,* ***2014***, 53-60.
- Oliveira, A.P., Pereira, D.M., Andrade, P.B., Valentão, P., Sousa, C., Pereira, J.A., Bento, A., Rodrigues, M.Â., Seabra, R.M., & Silva, B.M. (2008). Free amino acids of tronchuda cabbage (Brassica oleracea L. Var. costata DC): Infuence of leaf position (internal or external) and collection time. *J Agric Food Chem,* ***56***, 5216–5221.
- Omote, K., Kawamata, T., Kawamata, M., & Namiki, A. (1998). Formalin-induced release of excitatory amino acids in the skin of the rat hindpaw. *Brain Res,* ***787***, 161–164.
- Osborne, D.W. & Musakhanian, J. (2018). Skin Penetration and Permeation Properties of Transcutol®—Neat or Diluted Mixtures. *AAPS PharmSciTech,* ***19***, 3512–3533.
- Otberg, N., Patzelt. A., Rasulev, U., Hagemeister, T., Linscheid, M., Sinkgraven, R., et al. (2008). The role of hair follicles in the percutaneous absorption of caffeine. *Br. J. Clin. Pharmacol,* ***65***, 488–492.
- Otto, A., Plessis, J., & Wiechers, J.W. (2009). Formulation effects of topical emulsions on transdermal and dermal delivery. *Int. J. Cosmet. Sci,* ***31***, 1–19.

- Palace, G.P., Fitzpatrick, R., Tran, K.V., Phoebe, H.C., & Norton, K. (1999). Determination of amino acids in diverse polymeric matrices using HPLC, with emphasis on agars and agaroses. *Biochim Biophys Acta,* ***1472***, 509-18.
- Palmer, C.N., Irvine, A.D., Terron-Kwiatkowski, A., Zhao, Y., Liao, H., Lee, SP, et al. (2006). Common loss of-function variants of the epidermal barrier protein filaggrin are a major predisposing factor for atopic dermatitis. *Nat Genet,* ***38***, 441-6.
- Panaite, T., Ropota, M., Turcu, R., Olteanu, M., Corbu, A.R., & Nour, V. (2017). Flaxseeds: nutritional potential and bioactive compounds. *Bull Univ Agric Sci Vet Med Cluj-Napoca Food Sci Technol,* ***74***, 65.
- Panchagnula, R., Desu, H., Jain, A., & Khandavilli, S. (2004). Effect of lipid bilayer alteration on transdermal delivery of a high molecular-weight and lipophilic drug: studies with paclitaxel. *J. Pharm. Sci,* ***93***, 2177–2183.
- Park, J.H., & Lee, S.Y. (2008). Towards systems metabolic engineering of microorganisms for amino acid production. *Curr Opin Biotechnol,* ***19***, 454–460.
- Pathan, I.B., & Setty, C.M. (2009). Chemical penetration enhancers for transdermal drug delivery systems. *Trop J Pharm Res,* ***8***, 173–9.
- Peck, K.D., Ghanem, A.H., & Higuchi, W.I. (1994). Hindered diffusion of polar molecules through and effective pore radii estimates of intact and ethanol treated human epidermal membrane. *Pharm. Res,* ***11***, 1306–1314.
- Peppelman, M., van den Eijnde, W.A., Jaspers, E.J., Gerritsen, M.J., & van Erp, P.E. (2015). Combining tape stripping and non-invasive reflectance confocal microscopy: an in vivo model to study skin damage. *Skin Res. Technol,* ***21***, 474–484.
- Phillipson, J.D. (2001). Phytochemistry and medicinal plants. *Phytochemistry,* ***56***, 237–243.
- Podlogar. F., Gasperlin, M., Tomsic, M., Jamnik, A., Rogac, M.B. (2004). Structural characterization of water-Tween 40/Imwitor 308-isopropyl myristate micro emulsions using different experimental methods. *Int J Pharm,* ***276***, 115–128.
- Potts, R.O., Guy, R.H. (1992). Predicting skin permeability. Pharm Res, **9**: 663–669.
- Proksch, E., Brandner, J., & Jensen, J.M. (2008). The skin: an indispensable barrier. *Exp. Dermatol,* ***17***,1063–1072.
- Rawlings, A.V., & Harding, C.R. (2004). Moisturization and skin barrier function. *Dermatol Ther,* ***17***, 43–8.
- Rawlings, A.V., Hope, J., Watkinson, A.W., Harding, C.R., Egelrud, T. (1993): The biology effect of glycerol. *J Invest Dermatol,* ***100***, 526-530
- Rawlings, A.V., Scott, I.R., Harding, C.R., & Browser, P.A. (1994). Stratum corneum moisturization at the molecular level. *J Invest Dermatol,* ***103***, 731–40.

- Raykar, P.V., Fung, M.C., & Anderson, B.D. (1988). The Role of Protein and Lipid Domains in the Uptake of Solutes by Human Stratum Corneum. *Pharm. Res,* ***5***, 140–150.
- Rhee, Y.S., Choi, J.G., Park, E.S., & Chi, S.C. (2001). Transdermal delivery of ketoprofen using micro emulsions. *Int. J. Pharm,* ***228***, 161.
- Robinson, R.G. (1975). Amino acid and elemental composition of sunfower and pumpkin seeds 1. *Agron J,* ***67***, 541–544.
- Roohinejad, S., Oey, I., Wen, J., Lee, S.J., Everett, D.W., & Burritt, D.J. (2015). Formulation of oil-in-water β-carotene microemulsions: effect of oil type and fatty acid chain length. *Food Chem,* ***174***, 270-8.
- Rougier, A., Lotte, C., & Maibach, H.I. (1987). *In vivo* percutaneous penetration of some organic compounds related to anatomic site in humans: predictive assessment by the stripping method. *J. Pharm. Sci,* ***76***, 451–545.
- Rougier, A., Rallis, M., Krien, P., & Lotte, C. (1990). *In vivo* percutaneous absorption: a key role for stratum corneum/vehicle partitioning. *Arch Dermatol Res,* ***282***, 498-505.
- Rubio, L., Alonso, C., Lopez, O., Rodriguez, G., Coderch, L., Notario, J., et al. (2011): Barrier function of intact and impaired skin: percutaneous penetration of caffeine and salicylic acid. *Int J Dermatol,* ***50***, 881–889.
- Ruhsam, M., & Hollingsworth, P.M. (2018). Authentication of Eleutherococcus and Rhodiola herbal supplement products in the United Kingdom. *J Pharm Biomed Anal,* ***149***, 403–409.
- Saboori-Robat, E., Joshi, J., Pajak, A., Renaud, J., Marsolais, F., et al. (2019). Common bean (Phaseolus vulgaris L.) accumulates most S-Methylcysteine as its glutamyl dipeptide. *Plants,* ***8***, 126.
- Sahle, F., Wohlrab, J., & Neubert, R.H.H. (2014). Controlled penetration of ceramides into and across the stratum corneum using various types of microemulsions and formulation associated toxicity studies. *Eur J Pharm Biopharm,* ***86***, 244-250.
- Sahle, F.F., Metz, H., Wohlrab, J., & Neubert, R.H.H. (2012). Polyglycerol fatty acid ester surfactant-based microemulsions for targeted delivery of ceramide AP into the stratum corneum: formulation, characterisation, in vitro release and penetration investigation. *Eur J Pharm Biopharm,* ***82***, 139-50.
- Sahle, F.F., Metz, H., Wohlrab, J., & Neubert, R.H.H. (2013). Lecithin-based microemulsions for targeted telivery of ceramide AP into the stratum corneum: formulation, characterizations, and in vitro release and penetration studies. *Pharm Res,* ***30***, 538–551.
- Sahle, F.F., Wohlrab, J., & Neubert, R.H.H. (2014). Controlled penetration of ceramides into and across the stratum corneum using various types of microemulsions and formulation associated toxicity studies. *Eur. J. Pharm. Biopharm,* ***86*****,** 244-250.

- Salerno, C., Gorzalczany, S., Arechavala, A., Scioscia, S.L., Carlucci, A.M., & Bregni, C. (2015). Novel gel-like micro emulsion for topical delivery of Amphotericin B. *Rev. Colomb. Cienc. Quím. Farm, **44***, 359-381.
- Sandberg, F., & Corrigan, D. (2001). Natural remedies. Their origins and uses. Taylor and Francis, New York.
- Santos P, Watkinson AC, Hadgraft J, Lane ME (2012). Influence of penetration enhancer on drug permeation from volatile formulations. *Int J Pharm, **439***, 260–268.
- Scheuplein, R.J., & Blank, I.H. (1971). Permeability of the skin. *Physiol Rev, **51***, 702-747.
- Schulman, J.H., Stoeckenius, W., & Prince, L.M. (1959). Mechanism of formation and structure of microemulsions by electron microscopy. *J Phys Chem, **63***,1677–1680.
- Schwarz, J., Weisspapir, M., & Friedman, D. (1995). Enhanced transdermal delivery of diazepam by submicron emulsion (sme) creams. *Pharm. Res, **12***, 687–692.
- Segneanu, A., Velciov, S.M., Olariu, S., Cziple, F., Damian, D., & Grozescu, I. (2017). Bioactive molecules profile from natural compounds. Amino acid–new insights and roles in plant and animal. IntechOpen, pp 209–228
- Seguchi, T., Chang-Yi, C., Kusuda, S., Takahashi, M., Aisu, K., & Tezuka, T. (1996). Decreased expression of filaggrin in atopic skin. *Arch Dermatol Res, **288***, 442–446.
- Sekkat, N., Kalia, Y.N., & Guy, R.H. (2002). Biophysical study of porcine ear skin in vitro and its comparison to human skin in vivo. *J. Pharm. Sci, **91***, 2376-2381.
- Shafiq, S., Shakeel, F., Talegaonkar, S., Ahmad, F., Khar, R., & Ali, M. (2007). Development and bioavailability assessment of ramipril nanoemulsion formulation. *Eur J Pharm Biopharm, **66***, 227–243.
- Shangguan, D., Zhao, Y., Han, H., Zhao, R., & Liu, G. (2001). Derivatization and Fluorescence Detection of Amino Acids and Peptides with 9-Fluorenylmethyl Chloroformate on the Surface of a Solid Adsorbent. *Anal. Chem, **73***, 2054–2057.
- Sharma, N., Singh, P., & Gupta, S.K. (2019). A review on role of various medicinal plants in cosmetics and cure health. *Curr Res Pharm Sci, **9***, 37–41
- Shavandi, A., Silva, T.H., Bekhit, A.A., & Bekhit, A.E. (2017). Keratin: dissolution, extraction, and biomedical application. *J Biomaterials science, **5***, 1699-1735.
- Shi, H.P., Fishel, R.S., Efron, D.T., Williams, J.Z., Fishel, M.H., & Barbul, A. (2002). Effect of supplemental ornithine on wound healing. *J Surg Res, **106***, 299–302.
- Shi, H.P., Most, D., Efron, D.T., Witte, M.B., & Barbul, A. (2003). Supplemental L-arginine enhances wound healing in diabetic rats. *Wound Repair Regen, **11***, 198–203.

- Shi, Z., Li, H., Li. Z., Hu. J., & Zhang, H. (2013). Pre-column derivatization RP-HPLC Determination of Amino Acids in Asparagi Radix before and after Heating Process. *IERI Procedia, **5***, 351–356.
- Singh, O., Khanam, Z., Misra, N., & Srivastava, M.K. (2011). Chamomile (Matricaria chamomilla L.): an overview. *Pharmacogn Rev, **5***, 82–95
- Singh, S., Zhao, K., & Singh, J. (2002). In vitro permeability and binding of hydrocarbons in pig ear and human abdominal skin. *Drug Chem Toxicol, **25***, 83–92.
- Solano, F. (2020). Metabolism and Functions of Amino Acids in the Skin. In G. Wu (ed.), Amino Acids in Nutrition and Health. *Adv. Exp. Med. Biol, **1265**,*187- 199.
- Sølberg, J., Ulrich, N.H., Krustrup, D., Ahlström, M.G., Thyssen, J.P., Menné, T., Bonefeld, C.M.,3, Gadsbøll, A., Balslev, E., & Johansen, J.D. (2019). Skin tape stripping: Which layers of the epidermis are removed? *Contact Dermatitis, **80***, 319–321.
- Sommer, E., Neubert, R.H.H., Mentel, M., Tuchscherer, B., Mrestani, Y., & Wohlrab, J. (2018). Dermal peptide delivery using enhancer molecules and colloidal carrier systems. Part III: Tetrapeptide GEKG. *Eur J Pharm Sci, **124***, 137–144.
- Souto, E.B., Cano, A., Martins-Gomes, C., Coutinho, T.E., Zielinska, A., & Silva, A.M. (2022). Review: Microemulsions and Nanoemulsions in Skin Drug Delivery. *Bioengineering, **9***, 158.
- Srivastava, A., Srivastava, P., Pandey, A., Khanna, V.K., & Pant, A.B. (2018). Phytomedicine: a potential alternative medicine in controlling neurological disorders. New look to phytomedicine: advancements in herbal products as novel drug leads. Elsevier, pp. 625–655
- Stechmiller, J.K., Childress, B., & Cowan, L. (2005). Arginine supplementation and wound healing. *Nutr Clin Pract, **20***, 52–61.
- Stenn, K.S., Link, R., Moellmann, G., Madri, J., & Kuklinska, E. (1989). Dispase, a neutral protease from Bacillus polymyxa, is a powerful fibronectinase and type IV collagenase. *Br. J. Dermatol, **93***, 287-290.
- Stoimenova, A., Ivanov, K., Obreshkova, D., & Saso, L. (2013). Biotechnology in the production of pharmaceutical industry ingredients: amino acids. *Biotechnol Biotechnol Equip, **27***, 3620–3626
- Strianse, S.J. (1974). The search for the ideal moisturizer. *Cosmet Perfum, **89***, 57.
- Sun, L., Liu, Q., Bao, C., & Fan, J. (2017). Comparison of free total amino acid compositions and their functional classifications in 13 wild edible mushrooms. *Molecules, **22***, 350.
- Surber, C. (1990). Partitioning of chemicals into human stratum corneum: Implications for risk assessment following dermal exposure. Fundam. *Appl. Toxicol, **15***, 99–107.
- Surber, C. Wilhelm, K.P., Hori, M., Maibach, H.I., Guy, R.H. (1990). Optimization of Topical Therapy: Partitioning of Drugs into Stratum Corneum. *Pharm. Res, **7***, 1320–1324.

- Sybert, V.P., Dale, B.A., & Holbrook, K.A. (1985). Ichthyosis vulgaris: identification of a defect in synthesis of filaggrin correlated with an absence of keratohyaline granules. *J Invest Dermatol, **84***, 191-4.
- Sznitowska, M., Janicki, S., & Williams, A.C. (1998). Intracellular or intercellular localization of the polar pathway of penetration across stratum corneum. *J. Pharm. Sci, **87***, 1109–1114.
- Takada, S., Naito, S., Sonoda, J., & Miyauchi, Y. (2012). Noninvasive *in vivo* measurement of natural moisturizing factor content in stratum corneum of human skin by attenuated total reflection infrared spectroscopy. *Appl Spectrosc, **66***, 26–32.
- Takahashi, M., Uematsu, Y., Kashiwaba, K., Yagasaki, K., Hajika, M., Matsunaga, R., Komatsu, K., & Ishimoto, M. (2003). Accumulation of high levels of free amino acids in soybean seeds through integration of mutations conferring seed protein defciency. *Planta, **217***, 577–586.
- Takaoka, M., Okumura, S., Seki, T., & Ohtani, M. (2019). Effect of aminoacid intake on physical conditions and skin state: a randomized, doubleblind, placebocontrolled, crossover trial. *J Clin Biochem Nutr, **65***, 52–58.
- Tan, S.P., Brown, S.B., Griffiths, C.E., Weller, R.B., & Gibbs, N.K. (2017). Feeding filaggrin: effects of l-histidine supplementation in atopic dermatitis. *Clin Cosmet Investig Dermatol, **10***, 403–411.
- Tang, C.H., Ten, Z., Wang, X.S., & Yang, X.Q. (2006). Physicochemical and functional properties of hemp (Cannabis sativa L.) protein isolate. *J Agric Food Chem, **54***, 8945–8950.
- Tang, L., Zhang, Y.X., & Hutchinson, C.R. (1994). Amino acid catabolism and antibiotic synthesis: valine is a source of precursors for macrolide biosynthesis in Streptomyces ambofaciens and Streptomyces fradiae. *J Bacteriol, **176***, 6107–6119.
- Tenjarla, S. (1999) Microemulsions: an overview and pharmaceutical applications. *Crit Rev Ther Drug Carrier Syst, **16***, 461–521.
- Thornfeldt, C. (2005). Cosmeceuticals containing herbs: fact, fiction, and future. *Dermatol Surg, **31***, 873–881.
- Toghrol, F., & Daneshpejouh, H. (1974). Estimation of free amino acids, protein and amino acid compositions of cumin seed (*Cuminum cyminum*) of Iran. *J Trop Pediatr, **20***, 109–111.
- van Hal, D.A., Jeremiasse, E., Junginger, H.E., Spies, F., & Bouwstra, J.A. (1996). Structure of Fully Hydrated Human Stratum Corneum: A Freeze-Fracture Electron Microscopy Study. *J Invest Dermatol, **106***, 89-95.
- Vecchia, B.E., & Bunge, A.L. (2002). Partitioning of Chemicals into Skin: Results and Predictions. In Guy, R.H., Hadgraft, J. (eds.), Transdermal Drug Delivery (2nd ed., pp. 143– 198), Marcel Dekker: Inc. New York.
- Verdier-Sévrain, S., & Bonté, F. (2007). Skin hydration: a review on its molecular mechanisms. *J. Cosmet. Dermatol, **6**, 75–82*.

- Walkley, K. (1972). Bound water in stratum corneum measured by differential scanning calorimetry. *J. Invest. Dermatol, **50**, 225–227*.
- Walters, K.A., & Roberts, M.S. (2019). Skin Morphology, Development and Physiology. In Heather, A.E., Benson, M.S., Roberts, V.R.L, Kenneth W. (eds.), Cosmetic Formulation: Principles and Practice (1st Edition, pp. 29-46). Boca Raton, CRC Press.
- Walzer, C., Benathan, M., & Frenk, E. (1989). Thermolysin treatment: a new method for dermo-epidermal separation. *J Invest Dermatol, **92***, 78–81.
- Waterbeemd, H., Karajiannis, H., & Tayar, N. (1994). Lipophilicity of amino acids. *Amino acids, **7***, 129–145.
- Watkinson, A., Harding, C., Moore, A., & Coan, P. (2001). Water modulation of stratum corneum chymotryptic enzyme activity and desquamation. *Arch Dermatol Res, **293***, 470–476.
- Wertz, P.W., & Downing, D.T. (1989). Stratum corneum: biological and biochemical considerations. In Hadgraft, J., Guy, R.H. (Eds.), Transdermal Drug Delivery (pp. 1–17). Marcel Dekker, New York.
- Wester, R.C., & Maibach, H.I. (1983). Cutaneous pharmacokinetics: 10 steps to percutaneous absorption. *Drug Metab Rev, **14***, 169–205.
- Wester, R.C., Melendres, J., Sedik, L., Maibach, H., & Riviere, J.E. (1998). Percutaneous absorption of salicylic acid, theophylline, 2, 4-dimethylamine, diethyl hexyl phthalic acid, and p-aminobenzoic acid in the isolated perfused porcine skin flap compared to man in vivo. *Toxicol Appl Pharmacol, **151***, 159–165.
- Williams, A.C. & Barry BW (2012). Penetration enhancers. *Adv. Drug Deliv. Rev, **64***, 128–137.
- Williams, A.C. & Barry, B.W. (2004). Penetration enhancers. *Adv. Drug Deliv. Rev, **56***, 603–618.
- Williams, C., Wilkinson, S.M., McShane, P., Lewis, J., Pennington, D., Pierce, S., & Fernandez, C. (2010). A double-blind, randomized study to assess the effectiveness of different moisturizers in preventing dermatitis induced by hand washing to simulate healthcare use. *Br J Dermatol,**162***, 1088–1092.
- Williams, J.Z., Abumrad, N., & Barbul, A. (2002). Effect of a specialized amino acid mixture on human collagen deposition. *Ann Surg, **236***, 369–374.
- Wilschut, A., ten Berge, W.F., Robinson, P.T., McKone, T.E. (1995). Estimating skin permeation. The validation of five mathematical skin permeation models. *Chemosphere, **30***, 1275–1296.
- World Health Organization (WHO) (2013). WHO traditional medicine strategy 2014–2023. WHO 2009, 1–76.
- Wu, G. (2013). Amino acids: biochemistry and nutrition. CRC Press, Boca Raton.

- Wu, G., Bazer, F.W., Burghardt, R.C., Johnson, G.A., Kim, S.W., Knabe, D.A., Li, P., et al. (2011). Proline and hydroxyproline metabolism: implications for animal and human nutrition. *Amino Acids,* ***40***, 1053–1063.
- Wu. G. (2009). Amino acids: metabolism, functions, and nutrition. *Amino Acids,* ***37***, 1–17.
- Xi, P.B., Jiang, Z.Y., Dai, Z.L., Li, X.L., Yao, K., Zheng, C.T., Lin, Y.C., Wang, J.J., & Wu, G. (2012). Regulation of protein turnover by L-glutamine in porcine intestinal epithelial cells. *J Nutr Biochem,* ***23***, 1012–1017.
- Yang, R., Wei, T., Goldberg, H., Wang, W., Cullion, K., & Kohane, D.S. (2017). Getting Drugs Across Biological Barriers. *Adv Mater Weinheim,* ***29***, 1-25.
- Yannas, I.V. (2001). Regeneration of skin, Tissue and Organ Regeneration in Adults, Springer New York, New York, NY, pp. 89–136.
- Yimer, E.M., Tuem, K.B., Karim, A., Ur-Rehman, N., & Anwar, F. (2019). Nigella sativa L. (Black Cumin): a promising natural remedy for wide range of illnesses. Evid Based Complement *Altern Med,* ***2019***, 1-16.
- You, J., Liu, L., Zhao, W., Zhao, X., Suo, Y., Wang, H., & Li, Y. (2007). Study of a new derivatizing reagent that improves the analysis of amino acids by HPLC with fluorescence detection: application to hydrolyzed rape bee pollen. *Anal. Bioanal. Chem,* ***387***, 2705–2718.
- Yu, B., Kim, K.H., So, P.T., Blankschtein, D., & Langer, R. (2003). Evaluation of fluorescent probe surface intensities as an indicator of transdermal permeant distributions using wide-area two-photon fluorescence microscopy. *J. Pharm. Sci,* ***92***, 2354– 2365.
- Zeng, F., Ou, J., Huang, Y., Li, Q., Xu, G., Liu, Z., & Yang, S. (2015). Determination of 21 free amino acids in fruit juices by HPLC using a modifcation of the 6-aminoquinolyl-N-hydroxysuccinimidyl carbamate (AQC) method. *Food Anal Methods,* ***8***, 428–437.
- Zhai, H, & Maibach, H.I. (1996). Effect of barrier creams: human skin in vivo. *Contact Dermatitis,* ***35***, 92–96.
- Zhang, J., & Michniak-Kohn, B. (2011). Investigation of micro emulsion microstructures and their relationship to transdermal permeation of model drugs: Ketoprofen, lidocaine, and caffeine. *Int. J. Pharm,* ***421***, 34–44.
- Zhang, L.Y., & Sun, M.X. (2004). Determination of histamine and histidine by capillary zone electrophoresis with pre-column naphthalene-2, 3- dicarboxaldehyde derivatization and fluorescence detection. *J. Chromatogr A,* ***1040***, 133–140.
- Zhang, X.J., Chinkes, D.L., & Wolfe, R.R. (2004). Leucine supplementation has an anabolic effect on proteins in rabbit skin wound and muscle. *J Nutr,* ***134***, 3313–3318.

- Zhang, X.L., Zhao, T., Cheng, T., Liu, X.Y., & Zhang, H.X. (2012). Rapid resolution liquid chromatography (RRLC) analysis of amino acids using pre-column derivatization. *J. Chromatogr B,* ***906*****,** 91– 95.
- Zhao, M., Ma, Y., Dai, L., Zhang, D, Li, J., Yuan, W., & Zhou, H. (2012). A High-Performance Liquid Chromatographic Method for Simultaneous Determination of 21 Free Amino Acids in Tea. *Food Anal Methods,* ***6***, 69–75.
- Zhao, X., Yang, Z.B., Yang, W.R., Wang, Y., Jiang, S.Z., Zhang, G.G. (2011). Effects of ginger root (Zingiber ofcinale) on laying performance and antioxidant status of laying hens and on dietary oxidation stability. *Poult Sci,* ***90***, 1720–1727.
- Zhong, F.M., Yu, C.R., Luo, C., Shoemaker, Y., Li, S.Q., & Xia, J.G. (2009) Formation and characterisation of mint oil/S and CS/water micro emulsions. *Food Chem,* ***115***, 539–544.
- Zhou, H., Yue, Y., Liu, G., Li, Y., Zhang, J., Gong, Q., Yan, Z., & Duan, M. (2009). Preparation and characterization of a lecithin nanoemulsion as a topical delivery system. *Nanoscale Res. Lett,* ***5***, 224–230.
- Zidan, A.S., Kamal, N., Alayoubi, A., Seggel, M., Ibrahim, S., Rahman, Z., Cruz, C.N., & Ashraf, M. (2017) Effect of isopropyl myristate on transdermal permeation of testosterone from carbopol gel. *J Pharm Sci,* ***106***, 1805–3.
- Ziegler, J., Hussain, H., Neubert, R.H.H., & Abel, S. (2019). Sensitive and selective amino acid profling of minute tissue amounts by HPLC/electrospray negative tandem mass spectrometry using 9-fuorenylmethoxycarbonyl (Fmoc-Cl) derivatization. *Methods Mol Biol,* ***2030***, 365–379.
- Zou, Y., & Maibach, H.I. (2018). Dermal-epidermal separation methods: research implications. *Arch Dermatol Res,* ***310***, 1–9.
- Zou, Y., Ma, K., & Tian, M. (2015). Chemical composition and nutritive value of hot pepper seed (Capsicum annuum) grown in Northeast Region of China. *Food Sci Technol,* ***35***, 659–663.

APPENDIX

Annex 1: Some properties of FAAs

Table S1: Chemical name, Molecular weight, log P and water solubility of FAAs [Burnett et al., 2013].

S/N	Amino acid	Chemical name	3 letters Abbreviation	MWt (g/mol)	Log P	Solubility in water (g/l, 25 ^{0}C)	Melting point (^{o}C)
1	L-Arginine	α-Amino-delta-guanidino-n-valeric acid	L-Arg	174.20	-3.5	182.00	244
2	L-Asparagine	α-Aminosuccinamic acid	L-Asn	132.12	-3.5	29.40	235
3	L-Glutamin	α-Amino glutamic acid	L-Gln	146.14	-3.1	41.50	185
4	L-Serine	α-Amino-β-hydroxypropionic acid	L-Ser	105.09	-3.1	50.00	228
5	L-Aspartic acid	α-Aminosuccinic acid	L-Asp	133.10	-2.8	5.39	270
6	L-Glutamic acid	α-Aminoglutaric acid	L-Glu	147.13	-3.7	8.64	224
7	L-Threonine	α-Amino-β-hydroxy-n-butyric acid	L-Thr	119.12	-2.9	97.00	256
8	L-Glycine	Amino acetic acid	L-Gly	75.07	-3.2	249.00	262
9	L-Alanine	α-Aminopropionic acid	L-Ala	89.09	-3.0	164.00	300
10	L-Proline	Pyrrolidine-α-carboxylic acid	L-Pro	115.13	-2.5	162.00	221
11	L-Methionine	α-Amino-**γ**-methyl-thio-n-butyric acid	L-Met	149.21	-1.9	56.60	283
12	L-Valine	α-Aminoisovaleric acid	L-Val	117.15	-2.3	58.50	315
13	L-Phenalalanine	α-Amino-β-phenyl propionic acid	L-Phe	165.19	-1.5	26.90	283
14	L-Ileucine	α-Amino-β-methyl n-valeric acid	L-Ile	131.17	-1.7	34.40	285
15	L-Leucine	α-Aminoisocaproic acid	L-Leu	131.17	-1.5	21.50	293
16	L-Histidine	α-Amino-β-imidazolepropionic acid	L-His	155.15	-3.2	45.60	287
17	L-Ornithine	α-δ-Diamino-n-valeric acid	L-Orn	132.16	-3.6	172.00	245
18	L-Lysine	α-Diaminocaproic acid	L-Lys	146.19	-3.2	91.30	263
19	L-Trypthophan	α-Amino-β-indolepropionic acid	L-Trp	204.23	-1.1	11.40	290
20	L-Tyrosine	α-Amino-β-(p-hydroxyphenyl) propionic acid	L-Tyr	181.19	-2.3	0.45	343
21	L-Cystein	β-Mercaptoalanine	L-Cys	121.16	-2.5	277.00	240
22	L-Citrulline	2-Amino-5-(carbamoylamino)pentanoic acid	L-Cit	175.19	-4.3	200.00	235

Annex 2: Chemical structure of FAAs

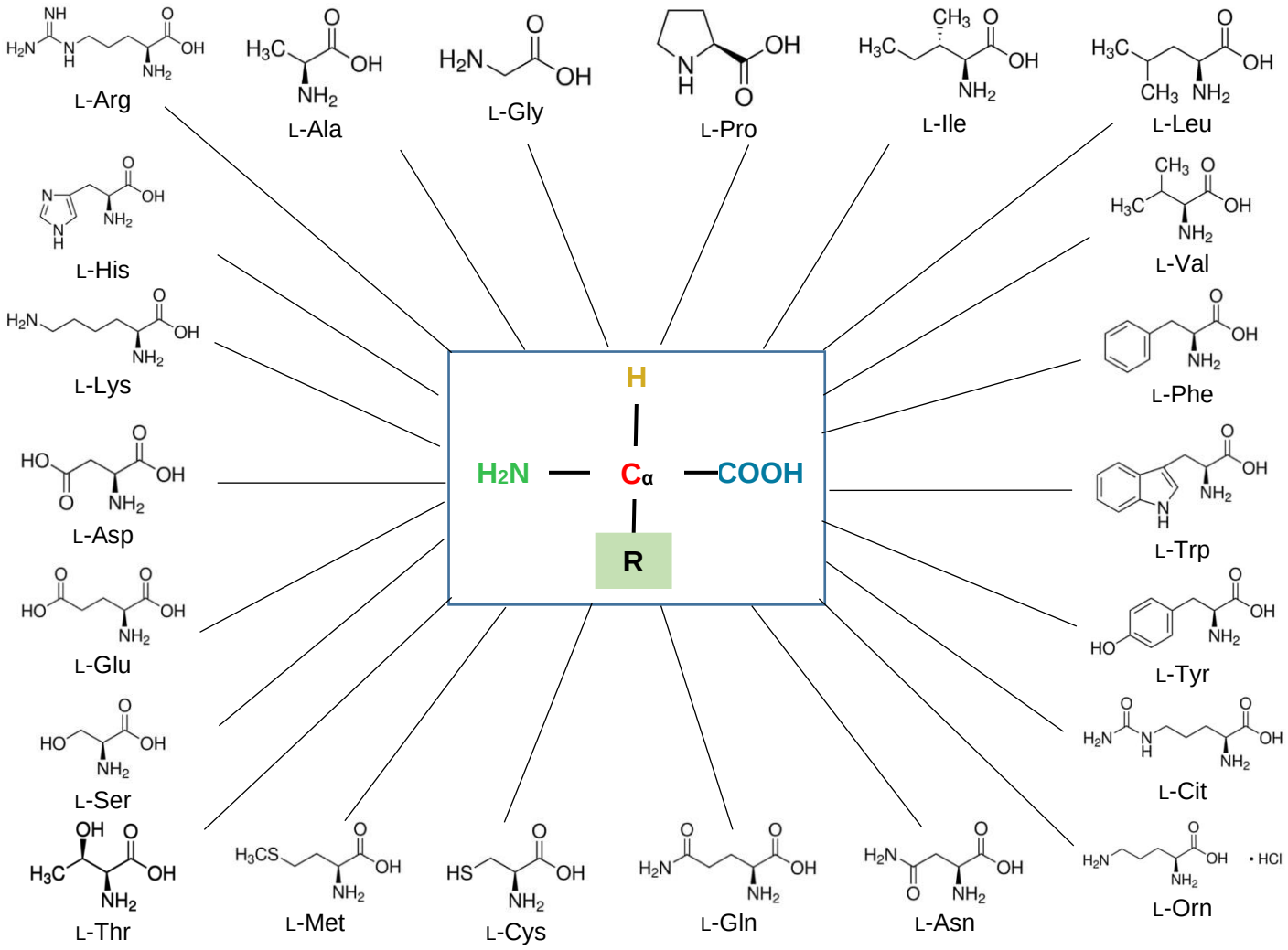

Fig. S1: Structure of L-amino acids